Report No. FAA-RD-71-52

ANALYSIS OF TECHNIQUES FOR DESCRIBING THE STATE OF SKY THROUGH AUTOMATION

R.O. Duda, R.L. Mancuso, P.F. Paskert
Stanford Research Institute
Menlo Park, California 94025

JULY 1971

FINAL REPORT

PREPARED FOR

DEPARTMENT OF COMMERCE
NATIONAL OCEANIC AND ATMOSPHERIC ADMINISTRATION
National Weather Service
Silver Spring, Maryland 20910

DEPARTMENT OF TRANSPORTATION
FEDERAL AVIATION ADMINISTRATION
Systems Research & Development Service
Washington, D.C. 20590

TECHNICAL REPORT STANDARD TITLE PAGE

1. Report No.	2. Government Accession No.	3. Recipient's Catalog No.
FAA-RD-71-52		

4. Title and Subtitle	5. Report Date
Analysis of Techniques for Describing the State of the Sky Through Automation	July 1971
	6. Performing Organization Code: SRI Project 7935
7. Author(s): R. O. Duda, R. L. Mancuso, P. F. Paskert	8. Performing Organization Report No.
9. Performing Organization Name and Address: Stanford Research Institute, 333 Ravenswood Avenue, Menlo Park, California 94025	10. Work Unit No.: 450-402-17C
	11. Contract or Grant No.: E-203-69(N)
12. Sponsoring Agency Name and Address: Department of Transportation, Federal Aviation Administration, SRDS, Washington, D.C. 20590; Department of Commerce, National Oceanic and Atmospheric Administration, NWS, Silver Spring, Md. 20910	13. Type of Report and Period Covered: Final Report
	14. Sponsoring Agency Code

15. Supplementary Notes

Prepared under FAA Inter-Agency Agreement No. FA65WAI-96.

16. Abstract

The problem of automatically describing cloud amount and cloud base height is studied through the use of statistical analysis and computer simulation. A simulation program is used to determine the response of a set of instruments to simulated cloud conditions. Relations are derived between the accuracy of cloud amount estimation and the number of instruments used, area covered, mean cloud size, cloud speed, sampling interval, and averaging time. Various clustering procedures are evaluated for use in determining the number of cloud layers, the mean height of each layer, and the cloud amount in layers. The physical limitations of such instruments as vertically-pointing ceilometers and scanning lidar systems are discussed. Finally, a simple cost comparison is made between the present manual and a possible automatic system.

17. Key Words	18. Distribution Statement
Sky cover Ceiling Cloud amount estimation Cloud base-height indicators	Availability is unlimited. Document may be released to the Clearinghouse for Federal Scientific and Technical Information, Springfield, Virginia 22151, for sale to the public.

19. Security Classif. (of this report)	20. Security Classif. (of this page)	21. No. of Pages	22. Price
Unclassified	Unclassified	156	$3.00 HC .95 MF

Form DOT F 1700.7 (8-69)

This is a contractor's report. The contents reflect the views of the Stanford Research Institute which is responsible for the facts and accuracy of the data presented herein. The contents do not necessarily reflect the official views or policies of the Department of Commerce or Department of Transportation. This report does not constitute a standard, specification, or regulation.

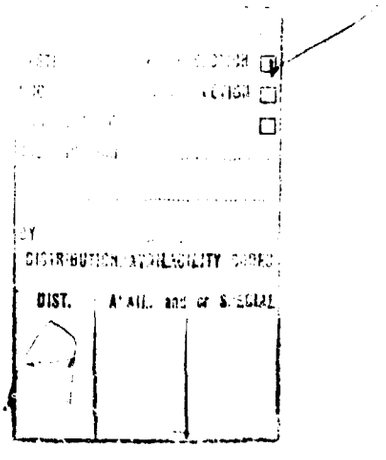

PREFACE

This research was supported jointly by the Systems Research and Development Service of the Federal Aviation Administration, Department of Transportation, and the National Oceanic and Atmospheric Administration/National Weather Service, Department of Commerce. Appendix A of this report was written by Roy H. Blackmer, Jr., and Appendix B was written by Ronald T. Collis. We would also like to acknowledge the contribution of Sidney M. Serebreny, Manager of the Atmospheric Analysis Program, who provided most valuable guidance and assistance during the entire project.

CONTENTS

ILLUSTRATIONS

TABLES

SYMBOLS

a	Reciprocal of ℓ_m	(/m)
A	Area	(m^2)
A_r	Receiver area	(m^2)
c	Speed of light	(m/s)
c_a	Cloud amount	(-)
$\tilde{c}$	Local cloud amount	(-)
$\hat{c}$	Single-instrument estimate of $\tilde{c}$	(-)
$\hat{c}(n)$	n-instrument estimate of $\tilde{c}$	(-)
$\hat{c}_m(n)$	m-reading n-instrument estimate of $\tilde{c}$	(-)
C	Cluster	(-)
d	Base-height correlation distance	(m)
d_{jk}	Distance from j^{th} to k^{th} cluster	(m)
e	Error	(m)
E	Expected value operator	(-)
f	Window function	(-)
g	Number of clusters	(-)
h	Cloud height	(m)
h_{max}	Maximum cloud height	(m)
h_{min}	Minimum cloud height	(m)
$\bar{h}$	Mean cloud height	(m)
$\hat{h}$	Estimate of $\bar{h}$	(m)
h^*	Cluster boundary	(m)
ℓ	Pulse length	(m)
ℓ_m	Mean cloud length	(m)
L	Number of cloud layers	(-)
m	Number of readings	(-)
n	Number of instruments	(-)
n	Number of samples	(-)
p	Probability density function	(/m)
p_n	n-sample estimate of p	(/m)
P_c	Probability of correct estimate	(-)
P_h	Percentage error in estimating base height	(-)

P_k	Observable cloud amount in k^{th} layer	(-)
P_r	Received power	(watts)
P_t	Transmitted power	(watts)
$\hat{P}_k$	Estimate of P_k	(-)
r	Range	(m)
R	Range	(m)
$\hat{s}^2$	Sample scatter	(m^2)
$\hat{s}_p^2$	Pooled sample scatter	(m^2)
t	Time	(s)
t_{add}	Computer add time	(s)
t_b	Layer beginning time	(s)
t_e	Layer ending time	(s)
t_{mul}	Computer multiply time	(s)
$\bar{t}$	Mean cloud layer thickness	(m)
T	Averaging time	(s)
T_{max}	Maximum allowed averaging time	(s)
T_o	Theoretical averaging time	(s)
u	Dummy variable	(-)
v	Cloud speed	(m/s)
w	Width	(m)
x	Coordinate pointing east	(m)
y	Coordinate pointing north	(m)
$\bar{z}$	Volume backscattering coefficient	(/m-ster)
Δ	Interval for P_c	(-)
Δh	Clustering parameter	(m)
ΔT	Sampling interval	(s)
$\Delta\theta$	Increment in elevation angle	(deg)
ζ	Correlation shift	(m)
θ	Elevation angle	(deg)
ϑ	Dummy variable	(-)
ς	Aspect ratio	(-)
σ	Volume extinction coefficient	(/m)
σ_b	Base height standard deviation	(m)
$\hat{\varepsilon}$	RMS error of $\hat{c}$	(-)

$\hat{\sigma}_b$	Sample standard deviation	(m)
$\hat{\sigma}_c$	RMS error requirement for cloud amount	(-)
$\hat{\sigma}_h$	RMS error requirement for cloud base height	(m)
$\hat{\sigma}_{min}$	Minimum value of $\hat{\sigma}$	(-)
$\hat{\sigma}(n)$	RMS error of $\hat{c}(n)$	(-)
$\hat{\sigma}_m(n)$	RMS error of $\hat{c}_m(n)$	(-)
$\hat{\sigma}_p$	Pooled sample standard deviation	(m)
τ	Pulse duration	(s)
ϕ	Aximuth angle	(deg)
ϕ_{xy}	Cross-correlation function	(-)
ψ_c	Cloud direction	(deg)

I INTRODUCTION AND SUMMARY

A. Background

The state of the sky is typically described by a few integrated parameters, such as the total sky cover, the cloud amount in layers, and the ceiling height. This summarizes what might be quite complicated phenomena, only small portions of which are sampled by ceilometers and other instruments. The present procedure for reporting the state of the sky relies heavily on human observers to make visual observations and interpret instrument readings. To automate this system, one must be able to specify the required instrument characteristics and the procedures for processing data to relate instrument readings to actual sky conditions.

In an earlier phase of this contract, we developed a mathematical cloud model as a tool for solving these problems (Duda, Mancuso and Blackmer, 1970). This model describes a sky composed of several layers of clouds at different mean base heights, each layer moving at a specified speed in a specified direction. The clouds in each layer are described by specifying a number of parameters, such as the mean length and percent sky cover. By varying these parameters, a wide variety of sky conditions can be obtained. This model was implemented as a digital computer program that calculates the responses of vertically-pointing ceilometers to the model sky conditions. By using this simulation program, the behavior of an automatic system for describing the state of sky can be determined.

B. Objectives

The basic objectives of the work described in this report were to gain insight into the cost/effectiveness of various sampling and processing strategies, and to compare the performance of various ceilometers, both to evaluate current sensors and to establish specifications for future instruments. The investigation involved three major tasks:

(1) Sampling and processing studies,

(2) Ceilometer studies, and

(3) Feasibility and cost comparisons.

In Task 1, the emphasis was on determining the spatial and temporal sampling and the data processing necessary to describe cloud amount and ceiling height to a specified degree of accuracy. Most of this work involved ideal or error-free instruments, although the effects of instrument limitations were also considered. The purpose of Task 2 was to evaluate the ability of vertically-pointing and scanning instruments to measure cloud amount and ceiling height, and to determine instrument characteristics needed to meet given operating specifications. Task 3 involved the use of the simulation program to determine the technical feasibility of an automatic system. It also included a cost comparison with a nonautomated system to determine economic feasibility.

The remainder of this report presents the results of our research on these three tasks. The organization of the report is based on the natural division of the problem into the separate problems of cloud-amount estimation, cloud base-height estimation, and cost comparisons. In the remainder of this section we summarize the major results of this work and show how they relate to the three major tasks.

C. Task 1--Sampling and Processing Studies

The basic sampling problem is to determine the spatial and temporal sampling required to determine cloud amount and cloud base height to a specified degree of accuracy. Since the determination of cloud amount or cloud base height required processing the data obtained from sampling, sampling and processing were often considered together. The primary processing technique for cloud amount estimation was the time averaging of readings from the various instruments. A greater variety of techniques were considered for cloud height estimation, including techniques for probability density function estimation, mixture density analysis, and clustering.

Most of our studies involved ideal instruments that gave exact reports of the conditions they sampled. The sampling error is due to the fact that not all points in space and time are sampled. In addition, intervening lower layers can interrupt the sampling of upper layers. A combination of mathematical analysis and computer simulation was used to show how the error depended on the following factors:

(1)	Sampling parameters	
	(a) Number of sensors	n
	(b) Area covered	A
	(c) Sensor configuration	-
	(d) Time between samples	ΔT
(2)	Processing parameters	
	(a) Averaging time	T
	(b) Window widths	w
	(c) Number of cluster centers	c
(3)	Cloud parameters	
	(a) Mean cloud length	ℓ_m
	(b) Cloud amount	c_a
	(c) Cloud speed	v
	(d) Mean base height	$\bar{h}$
	(e) Base-height standard deviation	σ_b
	(f) Base-height correlation distance	d

The major results of this study can be summarized as follows. The root mean square error $\hat{\sigma}$ in estimating cloud amount was found to depend primarily upon $\sqrt{A}/\ell_m$. Figure 6 shows the number of instruments needed to obtain a specified $\hat{c}$ for a worst case situation with $c_a = 0.5$ and no time averaging. By optimum time averaging, the required number of instruments can be reduced greatly, with four vertically-pointing instruments theoretically being able to exceed human performance.

The root mean square error in estimating the base height of a single cloud layer depends primarily upon σ_b and vT/d, and there exist theoretically optimum procedures for sampling and processing. The multiple-layer case is much more difficult. In our experiments, good results were obtained with a simple hierarchical clustering procedure described in Section IV-D-2. This procedure was able to determine the number of cloud layers, the mean height of each layer, and the cloud amount in layers for a variety of experimental conditions. These results may be sensitive to instrument limitations, and an investigation of ways to detect and overcome the effects of interference

and precipitation is needed. A discussion of these problems concludes Section IV.

D. Task 2--Ceilometer Studies

The goal of Task 2 was to evaluate the performance of both vertically-pointing and scanning instruments used to measure cloud amount and ceiling height, and to relate performance to required instrument characteristics. In this work, the model was used to provide information about the true sky conditions, allowing comparisons against an objective standard.

The performance of vertically pointing instruments is directly related to root mean square error $\hat{\sigma}$. A major result of our study was to relate $\hat{\sigma}$ to the time ΔT between measurements. Even if ΔT is zero, some error $\hat{\sigma}_{min}$ is unavoidable. The percentage increase in $\hat{\sigma}$ as a function of ΔT was determined, and a criterion for selecting ΔT is suggested in Section III-C-2. For cloud amount estimation, this criterion depends on the cloud speed v and the mean cloud length ℓ_m. For cloud base height estimation, it depends on the cloud speed and the base height correlation distance d. Actual selection of instrument parameters requires a decision about the range of cloud conditions over which a desired performance is to be achieved; such decisions were considered to be outside of the scope of this study.

Our original simulation model did not include provisions for scanning instruments. To add these instruments to our study, we limited our attention to a single cloud layer and worked in terms of an equivalent system of vertically-pointing instruments. The chief advantage of scanning instruments is that for intermediate and high clouds, one scanning instrument can replace many vertically-pointing instruments. However, it was found that the performance of scanning instruments was limited at low ceiling heights by geometrical constraints (see Section III-E). In addition to sampling problems, there are particular problems associated with the physics of different kinds of instruments. For example, the performance of scanning radars depends on the wavelength and pulse length used, and the usefulness of scanning lidars might be

limited by safety considerations. Appendix A contains a discussion of these considerations for radar systems, and Appendix B contains a similar discussion for lidar systems. The results of our sampling study also apply to other types of scanning sensors, such as the passive infra-red sensor, but only the radar and lidar systems were considered in detail.

E. Task 3--Feasibility and Cost Comparisons

The feasibility of an automatic system depends upon many factors, including the performance required and the nature of the conditions at the particular airport. To the extent that our model accurately describes sky conditions and instrument characteristics, we have demonstrated the technical feasibility of an automatic system for measuring cloud amount at least as accurately as is done at present. The technical feasibility of using clustering techniques to automatically determine cloud base heights was also demonstrated, both with the model data and with a small sample of actual ceilometer data. However, some further development of these techniques will probably be needed to accommodate possible bad effects of interference and precipitation.

Section V contains a comparison of the cost of an automatic system and the cost of the present manual system. In this comparison, it was assumed that both systems gave equivalent performance, and other possible benefits of either system were not considered. It was found that the results depended on the frequency with which cloud amount and ceiling height reports are needed. If the present frequency of one reading per hour is satisfactory, then the current manual system is less expensive. However, if readings are required every ten minutes or more often, automatic systems can be less expensive. The effects of cost uncertainties are included in this analysis.

F. Report Organization

The remainder of this report contains the technical material that justifies these conclusions. Section II reviews the cloud model. It describes the parameters involved in our study and their effects on the simulation sky conditions. Section III is concerned with cloud estimation. It includes precise definitions of terms, and separate

studies of estimation by single vertically-pointing instruments and scanning instruments. Section IV is concerned with cloud base-height estimation. It defines base heights for multiple-layer clouds in terms of the parameters in a mixture density function. The results of various techniques for estimating density functions and clustering cloud-height readings are reported. Section V shows how these theoretical results can be used to determine instrument and data processing requirements. Section VI presents the cost comparison, and Section VII presents the conclusions of the study.

II THE CLOUD MODEL

A. Introduction

In this section we give a brief review of those aspects of the cloud model that one must know to understand the rest of this report; a complete description of the cloud model is given in the report by Duda, Mancuso and Blackmer (1970). The cloud model describes a sky composed of one or more layers of clouds. The clouds in each layer have random characteristics, but their statistical properties are fixed by a small number of parameters. Since these parameters have constant values everywhere in a given layer, each layer is statistically homogeneous.

The geometrical parameters determine the sizes and shapes of the clouds. They fall into two classes, those that affect the plan view and those that affect the profile view. In plan view, a layer looks like an infinite plane covered with a scattering of possibly overlapping rectangles of different sizes. If the cloud amount is five tenths or less, these rectangles represent clouds, while if the cloud amount exceeds five tenths they represent holes. To simplify the following discussion, we shall assume that the rectangular areas are clouds. If the cloud amount exceeds five tenths, the statements made about clouds should be interpreted as pertaining to holes.

B. Plan-View Parameters

The appearance of the clouds in plan view is affected by the following parameters:

(1)	Mean length	ℓ_m	(m)*
(2)	Aspect ratio	ρ	(-)
(3)	Cloud amount	c_a	(-)
(4)	Cloud speed	v	(m/s)
(5)	Cloud direction	ψ_c	(rad)
(6)	Layer beginning time	t_b	(s)
(7)	Layer ending time	t_e	(s)

*In some cases distances will be reported in feet rather than meters.

The clouds generated by the model are rectangles of length ℓ in the direction of motion and width $\rho\ell$ normal to the direction of motion. The lengths ℓ have an exponential distribution that is completely specified by the mean length ℓ_m. The cloud amount c_a specifies the fraction of the entire infinite plane that is covered with clouds. The cloud amount over some specified area A may be either less than or greater than c_a, and will vary as the clouds move. All of the clouds in a given layer move in unison with the common speed v in a common direction specified by ψ_c. This greatly simplifies the computation of the instrument responses as a function of time. The instrument locations are given in a conventional, earth-referenced xy-coordinate system. If one wants to consider only part of the infinite cloud layer, a strip of clouds can be defined by t_b and t_e. The layer-beginning-time t_b specifies the time at which the leading edge of the layer passes over the origin, and the layer-ending time does the same thing for the trailing edge.

C. Profile-View Parameters

The appearance of the clouds in profile view is affected by the following parameters:

(1)	Mean thickness	$\bar{t}$	(m)
(2)	Mean base height	$\bar{h}$	(m)
(3)	Base-height standard deviation	σ_b	(m)
(4)	Base-height correlation distance	d	(m)

The tops of the clouds are always located at $\bar{h} + \bar{t}$. The base height h(x) is a randomly generated function of x, having mean $\bar{h}$ and standard deviation σ_b. The correlation coefficient between two base heights a distance ζ apart is given by $\exp[-\zeta/d]$, where d is the base-height correlation distance. Thus, adjacent base-height values are correlated, but the correlation is very small between points that are separated by distances much greater than d. As the clouds move, the base-height profile moves with them. Thus, if the x-axis is aligned with the direction of cloud motion, the base height function should really be written as h(x + vt), so that h(x) gives the base height at time t = 0.

D. Instrument Parameters and Normalization

Most of this report is concerned with the response of ideal instruments to sky conditions that can be generated by the cloud model. By an ideal instrument, we mean one that sights along a straight line, does not give a response when no clouds are intercepted, and gives the exact range to the first point of intersection when a cloud is intercepted. With an ideal vertically-pointing instrument, the line of sight is to the zenith. We do not assume that the base height readings are obtained continually, but rather that readings are made every ΔT seconds. For an ideal vertically-pointing instrument, this is the only instrument parameter of interest.

In general, an ideal vertically-pointing instrument provides samples of the base-height function $h(x)$. If we assume for simplicity that the instrument is located at the origin and that the x-axis is aligned with the direction of cloud motion, then at the k^{th} sampling instant we obtain the reading $h(kv\Delta T)$. This shows that not all of the parameters are independent variables. If v were doubled, ΔT were halved, and all other conditions were left the same, exactly the same sequence of readings would be obtained. By normalizing the dimensional parameters with respect to distance and time, we can reduce the number of variables and simplify the presentation of results. While normalization can be done in many ways, we most frequently will use the mean cloud length ℓ_m to normalize distances and the sampling interval ΔT to normalize time. Thus, the normalized correlation distance is d/ℓ_m, and the normalized cloud speed is $v\Delta T/\ell_m$.*

*This normalization is most convenient in the single-layer case. With multiple layers, one can use the mean cloud length in the lowest layer for normalization, but this is somewhat inconvenient. In such cases we occasionally use the square root of the airport area to normalize distances.

III CLOUD AMOUNT ESTIMATION

A. Definitions

When sky cover is estimated by human observers, it is usually reported as tenths or eighths of the sky covered by surface-based phenomena and by clouds or obscuring phenomena in each layer aloft. The evaluation is made in terms of the entire sky area above the local or apparent horizon, and is fundamentally a surface-based observation, limited to a roughly circular area of several miles radius centered about the observer.

When instruments are used to give an objective measure of cloud amount, it is necessary to be somewhat more precise in defining cloud amount, particularly with regard to the area involved. A single vertically-pointing instrument gives an excellent report of the cloud amount directly above that instrument, but may not give a correct report of the cloud amount in a circular area of, say, five-mile radius around that instrument. In fact, a human observer has a similar limitation, but since he can usually observe the entire area of interest for operations at one airport, this limitation is usually not noticed.

In this report, we define the cloud amount over a given area A as the fraction of that area covered by a vertical projection of the clouds onto the ground. When several layers are present, this defines the total cloud amount. In describing the cloud amount in layers, one must distinguish between the cloud amount actually observable from the ground and the cloud amount for an isolated layer. In accordance with conventional practice, we define the (observable) cloud amount for a given layer as the fraction of the area that is covered by clouds in that layer and not covered by clouds in lower layers. We also define the model cloud amount as the fraction of the area that is covered by clouds in that layer in the absence of other layers. In this section we shall only be concerned with estimating the total cloud amount; we shall return to the question of measuring the (observable) cloud amount in layers in Section IV.

B. Variables

When instruments are used to estimate the cloud amount over an area A, the results obtained depend on the following quantities:

(1)	The area	A	(m)
(2)	The number of instruments	n	(-)
(3)	The time interval between readings	ΔT	(s)
(4)	The total observation time	T	(s)
(5)	The plan-view parameters:		
	Mean length	ℓ_m	(m)
	Aspect ratio	ρ	(-)
	Cloud amount	c_a	(-)
	Cloud speed	v	(m/s)
	Cloud direction	ψ_c	(rad)
	Layer duration	$t_e - t_b$	(s)

Even when we normalize by ℓ_m and ΔT, we see that the performance depends on at least eight variables. It is not possible to consider all combinations of all of these variables in an experimental program to find the optimum sampling and processing procedures. In our investigations, we paid particular attention to what we thought were the most critical variables. In particular, we ignored the effects of the aspect ratio and the cloud direction, taking $\rho = 1$ and $\psi_c = 0$. Since our initial experiments disclosed that five-tenths cloud amount provided the greatest difficulty, we limited most of our experiments to this case. Finally, because of experimental difficulty, we considered only one case in which the layer duration was not infinite. This means that we studied mainly statistically uniform situations. We have tried to insert cautionary remarks whenever neglect of this variable might result in conclusions that are not valid in general.

In the remainder of this section we show how cloud amount estimates depend on the remaining variables. We consider first the performance of one instrument and show how it can be improved by time averaging. After that we consider the case where n instruments are used to give instantaneous ("snapshot") estimates of the cloud amount and show how the performance varies with n, A, and ℓ_m. Finally, we consider the additional improvement that can be obtained by averaging, and introduce the effects of ΔT, T, and v.

C. Single-Instrument Sampling

1. Without Time Averaging

An ideal vertically-pointing instrument can detect whether or not there is a cloud directly overhead. Let $c(x,y)$ indicate the presence or absence of a cloud above a given point (x,y), with $c = 1$ if a cloud is present and $c = 0$ if a cloud is absent. Let $\tilde{c}$ give the total cloud amount over a specified area A, and let c_a be the total cloud amount for the cloud layer. Then

$$\tilde{c} = \frac{1}{A} \iint_A c(x,y)\, dx\, dy \tag{1}$$

and

$$c_a = \lim_{A \to \infty} \tilde{c} \quad . \tag{2}$$

If a single instrument is located at (x_0,y_0), then its readings give $c(x_0,y_0)$. We want to use these readings to estimate $\tilde{c}$. Let $\hat{c}$ be our estimate of $\tilde{c}$. The simplest of all estimates is just to take $\hat{c} = c$, the instantaneous instrument reading. If the area A is small (relative to the square of the mean cloud length), then this estimate is very good. However, if A is large, this estimate is poor. The accuracy of the estimate is measured by the error $\hat{c} - \tilde{c}$, or, since c, $\hat{c}$ and $\tilde{c}$ are random variables, by the expected squared error*

$$\hat{\sigma}^2 = E[(\hat{c} - \tilde{c})^2] \tag{3}$$

$$= E[\hat{c}^2] - 2E[\hat{c}\,\tilde{c}] + E[\tilde{c}^2] \quad . \tag{4}$$

Under ordinary conditions, the probability of error for the estimate $\hat{c}$ can be related to the root-mean-square error $\hat{\sigma}$ by assuming that $\hat{c}$ is normally distributed with mean $\tilde{c}$ and variance $\hat{\sigma}^2$. In this

*Note that $\hat{\sigma}^2$ is not the variance of $\hat{c}$ unless the area is infinite, in which case $\tilde{c} = c_a = E[\tilde{c}]$.

case, the probability that $\hat{c}$ lies in the interval $-\Delta \leq \tilde{c} \leq \Delta$ is given by

$$P_c = \frac{1}{\sqrt{2\pi}\,\hat{\sigma}} \int_{\tilde{c}-\Delta}^{\tilde{c}+\Delta} e^{-\frac{1}{2}\left(\frac{\hat{c}-\tilde{c}}{\hat{\sigma}}\right)^2} d\hat{c} \quad . \tag{5}$$

This probability is shown graphically in Figure 1. Note that $\hat{\sigma}$ must be rather small to obtain good accuracy. For example, if one wants tht estimate to be within one tenth of the true cloud amount at least 68 percent of the time, $\hat{\sigma}$ must be less than 0.1. For this same performance 95% of the time, $\hat{\sigma}$ must be less than 0.05. According to Galligan, when the cloud amount is near five tenths, human observers have a $\hat{\sigma}$ from 0.107 to 0.123 (Galligan, 1953). This should be kept in mind when specifying the desired performance for an automatic system.

In Section III-D-2 we shall see how $\hat{\sigma}^2$ increases as a function of A. At this point, however, we consider only the limiting situation as A approaches infinity. For this case, $\tilde{c} \rightarrow c_a$, and

$$\lim_{A \rightarrow \infty} \hat{\sigma}^2 = E[\hat{c}^2] - 2\, c_a\, E[\hat{c}] + c_a^2 \quad . \tag{6}$$

Since $\hat{c}$ is either one or zero, being one with probability c_a and zero with probability $1 - c_a$,

$$E[\hat{c}^2] = E[\hat{c}] = c_a \quad . \tag{7}$$

Thus,

$$\lim_{A \rightarrow \infty} \hat{\sigma}^2 = c_a(1 - c_a) \quad . \tag{8}$$

This shows that the accuracy of the estimate varies with the cloud amount. It is very good if c_a is near either zero or one, and is worst if $c_a = 0.5$. This is a very reasonable result, and is in agreement with observations on the accuracy of human observers

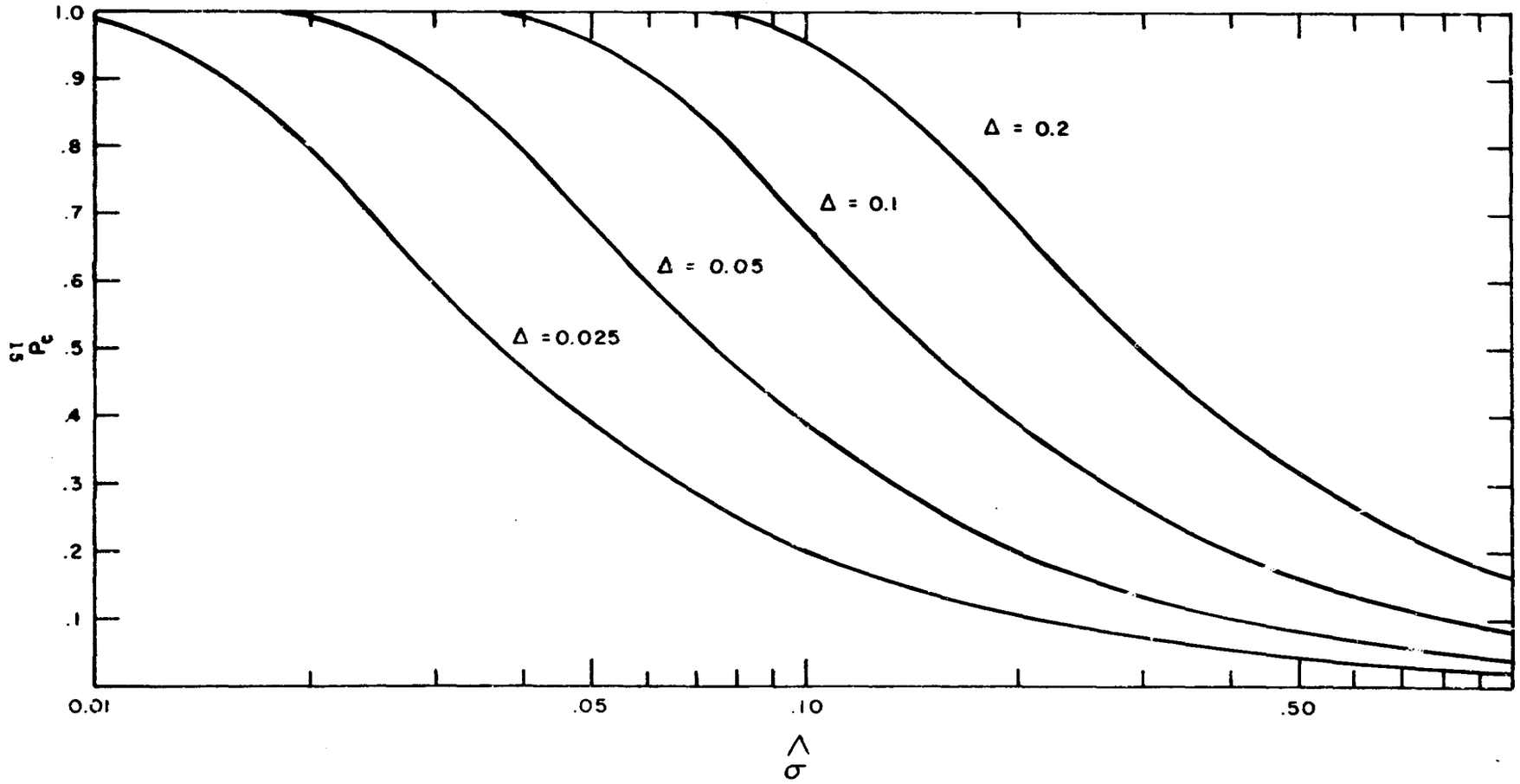

FIGURE 1 PROBABILITY THAT THE ESTIMATED CLOUD AMOUNT IS WITHIN ± Δ OF THE TRUE CLOUD AMOUNT

in estimating cloud amount (Galligan, 1953). Since the worst case occurs for $c_a = 0.5$, and since this is not an anomolous situation, we have used this result to justify limiting most of our experimental work to this case.

2. With Time Averaging

The estimate $\hat{c} = c$ takes no account of the spatial and temporal continuity of the cloud cover. It jumps back and forth between $\hat{c} = 0$ and $\hat{c} = 1$, and would not be considered seriously in practice. A more reasonable estimate can be obtained by smoothing or averaging the readings taken at previous times. Suppose that readings are taken every ΔT seconds. If c_k denotes the reading obtained at the k^{th} sampling time, then the estimate of $\tilde{c}$ obtained by averaging m readings is given by

$$\hat{c}_m = \frac{1}{m} \sum_{k=1}^{m} c_k \quad . \tag{9}$$

The physical interpretation of this estimate is simple. If the clouds are moving, then the instrument is sampling the clouds along a line in plan view that goes through the instrument location and along the direction of cloud motion. If the cloud speed is v, then the samples are a distance $v\Delta T$ apart in space, and the samples used to compute $\hat{c}_m$ extend over a distance of $mv\Delta T = vT$, where T is the total averaging time. Note that if we keep T fixed and decrease ΔT, then $m = T/\Delta T$ will increase. In the limit as ΔT goes to zero, $\hat{c}_m$ approaches the average of $c(x,y)$ along the line of length vT. This line is as close as a single instrument can come to obtaining $\tilde{c}$, the average of $c(x,y)$ over the entire area A.

Appendix C gives a derivation of the expected squared error $\hat{\sigma}_m^2$ for the estimate $\hat{c}_m$. The analysis is limited to the special case where $A = \infty$ and $c_a = 0.5$, and neglects the effects of cloud overlap. Its chief significance is that it provides us with a criterion for determining the sampling interval ΔT. The results of that analysis show that if the averaging time T is fixed and if $m = T/\Delta T$ is increased

by letting ΔT approach zero, then the expected squared error decreases to a minimum value $\hat{\sigma}_{min}^2$ given by

$$\hat{\sigma}_{min}^2 = \frac{c_a^2}{vT/\ell_m}\left[1 - \frac{1-e^{-2vT/\ell_m}}{2vT/\ell_m}\right] \quad . \tag{10}$$

The variation of $\hat{\sigma}_{min}^2$ with vT/ℓ_m is shown in Figure 2. If ΔT is not zero, $\hat{\sigma}_m^2$ is greater than $\hat{\sigma}_{min}^2$, but it may not be much greater. The exact increase in $\hat{\sigma}_m^2$ depends on both $v\Delta T/\ell_m$ and vT/ℓ_m, and the details are discussed in Appendix C. The basic result of this analysis is that the percentage increase in $\hat{\sigma}_m^2$ must lie between the two bounds shown in Figure 3. The upper bound corresponds to the no-averaging case where $T = \Delta T$, and the lower bound corresponds to the infinite-averaging case where $T = \infty$.

Note that in the worst case $\hat{\sigma}_m^2$ is less than 20% greater than $\hat{\sigma}_{min}^2$ if $\Delta T = 0.25\ \ell_m/v$, and a further reduction in ΔT does not yield much further benefit. Thus, for example, if the mean cloud length is 200 ft. and the cloud speed is 10 ft/sec, there is little value in sampling faster than once every five seconds. A very similar analysis shows that the percentage increase in the variance of the base height estimate is small if $\Delta T = 0.5d/v$, where d is the correlation distance (see Appendix E). We suggest the use of this criterion of percentage increase in the minimum expected squared error for determining the required sampling interval ΔT.

It might appear that Eq. (10) also supplies a criterion for determining the averaging time T. Unfortunately, an uncritical use of this result suggests making the averaging time infinite to obtain $\hat{\sigma}_{min}^2 = 0$. This is a limitation of the analysis, which was for the special case $A = \infty$. When the area is finite, the use of a long averaging time will prevent the estimate $\hat{c}$ from being able to follow fluctuations in $\tilde{c}$, the cloud amount over the area. In general, the averaging time is also the time that is required for $\hat{c}$ to be able to respond to a systematic change in the cloud amount. This, not Eq. (10), is the criterion that should be used in selecting T. We shall return to this question when we examine the results of averaging the responses of several instruments.

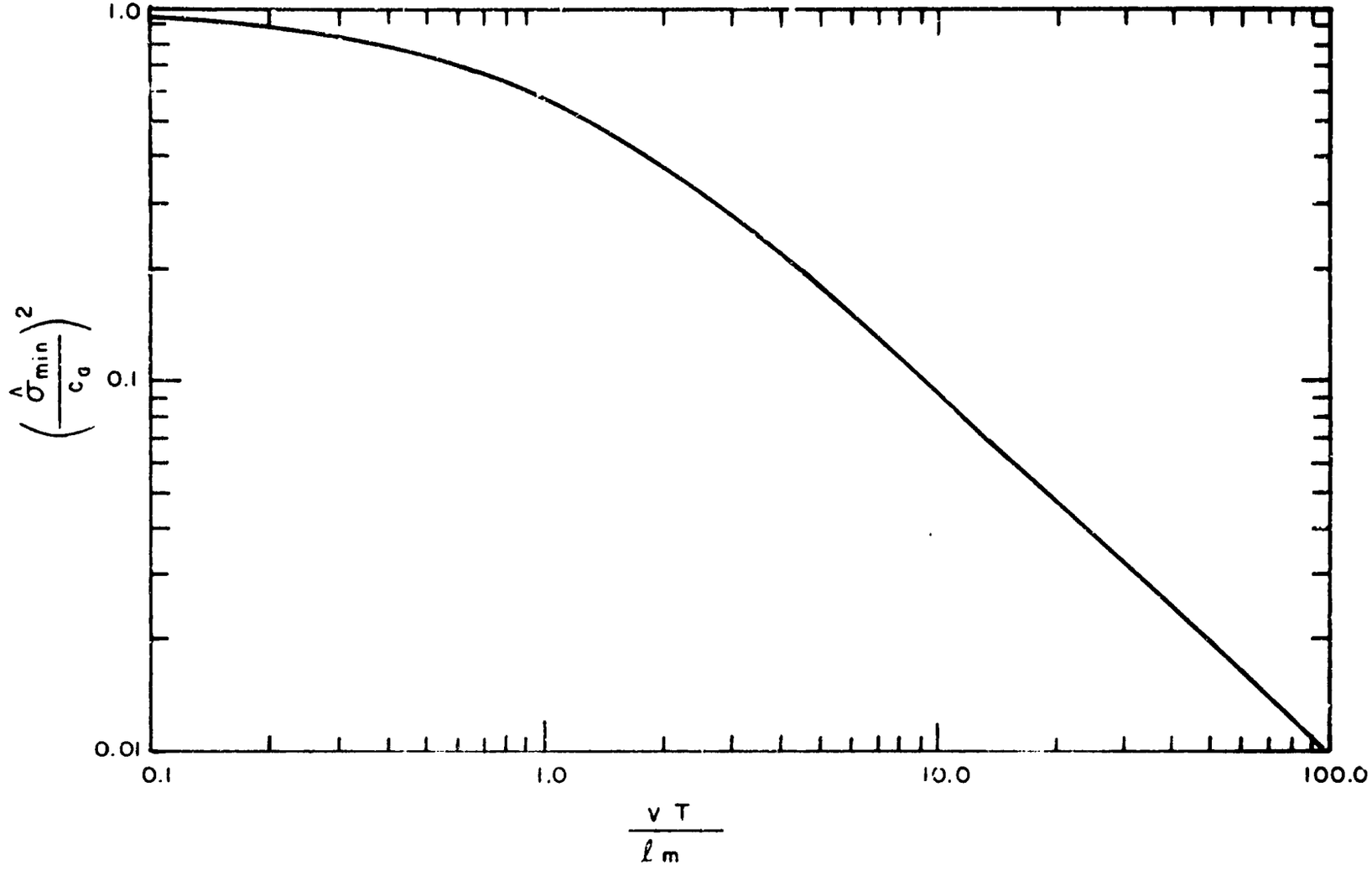

FIGURE 2 DEPENDENCE OF THE MINIMUM EXPECTED SQUARED ERROR ON AVERAGING TIME

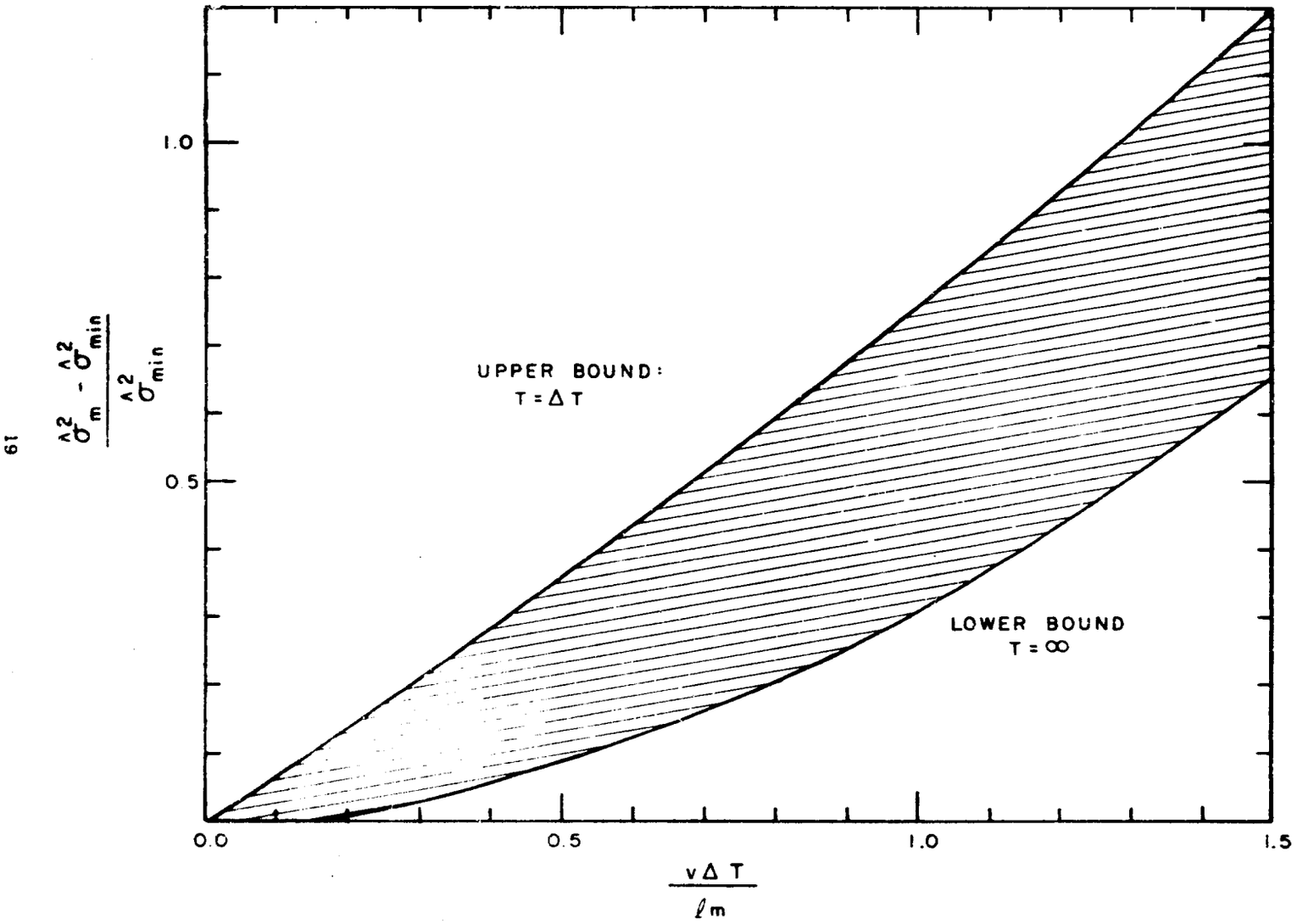

FIGURE 3 BOUNDS ON THE FRACTIONAL INCREASE IN EXPECTED SQUARED ERROR DUE TO TIME SAMPLING

D. Multiple-Instrument Sampling

1. Spatial Sampling

The use of more than one instrument allows the sampling of cloud conditions at various points in the area A. In particular, if an infinite number of instruments are used, $c(x,y)$ can be determined at every point in the area. Thus, the average cloud amount $\tilde{c}$ can be determined exactly, and zero expected squared error can be obtained. This is in contrast with the case of a single instrument, which in theory can not achieve an expected squared error less than $\hat{\sigma}_{min}^2$.

In considering the use of more than one instrument, one of the first questions that arises concerns the instrument locations. This is the problem of spatial sampling. Intuitively, it is clear that the instruments should not be concentrated in one locality, but should be distributed over the area to obtain more independent information. Whether or not the distribution should be isotropic depends on prior information. For example, if at a particular airport the clouds almost always come from a particular direction, it seems clear that the instruments should be arranged along a line at right angles to that direction. However, if the clouds are equally likely to come from any direction, then it would appear that the instrument configuration should not have preferred directions, if that is possible.

In general, the optimum instrument configuration is one that minimizes the expected squared estimation error, where the expectation is with respect to all of the random variables. To obtain an analytical solution to this problem would require knowledge of the joint probability that a given subset of the n instruments is detecting a cloud. This joint probability is a complicated function of the relative positions of the instruments, and an analysis of the problem is very difficult. Lacking an analytical solution, we have adopted a heuristic procedure that seems to provide an acceptable solution. This procedure is based on the observation that if a cloud is present above point (x_1,y_1), and if the cloud statistics are isotropic, then the probability that a cloud is also present above point (x_2,y_2) is the same for all points (x_2,y_2) on a circle centered at (x_1,y_1). This suggests

that the instruments should be located to maximize the minimum distance from any instrument to either another instrument or the boundary of the area A. Some solutions for a square area are shown in Figure 4; other solutions can be obtained from these by rotation or reflection.

2. Without Time Averaging

Let (x_i, y_i) give the location of the i^{th} instrument, $i = 1, \ldots, n$. Then the response of the i^{th} instrument yields $c(x_i, y_i)$. If all instruments are read at the same instant, then the average of their responses provides an instantaneous estimate for $\tilde{c}$:

$$\hat{c}(n) = \frac{1}{n} \sum_{i=1}^{n} c(x_i, y_i) \quad . \tag{11}$$

Figure 5 illustrates the behavior of $\tilde{c}$ and $\hat{c}(n)$ for a typical case. The solid curve in this figure shows the time variation of the cloud amount $\tilde{c}$ for a 5 km-by-5 km airport area. The plan-view parameters for the cloud layer were $c_a = 0.1$, $\ell_m = 0.5$ km, $v = 5$ m/sec, $\rho = 1$, and $\psi_c = 0$. Note that the average of $\tilde{c}$ over the 6-hour period was close to the large-area cloud amount c_a, but that significant fluctuations in $\tilde{c}$ occurred as clouds moved in and out of the area. The dotted line shows the behavior of $\hat{c}(n)$ when $n = 4$ instruments sampled the sky. When no time averaging is used, $\hat{c}(n)$ jumps back and forth between its $n + 1$ possible values--0, 1/n, 2/n, ..., 1. This erratic behavior is typical for this instantaneous estimate of the cloud amount.

Appendix D contains a derivation of the expected squared error for this estimate for a special case in which $c_a = 0.5$ and in which the n instruments are uniformly arrayed along a line segment of length w. If we assume that the area A is a square having sides of length $w = \sqrt{A}$, then the results of this analysis are as follows:

$$\hat{\sigma}^2(n) = E[(\hat{c}(n) - \tilde{c})^2]$$

$$= \frac{1}{4u} \left\{ \frac{u}{n} \frac{1+\theta}{1-\theta} + \frac{2\theta(1-\theta^n)}{n(1-\theta)} \left[1 - \frac{u}{n(1-\theta)} \right] - 1 - e^{-u} \frac{\sinh u}{u} \right\} , \tag{12}$$

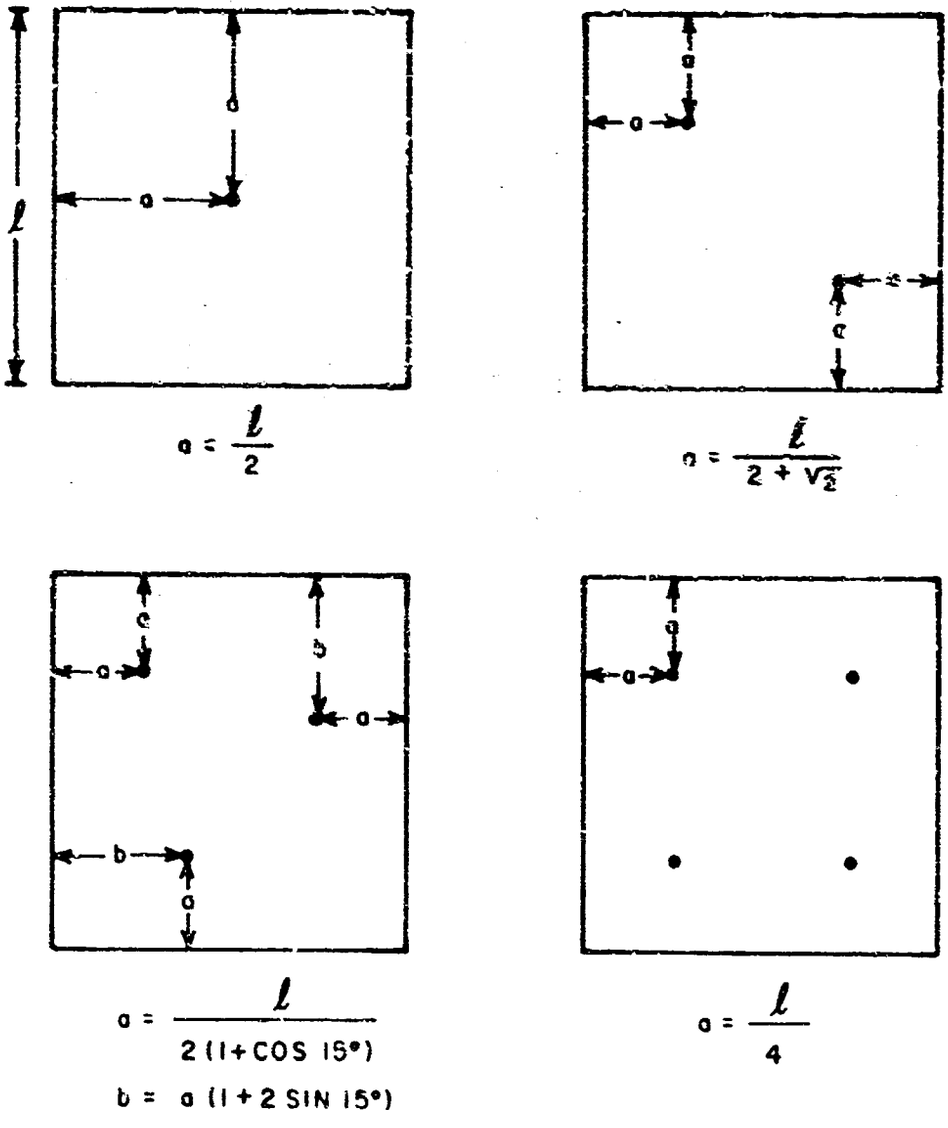

FIGURE 4 SPATIAL SAMPLING CONFIGURATIONS

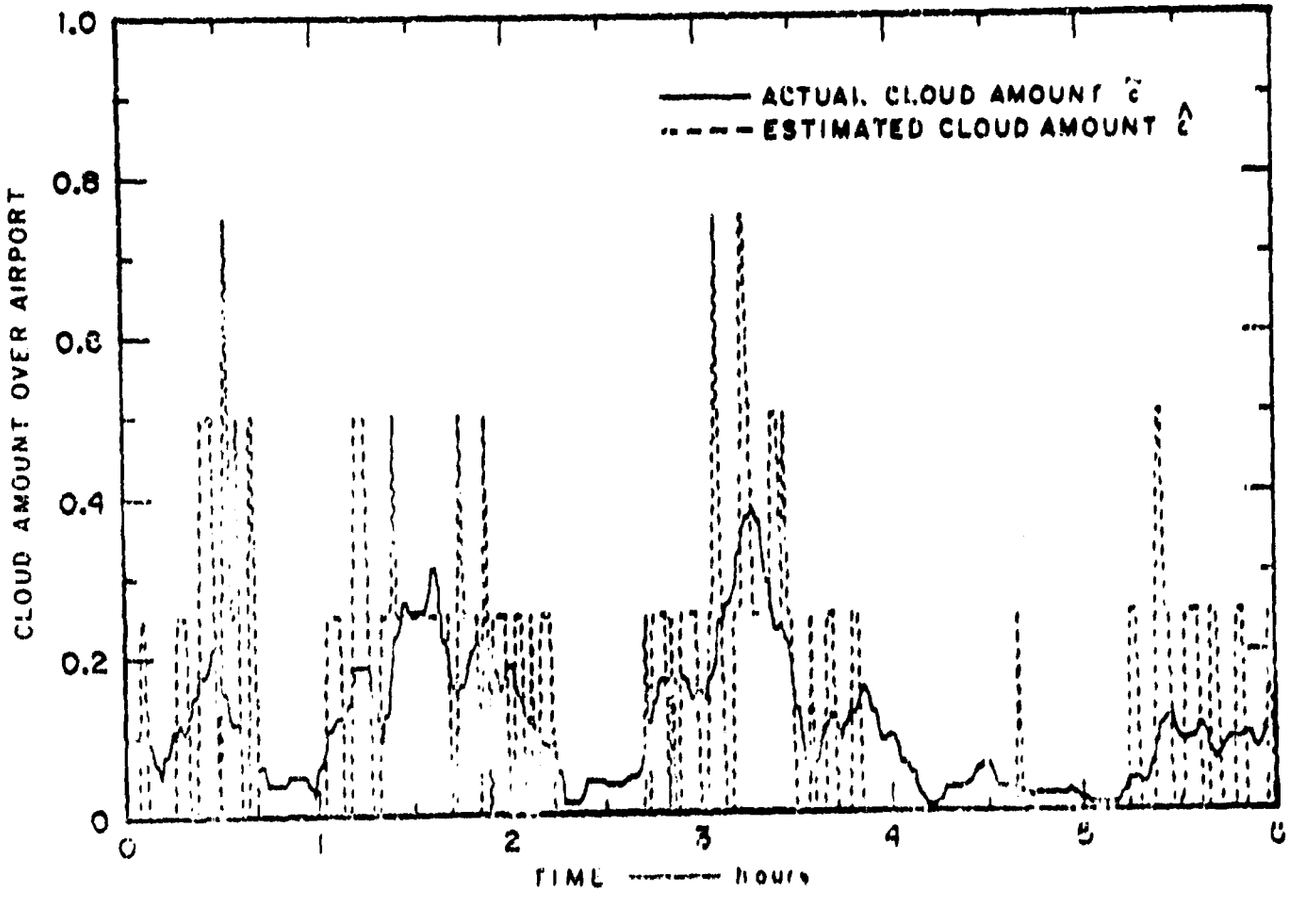

FIGURE 6 INSTANTANEOUS CLOUD AMOUNT ESTIMATED BY FOUR INSTRUMENTS

where

$$u = \sqrt{A}/L_n \quad , \tag{13}$$

and

$$\beta = e^{-\frac{2u}{u+1}} \quad . \tag{14}$$

Thus, for this case the expected squared error depends only on the number n of instruments and the normalized area A/L_n^2. For applications, it is interesting to ask how many instruments are needed to obtain a given expected squared error. When Eq. (12) was solved numerically for n as a function of β and $\sqrt{A}/L_n$, the results shown in Figure 6 were obtained. In this graph n is treated as a continuous variable, although, of course, only integral values make sense. The actual number of instruments needed to obtain a given expected squared error is the first integer greater than or equal to n.

Note that n is an increasing function of $\sqrt{A}/L_n$. If $\sqrt{A}/L_n = 0$, error-free performance can be obtained with only one instrument. As $\sqrt{A}/L_n$ approaches infinity, the number of instruments needed approaches $1/4\,\beta^2$; this corresponds to the formula

$$E[(\hat{c}(n) - c_a)^2] = \frac{c_a(1-c_a)}{n} \quad , \tag{15}$$

which is valid if the instrument readings are statistically independent.

Because Eq. (12) was derived for a special one-dimensional case, a series of twenty-four experiments were performed to see whether or not it remained valid for our more general cloud model. In all of these experiments the airport area was square, and the large-area cloud amount, c_a, was five tenths. The size of the area and the mean length of the clouds were varied to investigate the range $0.1 \le \sqrt{A}/L_n \le 25$, and the number of instruments used ranged from 1 to 4. When the area was aligned so that two sides were parallel to the direction of cloud motion, the differences between the sample mean squared errors and the value of $\beta(n)$ given by Eq. (12) were not statistically significant. When the instrument configuration was rotated 45° within the airport area, some variation in the results was observed, the greatest change

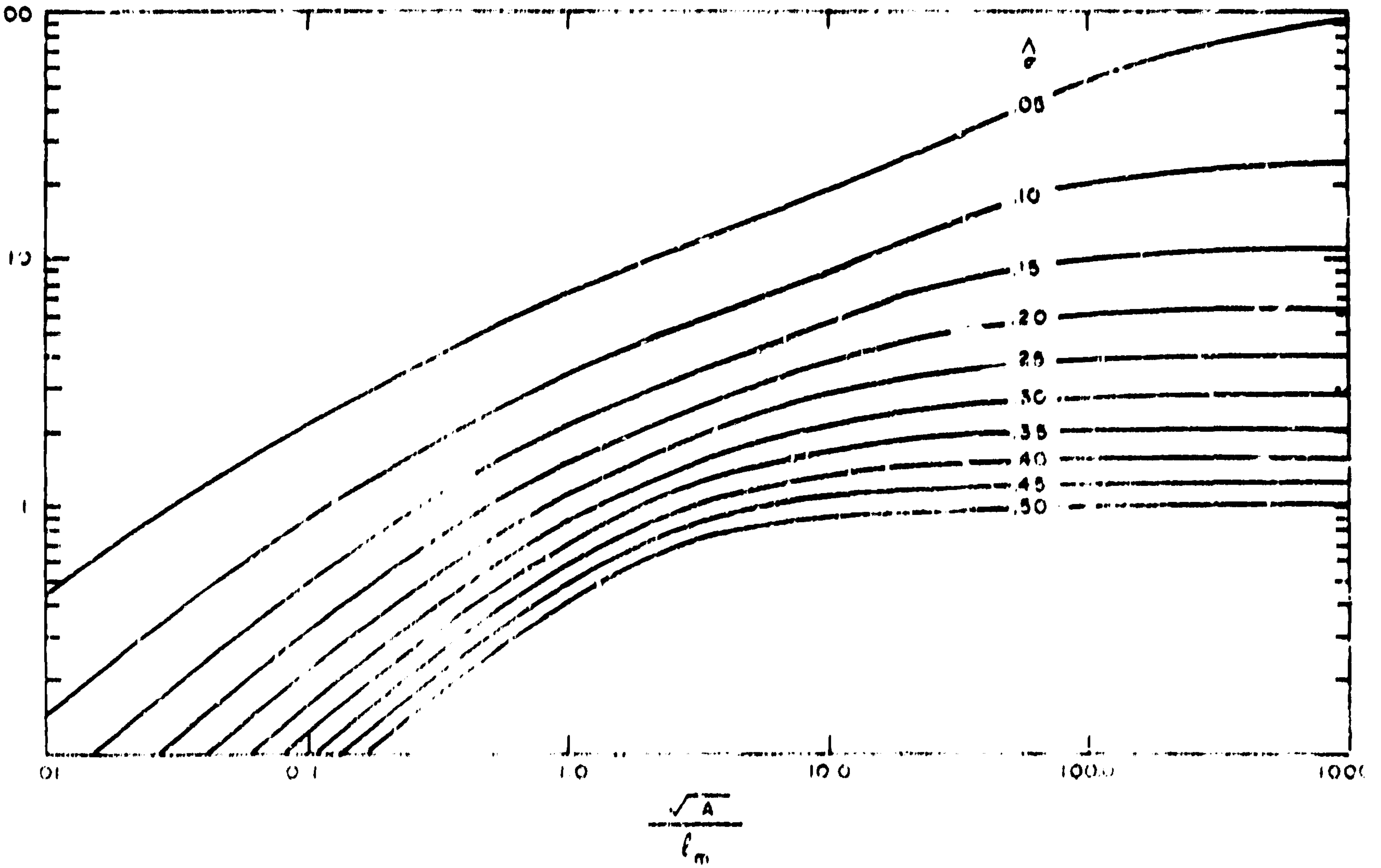

FIGURE 6 ... NUMBER OF INSTRUMENTS NEEDED TO OBTAIN A ROOT MEAN SQUARED ...

being a 20 percent increase in $\hat{\sigma}(n)$ over the theoretical value. This suggests that $\hat{\sigma}(n)$ depends on the shape and orientation of the clouds as well as their mean length. However, the general validity of the results was verified and we believe that Eq. (12) provides a good approximate solution for the general case.

3. With Time Averaging

As in the single-instrument case, the expected squared error can be reduced by forming a time average of the estimate $\hat{c}(n)$. If we let $c_k(x_i,y_i)$ denote the reading obtained from the instrument at (x_i,y_i) at the k^{th} sampling time, then the estimate of $\tilde{c}$ obtained by averaging m readings is given by

$$\hat{c}_m(n) = \frac{1}{m}\sum_{k=1}^{m}\left[\frac{1}{n}\sum_{i=1}^{n} c_k(x_i,y_i)\right]$$

$$= \frac{1}{n}\sum_{i=1}^{n}\left[\frac{1}{m}\sum_{k=1}^{m} c_k(x_i,y_i)\right] \quad . \tag{16}$$

The physical interpretation of this estimate of $\tilde{c}$ is similar to that given for a single instrument. If the clouds are moving, then each instrument is sampling the clouds along a line in plan view that goes through the instrument location and along the direction of cloud motion. If the cloud speed is V, and if the averaging extends over a time T, then the term

$$\frac{1}{m}\sum_{k=1}^{m} c_k(x_i,y_i)$$

is essentially the average of $c(x,y)$ along a line of length VT. The n-instrument estimate $\hat{c}_m(n)$ is merely the average of these estimates.

In considering the expected squared error for $\hat{c}_m(n)$, one must remember that both this estimate and the quantity being estimated, $\tilde{c}$, vary with time. Since the computation of $\hat{c}_m(n)$ involves readings during the past T seconds, $\hat{c}_m(n)$ at time t tends to be a better estimate of $\tilde{c}$ at time t-T/2 than of $\tilde{c}$ at time t. Here we see an important

distinction between needs for aviation applications and needs for general meteorological purposes, since the former is concerned with present cloud amount, while the latter can usually tolerate the delay of T/2 seconds. In our experiments, the optimum averaging time for aviation applications was found to be approximately one half the optimum averaging time for general meteorological applications. Thus, by computing two running averages over consecutive periods of duration T/2 seconds, both estimates can be provided with no more computation that that needed for general meteorological purposes alone.

In the remainder of this section we define the error to be the difference between the value of $\hat{c}_m(n)$ at time t and the value of $\tilde{c}$ at time t-T/2. Let $\hat{\sigma}_m^2(n)$ denote the expected squared error. In general, $\hat{\sigma}_m^2(n)$ is a function of all of the variables: A, n, ΔT, ℓ_m, ρ, c_a, v, ψ_c, and $t_e - t_b$. As usual, we neglect the effect of $t_e - t_b$, and to simplify the problem we take $\rho = 1$, $c_a = 0.5$, and $\psi_c = 0$. In the special case $A = \infty$, we can perform an analysis like that described in Section III-C-2. In that case, the n instruments can be located infinitely far apart, and it turns out that

$$\lim_{A \to \infty} \hat{\sigma}_m^2(n) = \frac{\hat{\sigma}_m^2}{n} \quad . \tag{17}$$

This kind of analysis is useful because it shows that the same criterion for choosing the sampling interval ΔT is valid in the n-instrument case, and thus ΔT can be eliminated from the list of variables. However, the dependence of $\hat{\sigma}_m^2(n)$ on A is of considerable interest for airport operations. Since analysis of this case is very difficult, we used the computer simulation program to investigate the behavior of $\hat{\sigma}_m^2(n)$ experimentally. In these experiments we kept $v\Delta T/\ell_m$ below 0.25, so that no appreciable improvement could be obtained by reducing ΔT.*

*For one case with $\sqrt{A}/\ell_m = 10$, we allowed $v\Delta T/\ell_m$ to reach 0.5. This is still a fairly small value, and should not have had significant influence on the results.

It was found convenient to normalize the remaining variables A, n, T, ℓ_m and v so that $\hat{\sigma}_m^2(n)$ was expressed in terms of n, $\sqrt{A/\ell_m}$, and $vT/\sqrt{A}$.

The experiments were restricted to the cases n = 1 and n = 4, $\sqrt{A/\ell_m}$ = 1,2,5 and 10, and $0 \le vT/\sqrt{A} \le 3.0$. For each of these cases, the simulation program was used to generate clouds having these statistics, and $\hat{\sigma}_m^2(n)$ was computed by computing the average of the squared error at 1080 different times.

The results of these experiments are shown in Figure 7. When $vT/\sqrt{A}$ is zero, $\hat{\sigma}_m^2(n)$ gives the standard deviation of the instantaneous (unaveraged) estimate. Thus, the ordinate intercepts of these curves give values corresponding to Figure 5. As $vT/\sqrt{A}$ is increased, $\hat{\sigma}_m^2(n)$ decreases to a minimum value, and then begins to increase again. Roughly speaking, a small amount of time averaging smooths the estimate and is beneficial, but with too much averaging, $\hat{c}_m(n)$ is unable to follow the fluctuations of $\tilde{c}$, and the error increases. If n is large and the instruments are arranged in a uniform array spaced a distance $\sqrt{A/n}$ apart, it can be argued that the optimum averaging time should be given by

$$T_0 = \frac{\sqrt{A/n}}{v} \quad , \tag{18}$$

since this is the longest averaging time that maintains the sampling within the area A. Inspection of Figure [illegible] shows that the optimum averaging [illegible] is generally larger than T_0 [illegible] ℓ_m [illegible]. This is probably because some [illegible] helps to make up for the lack of information at [illegible] within A. In any event, it is clear that the choice of [illegible] is not critical. This is fortunate, since one may [illegible] the averaging to changes in the cloud speed, and may have to accept a fixed averaging time. In addition, it should be kept in mind that these results are for a statistically uniform case, and the averaging time should never be allowed to become so long that the system is unable to respond to the onset of a new weather condition.

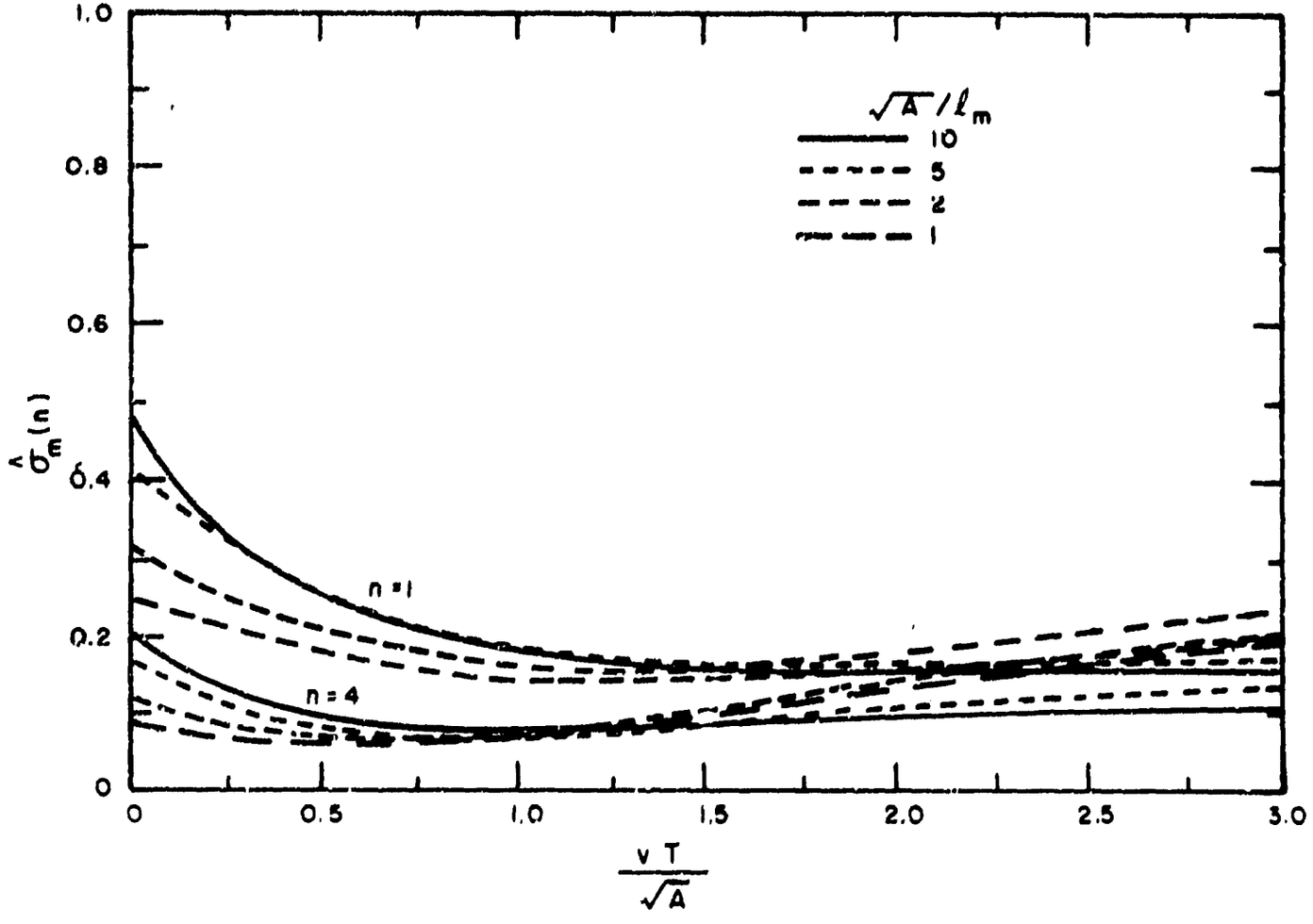

FIGURE 7 VARIATION OF ROOT MEAN SQUARE ERROR WITH AVERAGING TIME

In general, $\hat{\sigma}_m(n)$ depends on both $vT/\sqrt{A}$ and $\sqrt{A}/\ell_m$. If we choose T to minimize $\hat{\sigma}_m(n)$ and let

$$\hat{\sigma}_{min}(n) = \min_{vT/\sqrt{A}} \hat{\sigma}_m(n) \quad , \tag{19}$$

then $\hat{\sigma}_{min}(n)$ can be significantly less than $\hat{\sigma}(n)$, the root-mean-square error without averaging. The amount of improvement depends on $\sqrt{A}/\ell_m$. As $\sqrt{A}/\ell_m$ approaches zero, the optimum averaging time approaches zero, and no improvement can be obtained. On the other hand, as $\sqrt{A}/\ell_m$ approaches infinity, $\hat{\sigma}^2(n)$ approaches $c_a(1 - c_a)/n$, whereas $\hat{\sigma}_{min}(n)$ approaches zero. Since $\hat{\sigma}_{min}(n)$ also approaches zero as $\sqrt{A}/\ell_m$ approaches zero, it follows that $\hat{\sigma}_{min}(n)$ must reach a peak at some intermediate value of $\sqrt{A}/\ell_m$. The experimental results shown in Figure 7 confirm this prediction, with a maximum error near $\sqrt{A}/\ell_m = 4.0$ for $n = 1$ and near $\sqrt{A}/\ell_m = 10.0$ for $n = 4$.

These results make it clear that the instrument requirements suggested by Figure 6 are pessimistic. By averaging, one can obtain the same performance with fewer instruments. In particular, Figure 8 shows that a root-mean-square error of 0.17 or less can always be obtained with one instrument, and 0.085 or less can always be obtained with four instruments. Assuming that $\hat{\sigma}_{min}^2(n)$ varies inversely with n, we obtain the instrument/performance curve shown in Figure 9. This represents the best performance that can be obtained with a set of n ideal vertically-pointing instruments.

E. Scanning Instruments

An ideal scanning instrument measures the range r from the instrument to the intersection of its line of sight with a cloud. By changing the azimuth angle ϕ and the elevation angle θ, many ceiling height measurements can be obtained from a single instrument (see Figure 10). The basic sampling problem is to determine the number of values of θ and ϕ that are necessary to obtain a given performance.

In the case of a single cloud layer, one scanning instrument is equivalent to a number of vertically-pointing instruments. If the base height is h, and if the i^{th} range reading is taken at elevation θ_i and azimuth ϕ_i, then the equivalent vertically-pointing instruments are

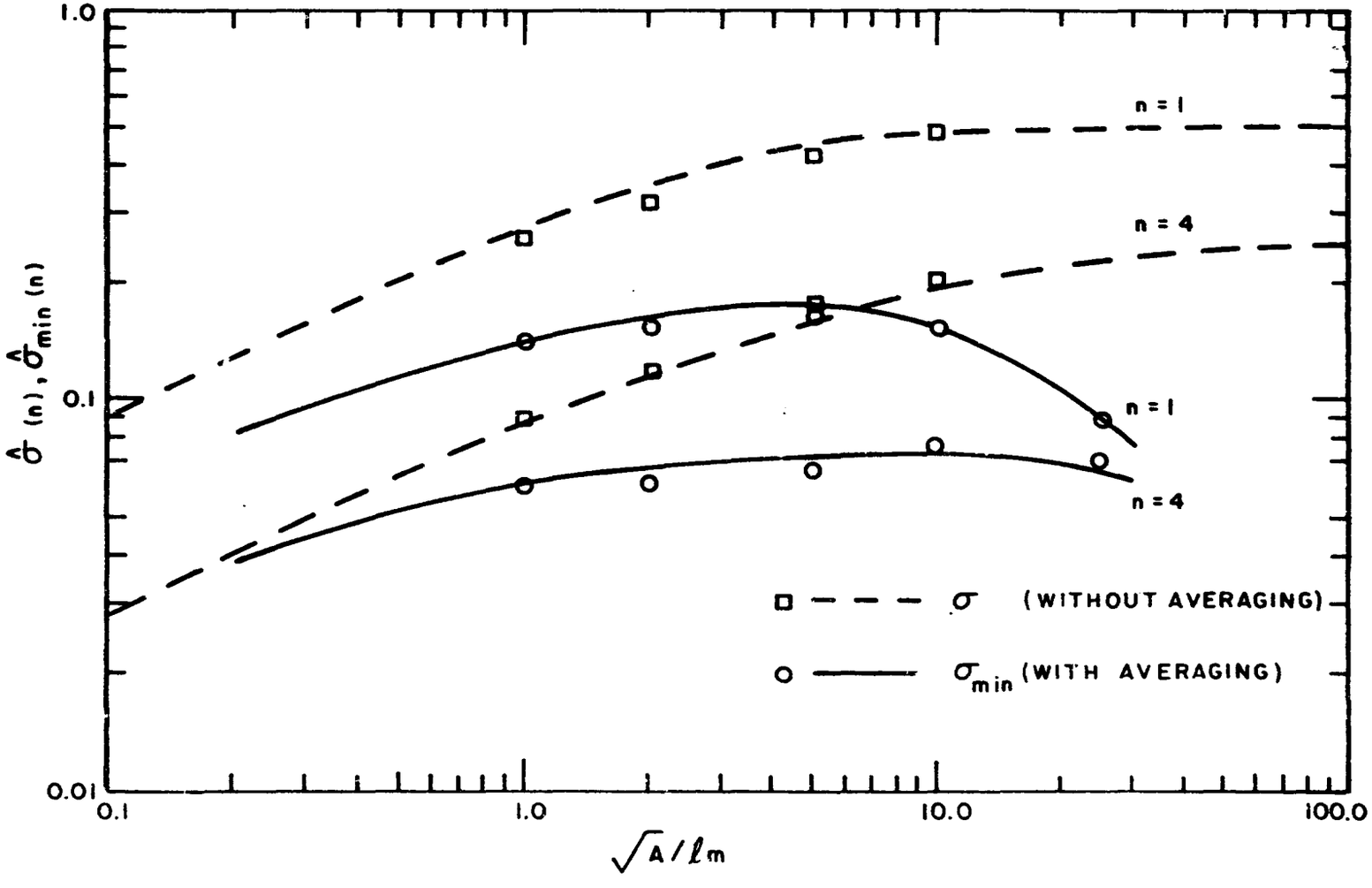

FIGURE 8 REDUCTION OF ROOT MEAN SQUARE ERROR BY OPTIMUM AVERAGING

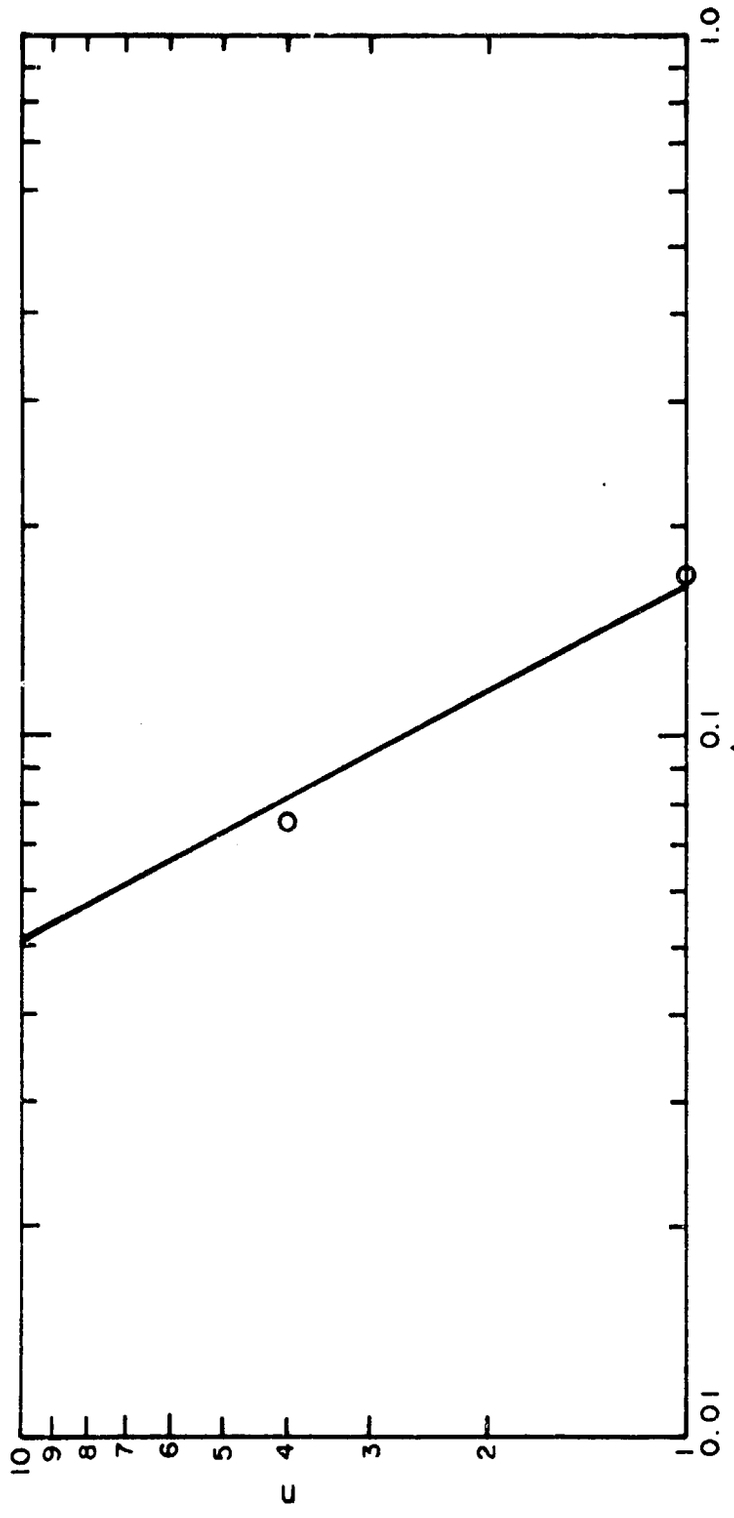

FIGURE 9 REQUIRED NUMBER OF INSTRUMENTS USING OPTIMUM AVERAGING

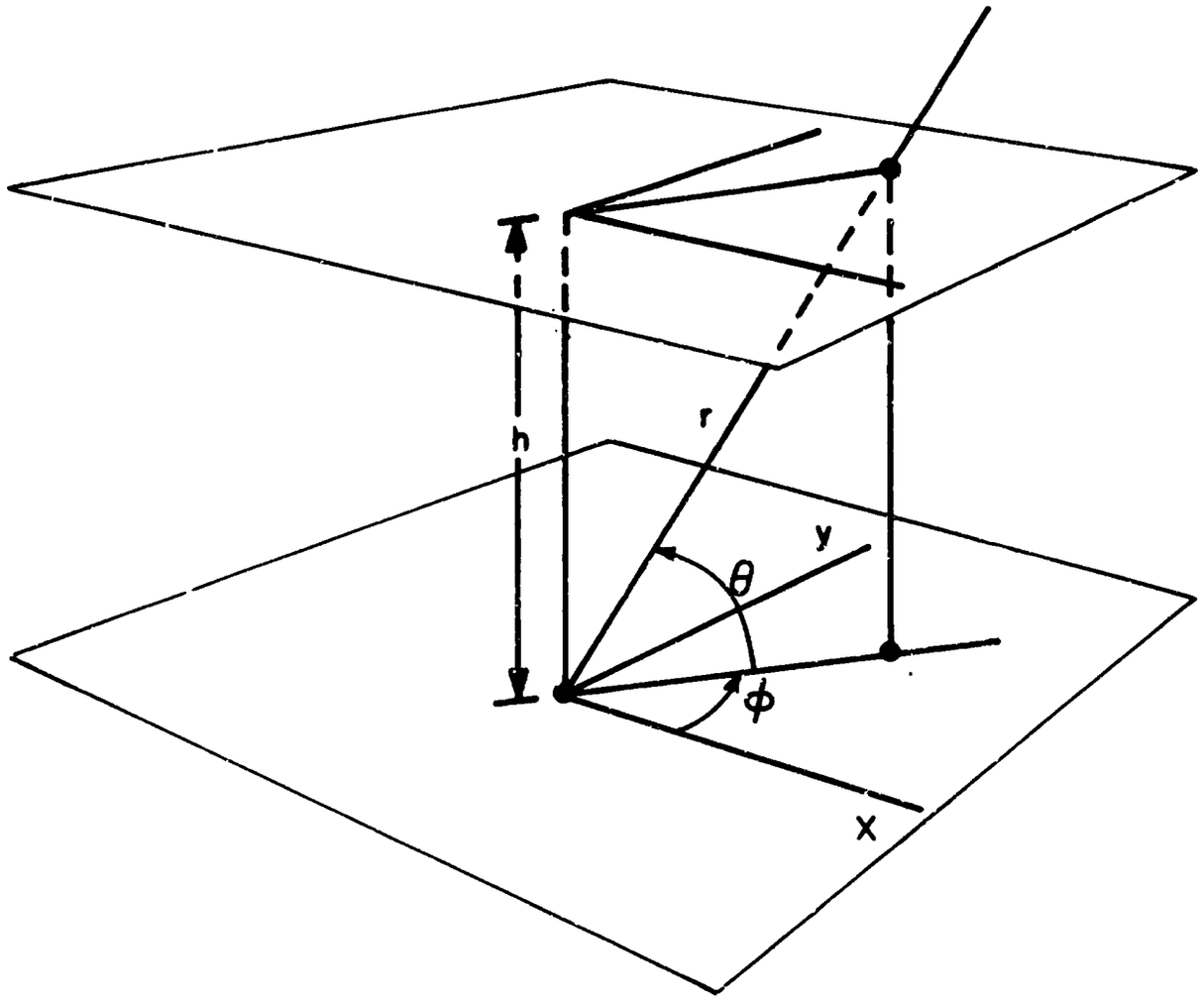

FIGURE 10 GEOMETRY FOR A SCANNING INSTRUMENT

located at

$$x_i = h \frac{\cos \phi_i}{\tan \theta_i} \tag{20}$$

and

$$y_i = h \frac{\sin \phi_i}{\tan \theta_i} \quad . \tag{21}$$

Thus, the equivalent instrument locations vary with the height of the cloud layer. If a fixed set of angles θ_i and ϕ_i are used, then the equivalent instruments move away from the origin as the cloud layer rises. At high enough altitudes, the only equivalent instrument that will remain within the airport area will be the one corresponding to $\theta_i = 90°$. If only those readings corresponding to equivalent instruments within the airport area are used to estimate cloud amount, then the effective number of equivalent instruments may become small for high clouds.

An even more serious problem arises when the clouds are very low and the equivalent instrument locations are near the origin. In this case a very small elevation angle must be used to get samples representing conditions some distance away, and accuracy problems become severe. Since low ceiling heights are of particular importance to aviation applications, this problem may limit the effectiveness of one scanning instrument as a substitute for several vertically-pointing instruments.

Figure 11 illustrates two different ways to choose elevation angles. In Figure 11(a) the angular increments are equal, while in Figure 11(b) the distances between adjacent samples are equal. The former method leads to simpler equipment, but results in nonuniform sampling for low cloud layers. These diagrams show scanning in a single vertical plane. Scanning in three dimensions can be done by scanning in several planes at different azimuth angles. An alternative that is a three-dimensional version of equal-increment sampling is to sample at points evenly distributed over a hemisphere. The three-dimensional version of the equal-distance case is to sample at points evenly distributed over a horizontal plane.

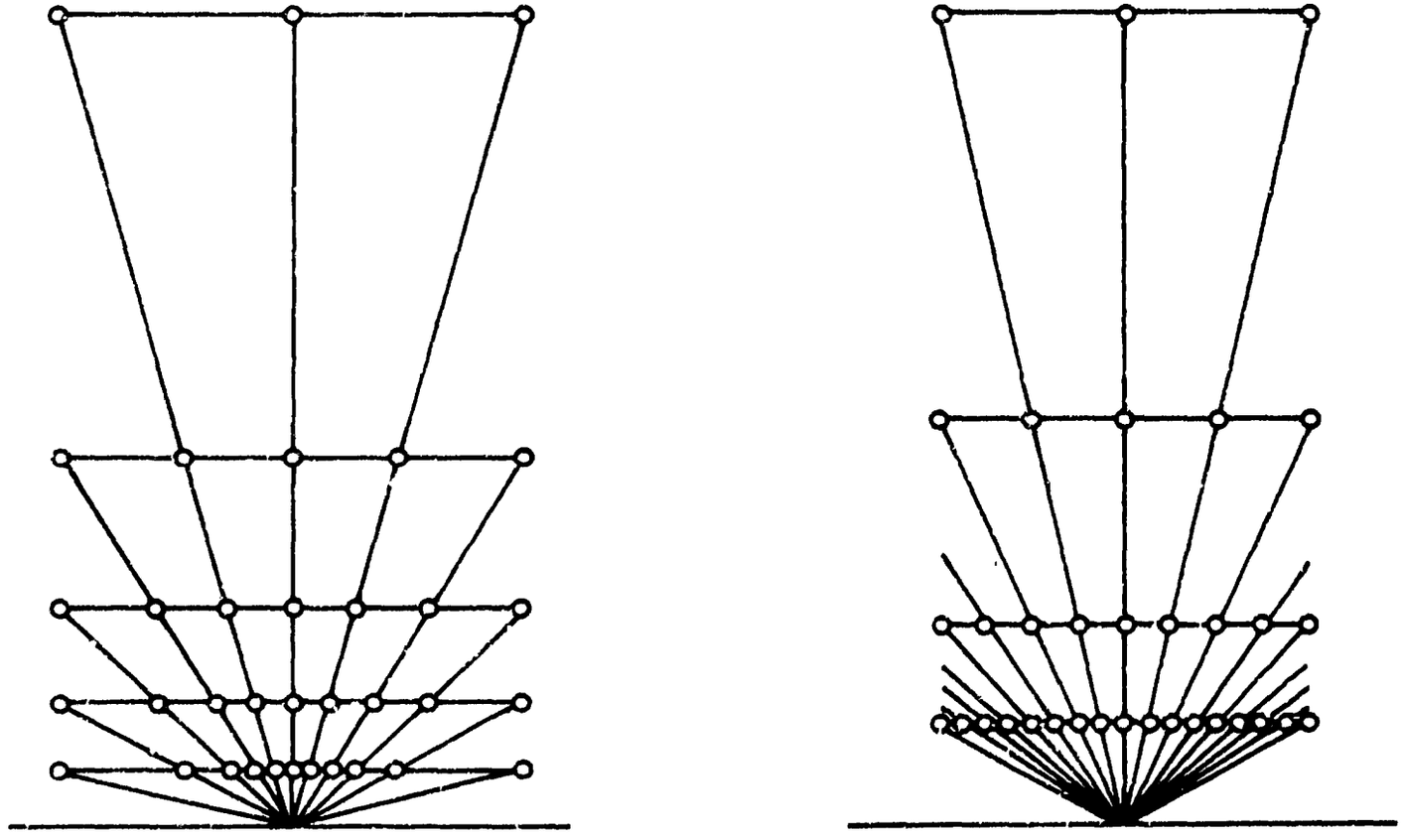

FIGURE 11 SCANNING IN A VERTICAL PLANE

The sampling requirements are most easily established when scanning is confined to a vertical plane. For the equal-increment case, the angular increment $\Delta\theta$ and the number of range readings are determined by the performance desired and the heights h_{min} and h_{max} of the lowest and highest layers of interest. By using the results of Section III-D-2, we can convert the desired performance into a specification of the number n of equivalent vertically-pointing instruments. If we let w denote the width of the airport area at the given azimuth angle, then the requirement that at least n samples of the highest layer fall within the area leads to the condition

$$\Delta\theta \leq \frac{2}{n-1} \tan^{-1} \frac{w}{2h_{max}} \quad . \tag{22}$$

Another restriction on $\Delta\theta$ is that the samples of the lowest cloud layer of interest must include points other than those points essentially directly overhead. If we require that one sample be at the boundary of the area and another be less than w/(n-1) away, then we obtain the condition

$$\Delta\theta \leq \tan^{-1} \frac{4h_{min}/w}{n-3 - 4(n-1)(h_{min}/w)^2} \quad . \tag{23}$$

Except for the cases n=2 and n=3, this requirement is usually more restrictive than Eq. (22). For example, if n=5, w=10000 ft, h_{max} = 5000 ft, and h_{min} = 100 ft, Eq. (22) gives $\Delta\theta \leq 22.5°$, while Eq. (23) gives $\Delta\theta \leq 1.15°$. An approximate guide is that the small angle solution to Eq. (23)

$$\Delta\theta \simeq \frac{4h_{min}/w}{n-3} \qquad \text{(radians)} \tag{24}$$

determines $\Delta\theta$ unless h_{max} is so large that $4(n-1)\, h_{max}\, h_{min} > (n-3)\, w^2$ and Eq. (22) becomes dominant. Exact solutions to Eq. (23) are shown in Figure 12.

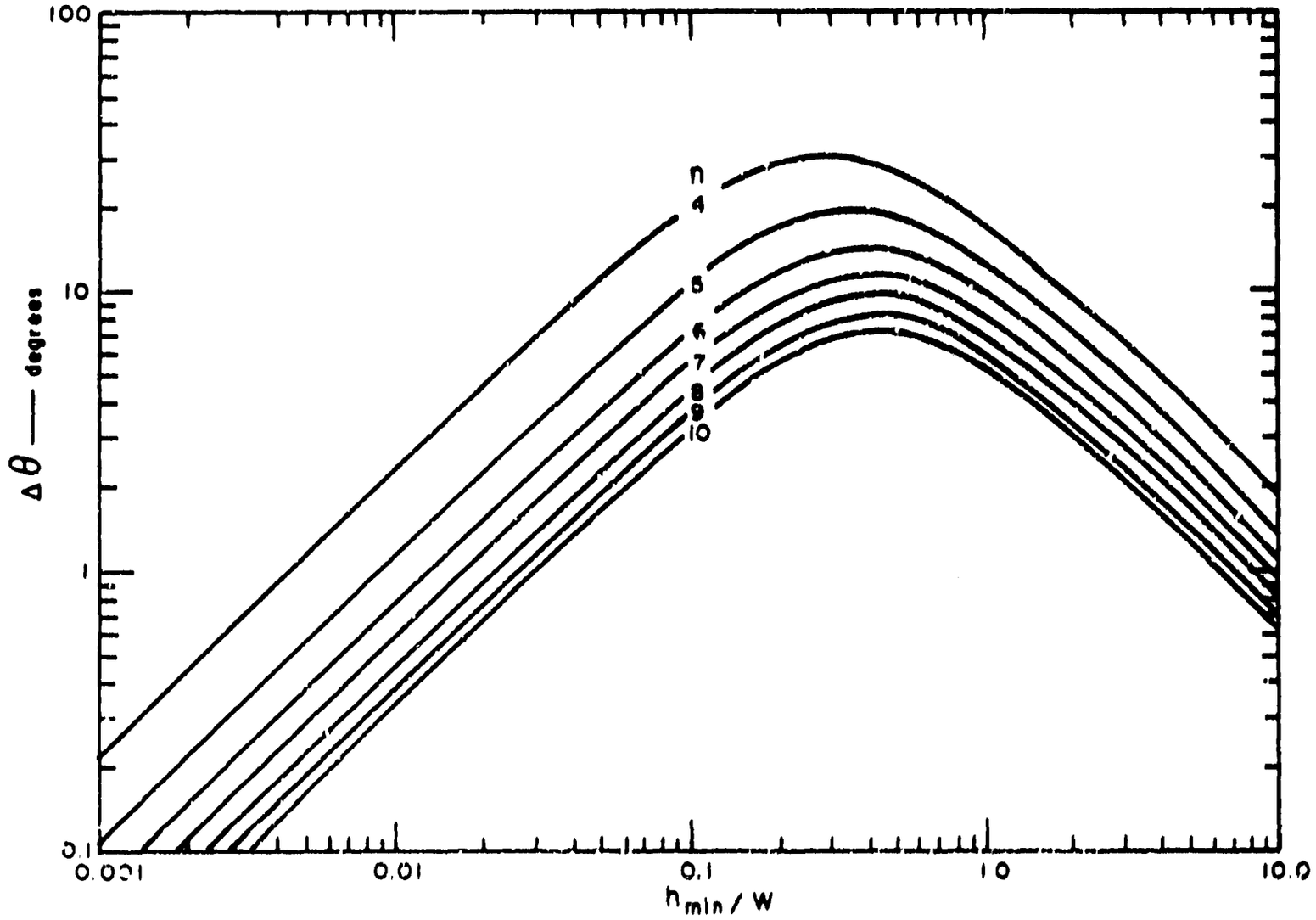

FIGURE 12 INCREMENT IN ELEVATION ANGLE REQUIRED TO OBTAIN THE SAME PERFORMANCE AS n VERTICALLY-POINTING INSTRUMENTS

These constraints place fairly severe conditions on the use of a single scanning instrument as a replacement for n vertically pointing instruments. In addition to the sampling problem, other difficulties arise when range readings at low elevation angles are attempted. These include interference by structures and personnel, atmospheric attenuation, and the effects of irregularities of the cloud base. If a single scanning instrument is to be used, it will probably be necessary to accept the fact that the effective area covered for low ceiling conditions must be reduced.

IV CLOUD BASE-HEIGHT ESTIMATION

A. Introduction

The estimation of cloud base heights introduces three new parameters, the mean base height $\bar{h}$, the base-height standard deviation σ_b, and the base-height correlation distance d. With our model, the height of the base of the cloud above a point (x,y) is assumed to be a random variable h(x,y) with mean $\bar{h}$ and variance σ_b^2. The correlation coefficient for values of h measured at two points a distance ξ apart is given by $\exp[-\xi/d]$.

The problem of base height estimation for a single layer is to estimate $\bar{h}$ from a series of readings of h(x,y). The estimation of σ_b is also of some interest, since that parameter measures the irregularity of the cloud base. However, the primary problem is to determine $\bar{h}$. An analysis for the case of a single cloud layer is given in Appendix E.

When several layers are present, the problem becomes more complicated. In this case, the problem is to separate the readings from the different layers. Once this is done, the mean base height for each layer can be estimated. In addition, the separation of readings according to layers allows the estimation of the cloud amount in layers.

The simplest of all situations is the case of a single layer of ten-tenths cloud cover. In this case, one can assume that the probability density function p(h) for a height reading h is normal:

$$p(h) = \frac{1}{\sqrt{2\pi}\sigma_b} \exp\left[-\frac{1}{2}\left(\frac{h-\bar{h}}{\sigma_b}\right)^2\right] \quad . \tag{25}$$

If we obtain n successive readings $h_1, \ldots, h_n$, then $\bar{h}$ and σ_b^2 can be estimated by computing the sample mean

$$\hat{h} = \frac{1}{n} \sum_{i=1}^{n} h_i \tag{26}$$

and the sample variance

$$\hat{\sigma}_b^2 = \frac{1}{n-1} \sum_{i=1}^{n} (h_i - \hat{h})^2 \quad , \tag{27}$$

respectively. If the readings are independently distributed according to Eq. (25), then it is well known that $\hat{h}$ converges to $\bar{h}$ and $\hat{\sigma}_b^2$ converges to σ_b^2 with probability one as n approaches infinity.

Unfortunately, this approach is not valid in all situations of interest. At least four complicating factors can arise:

(1) There may be holes in the cloud layer.

(2) There may be correlation between successive readings.

(3) There may be time variations in $\bar{h}$ and σ_b^2.

(4) There may be more than one cloud layer.

The presence of several of these factors in combination may be much more serious than their presence singly. For example, the mere presence of holes in an otherwise uniform, single layer causes no problems beyond the occasional absence of readings. Similarly, correlation between successive readings by itself presents no fundamental problem, but merely slows the convergence of $\hat{h}$ to $\bar{h}$ and $\hat{\sigma}_b^2$ to σ_b^2. The presence of both of these factors together can be more bothersome. Suppose, for example, that a hole interrupts a series of correlated readings $h_1, \ldots, h_{n-1}$ and that an n^{th} reading h_n is finally obtained. If enough time has elapsed so that h_n is essentially an independent reading, it is clear that it should receive more weight than the earlier readings, and not the equal weight provided by Eq. (26). A derivation of the optimum weighting is complicated even when simple Markov dependence can be assumed, and requires knowledge of the correlation coefficient for successive readings.

Probably the most serious combination of conditions in practice is the simultaneous presence of holes and multiple layers. While this situation can be complicated further by adding correlation and time variation, the basic problem of this combination is that one can no longer assume that h has a normal distribution. Instead, p(h) becomes a mixture of normal densities, one for each layer. To state this formally, let

L = number of cloud layers,

c_k = cloud amount for k^{th} layer,

$p_k(h)$ = probability density function for height readings for k^{th} layer,

$\bar{h}_k$ = mean cloud height for k^{th} layer,

and

σ_{hk}^2 = cloud-height variance for k^{th} layer.

We assume that c_k can be interpreted as the probability that the k^{th} layer will contain a cloud directly over the instrument, and that events in different layers occur independently. Under this assumption, the probability that the instrument sees through holes in the first k-1 layers and detects a hole in the k^{th} layer is given by*

$$P_k = \begin{cases} c_1 & k=1 \\ c_k \prod_{i=1}^{k-1} (1-c_i) & k=2,\ldots,L. \end{cases} \tag{28}$$

Then, ignoring the cases in which no cloud is detected, the law of total probability yields

$$p(h) = \sum_{k=1}^{L} p_k(h)\, P_k \quad . \tag{29}$$

This result, which shows that p(h) is a mixture of the probability density functions for each layer, is valid even if the component densities $p_k(h)$ are not normal. If no parametric assumptions can be made about the component densities, then all one can do is to estimate p(h)

---

*Note that this equation can be inverted to yield

$$c_k = \begin{cases} P_1 & k=1 \\ \dfrac{P_k}{1 - \sum_{i=1}^{k-1} P_i} & k=2,\ldots,L \quad . \end{cases}$$

However, it is the probability P_k, and <u>not</u> the cloud amount c_k, that constitutes the conventional report of cloud amount in the k^{th} layer.

and perhaps associate its modes (local maxima) with layers. If the component densities can be assumed to be normal, then the problem is to process the measurements $h_1, \ldots, h_n$ to determine the number of layers L, and the cloud amount P_k, mean base height $\bar{h}_k$, and base height variance σ_{bk}^2 for each layer. We shall consider first the case in which no parametric assumptions are possible.

B. Nonparametric Techniques for Density Estimation

Several nonparametric techniques are available for estimating probability density functions, including the Parzen window method (Parzen, 1962), the k_n-nearest-neighbor method (Loftsgaarden and Quesenberry, 1965), and the orthogonal-series method (Tarter and Kronmal, 1968). The Parzen window method is a generalization of the histogram idea, and is the simplest computationally. The k_n-nearest-neighbor method has some theoretically appealing properties, as does the orthogonal series method. However, because of their practical limitations, we shall discuss the former only briefly, and the latter not at all.

1. The Parzen Window Method

Let $h_1, \ldots, h_n$ be a set of n samples independently and identically distributed according to the unknown density p(h), and let f(u) be any function satisfying

$$f(u) \geq 0 \quad , \tag{30}$$

$$\int_{-\infty}^{\infty} f(u)\, du = 1 \quad , \tag{31}$$

and

$$\int_{-\infty}^{\infty} f^2(u)\, du < \infty \quad . \tag{32}$$

Then the Parzen window estimate for p(h) is given by

$$p_n(h) = \frac{1}{n} \sum_{i=1}^{n} \frac{1}{w_n} f\left(\frac{h-h_i}{w_n}\right) \quad , \tag{33}$$

where w_n is a parameter known as the window width. If w_n is small compared to the typical distance between adjacent samples, $p_n(h)$ is

irregular, with a local peak at each sample. If w_n is large, $p_n(h)$ is a smooth, "out-of-focus" estimate of $p(x)$. If the number of samples is fixed, one must settle for a value of w_n that gives a best compromise between an estimate that is too erratic and one that lacks resolution. If the number of samples is not fixed, one can let w_n become smaller as n gets larger, thereby gaining resolution without sacrificing stability. In theory, it can be shown that if w_n approaches zero as n approaches infinity in such a way that nw_n approaches infinity, then $p_n(x)$ converges to $p(x)$ in the mean-square sense at all points where $p(x)$ is continuous (Parzen, 1962). An example of a window width that satisfies these conditions is $w_n = w_1/\sqrt{n}$.

To see how this method might perform in practice, we used the model to generate ceiling height data for a three-layer problem having the following parameter values:

Layer	c_i	P_i	$\bar{h}_i$(m)	σ_{bi}(m)
1	.333	.333	500	20
2	.500	.333	600	20
3	1.000	.333	640	20

A sample of 180 readings taken at one-minute intervals is shown in Figure 13. The lower layer at 500 meters is clear to the eye, but it is harder to discriminate between the upper two layers. When these data were used with a rectangular window function, $f(u) = 0.5$ for $-1 \leq u \leq 1$ and zero elsewhere, and with $w_n = 100/\sqrt{n}$, the results shown in Figure 14 were obtained. (For clarity, the curves for successive values of n are displaced along the ordinate.) Note that the lower mode becomes visable after 30 samples, but even after 180 samples the structure of the data is not clear.

The use of a triangular window function, $f(u) = 1-|u|$ for $-1 \leq u \leq 1$ and zero elsewhere, gave curves having a smoother appearance (see Figure 15), but again the trimodal structure was not clearly revealed. Considerable improvement was obtained by fixing the window width at $w_n = 25$ meters (Figure 16) and by adding readings from two

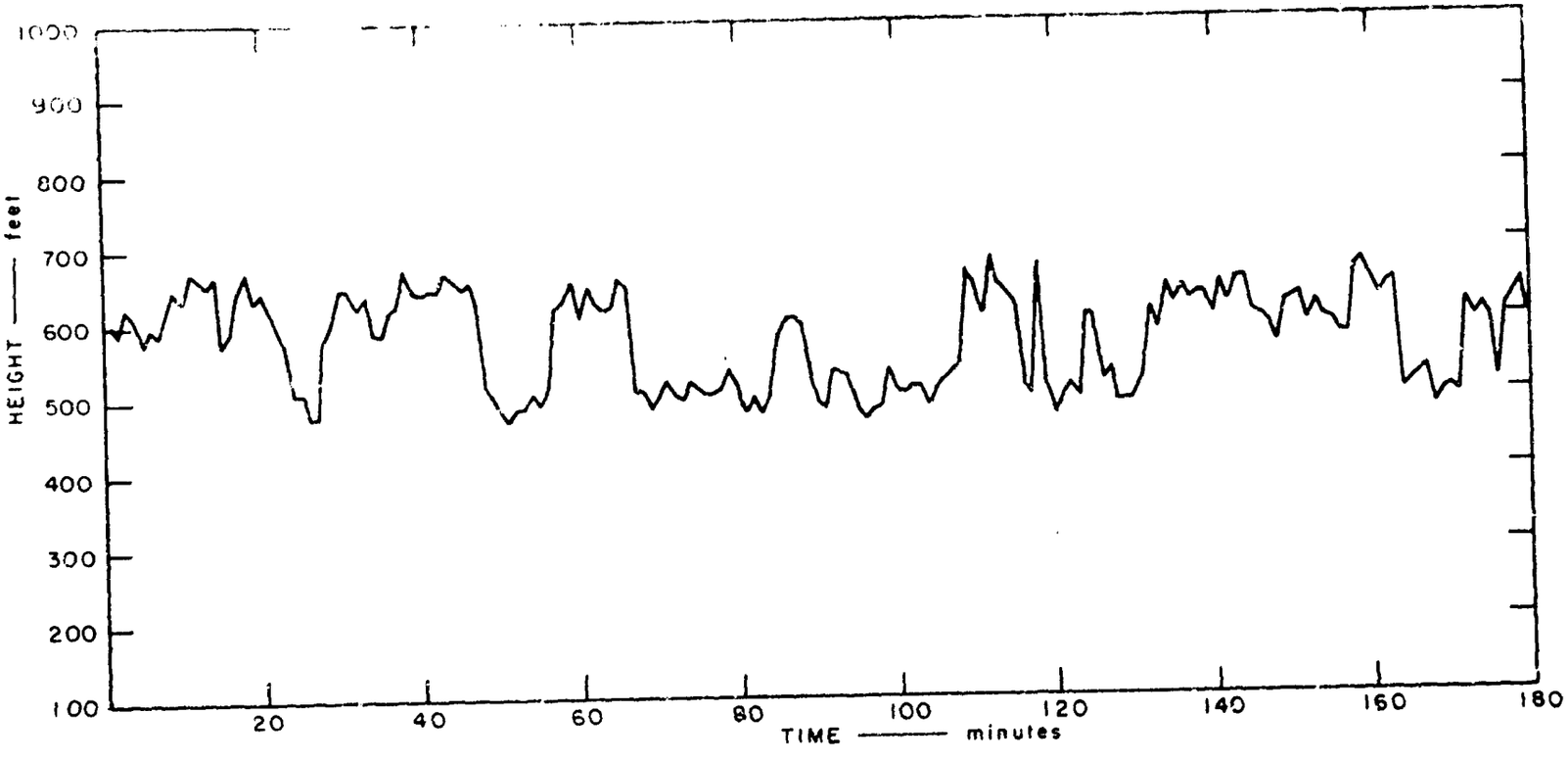

FIGURE 13 MODEL CEILING-HEIGHT DATA FOR A THREE-LAYER CASE

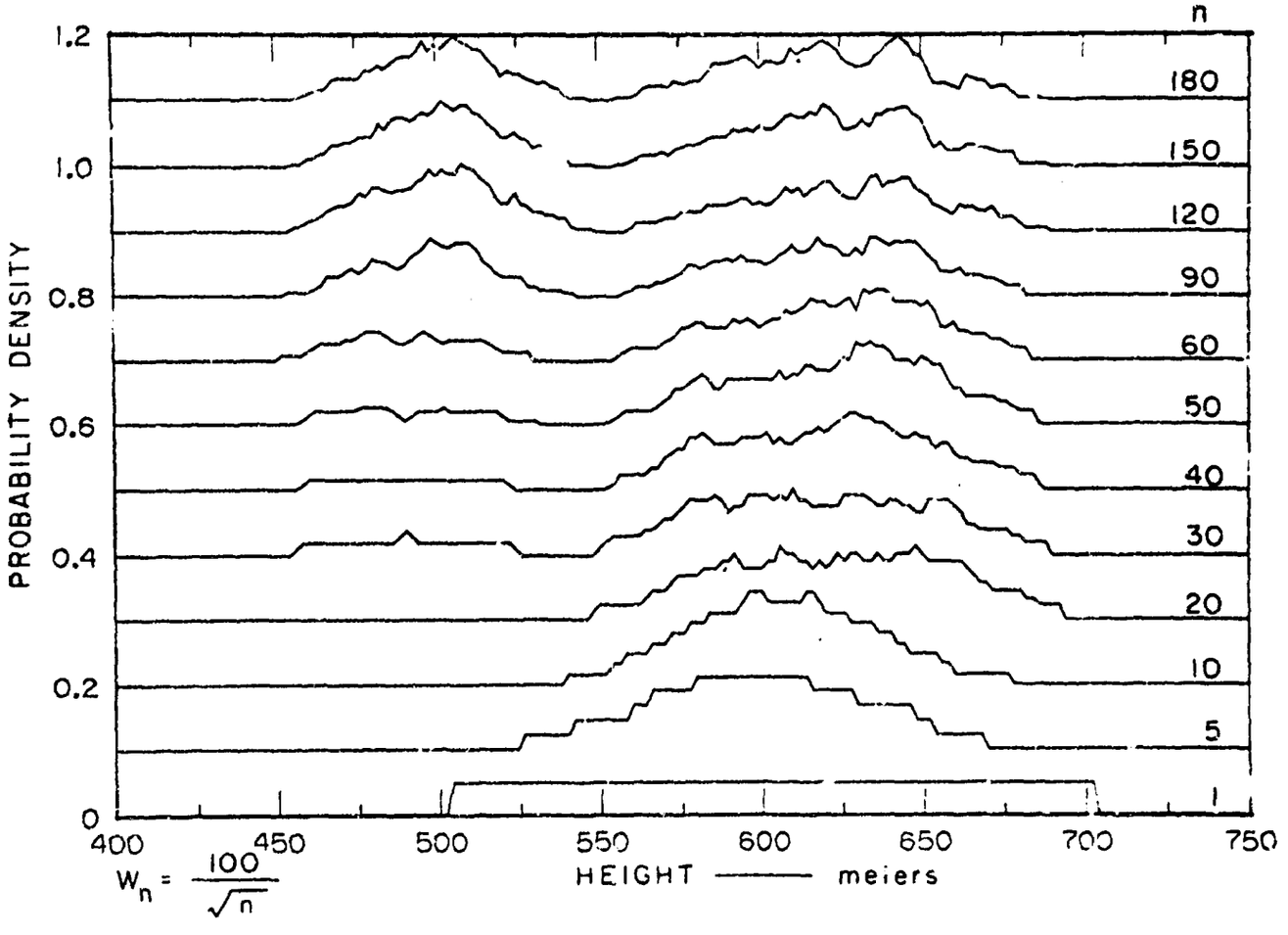

FIGURE 14 PARZEN WINDOW ESTIMATES USING A RECTANGULAR WINDOW

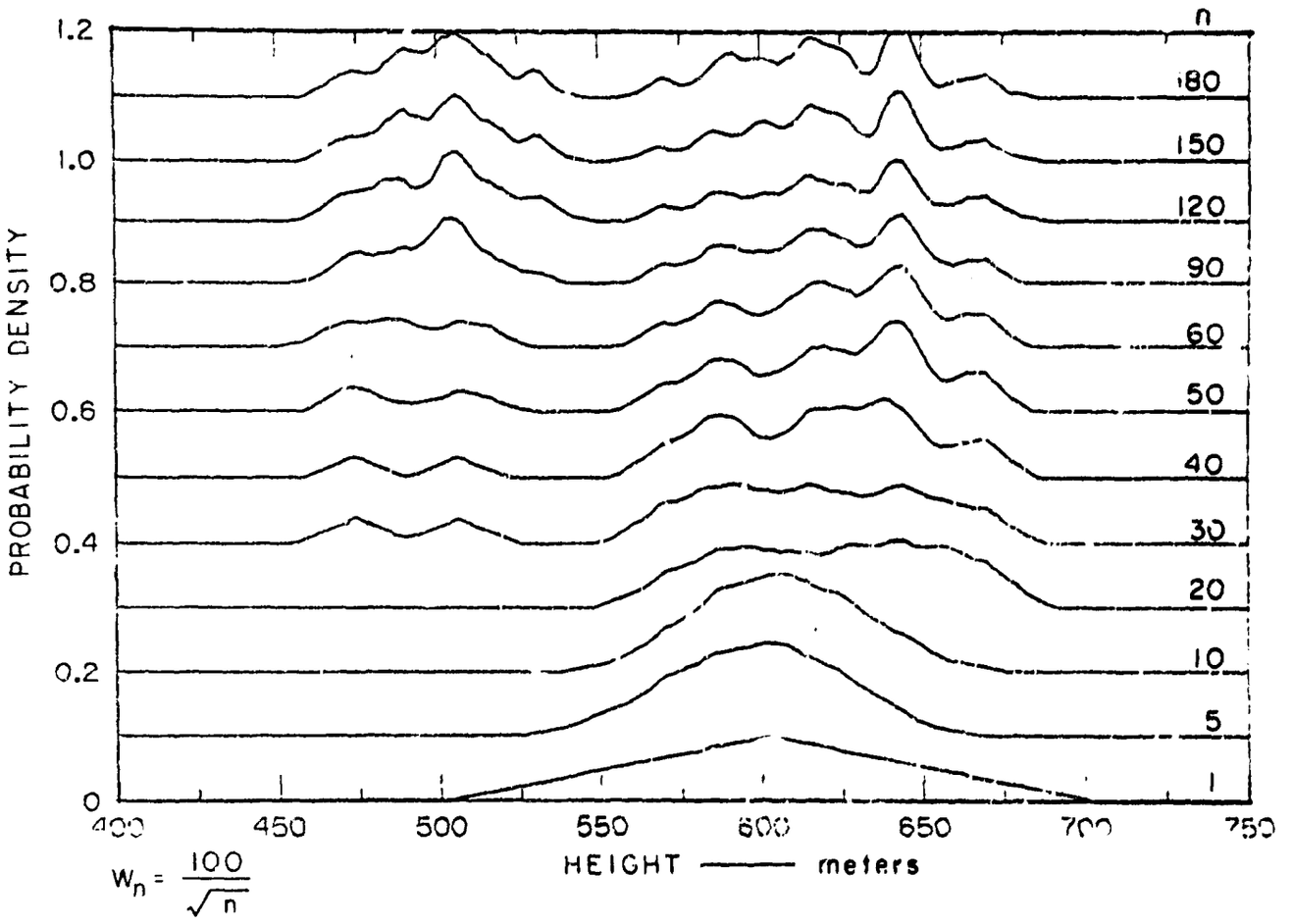

FIGURE 15 PARZEN WINDOW ESTIMATES USING A TRIANGULAR WINDOW

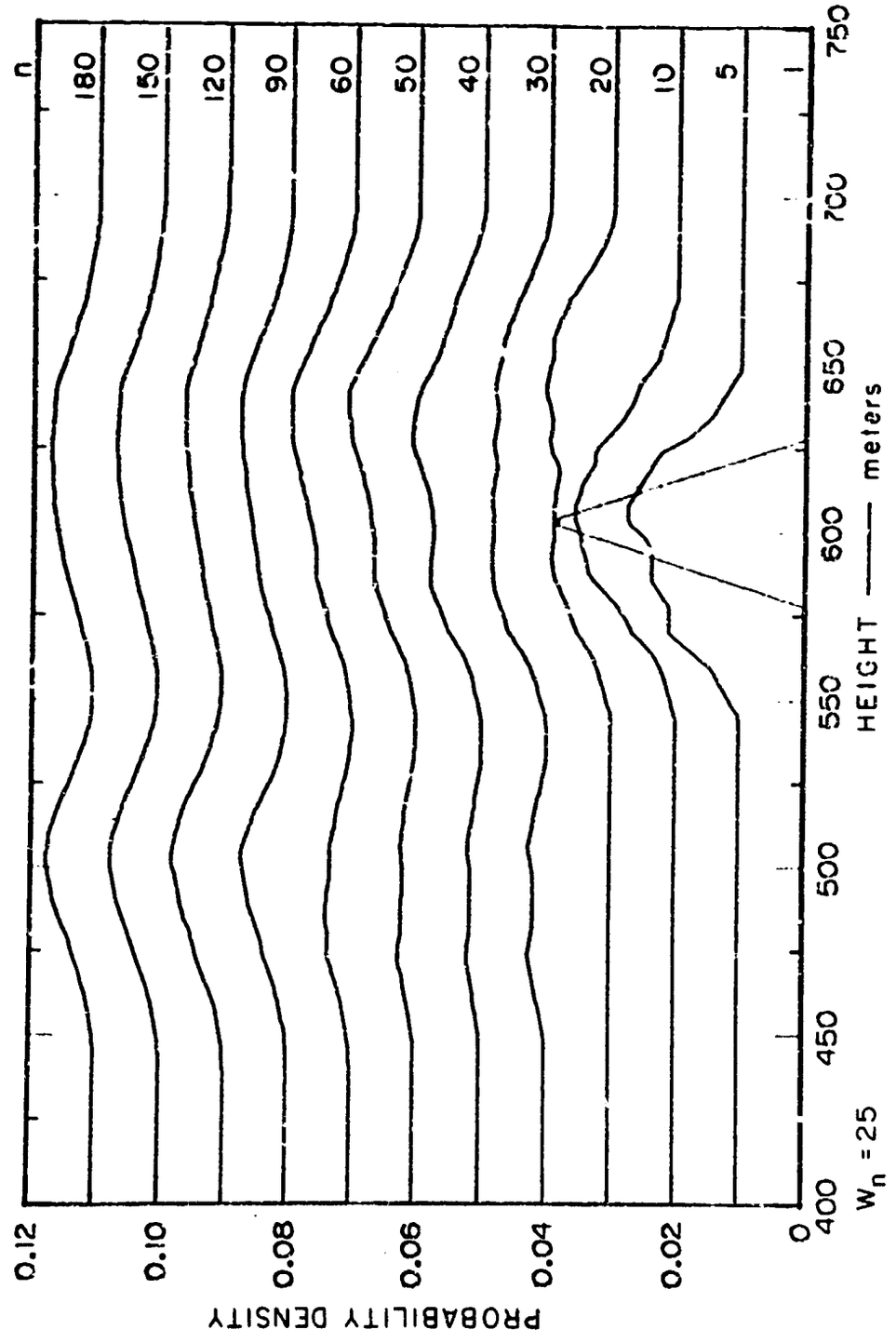

FIGURE 16 EFFECT OF FIXING THE WINDOW WIDTH

other simulated instruments (Figure 17). Under these conditions, the lower layer at 500 meters could be separated reliably from the upper two layers, but it was impossible to separate the upper layers by inspection. This last result could have been anticipated by the fact that the sum of two normal densities whose means differ by two or less than two standard deviations has only one local maximum.

2. The k_n-Nearest-Neighbor Method

The Parzen window method has been criticized on the grounds that the results obtained for finite n depend so strongly on the choice of the window function f(u) and the window width w_n. The k_n-nearest-neighbor method avoids this arbitrariness. To estimate p(h) at a particular value of h, one finds the k_n samples nearest to h, where k_n is a specified function of n, usually $\sqrt{n}$. Of these k_n nearest neighbors, let h′ be the sample farthest from h. Then the k_n-nearest-neighbor estimate is

$$p_n(h) = \frac{k_n/n}{2|h-h'|} \quad . \tag{34}$$

It can be shown that if k_n approaches infinity as n approaches infinity in such a way that k_n/n approaches zero, then $p_n(h)$ converges to p(h) in probability at all points where p(h) is continuous (Loftsgaarden and Quesenberry, 1965). Thus, the k_n-neighbor-method is a conceptually simple, convergent, general nonparametric method for estimating density functions. Unfortunately, when the k_n-nearest-neighbor method was programmed, the computation of $p_n(h)$ turned out to be quite time-consuming, and the results obtained had no evident advantage for ceiling-height estimation. Figure 18 shows the k_n-nearest neighbor estimate of p(h) based on the data of our previous example. While modes can be found by finding height intervals for which p(h) exceeds some threshold, nearly the same results can be obtained with the Parzen-window method with considerably less computation.

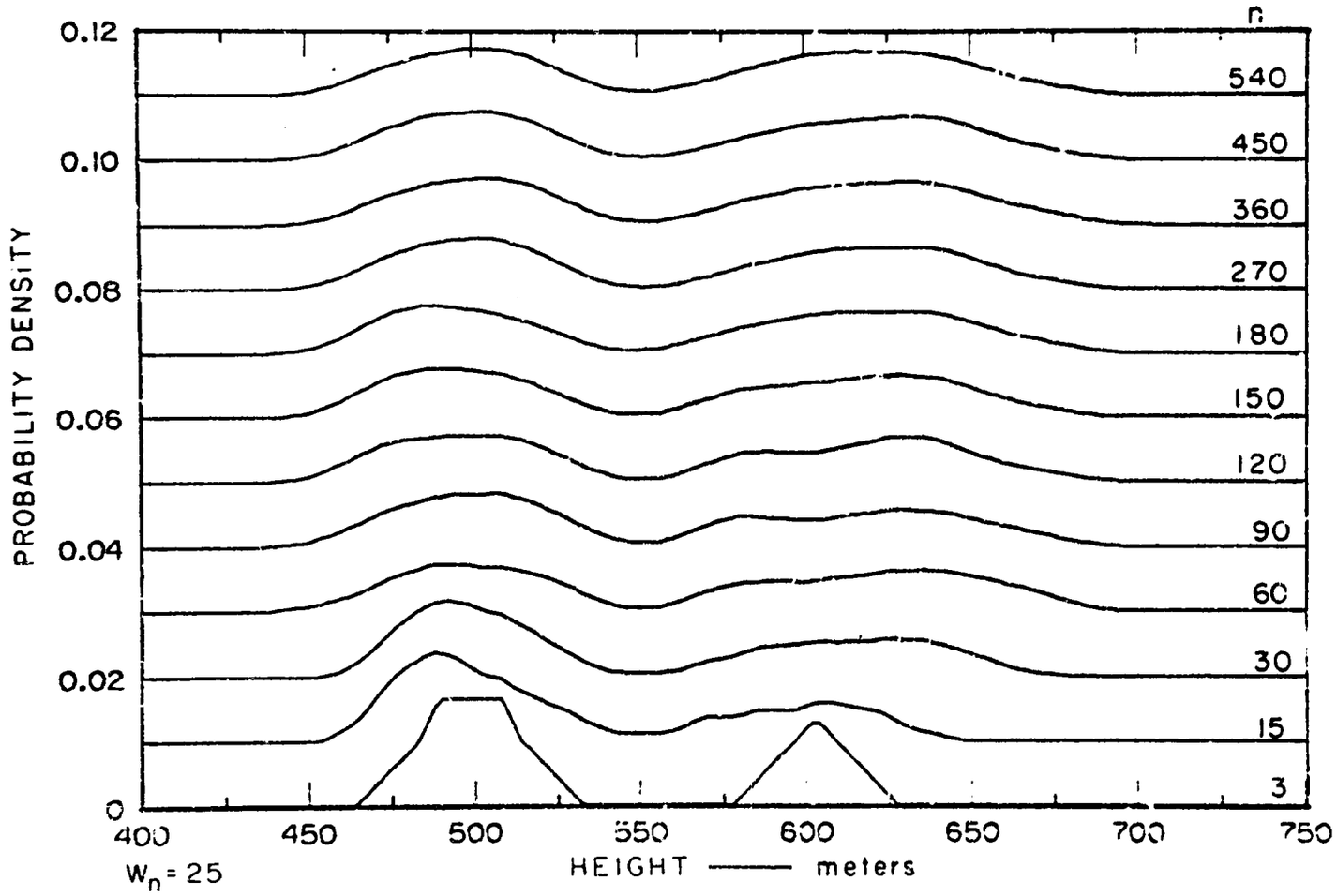

FIGURE 17 EFFECT OF USING THREE INSTRUMENTS

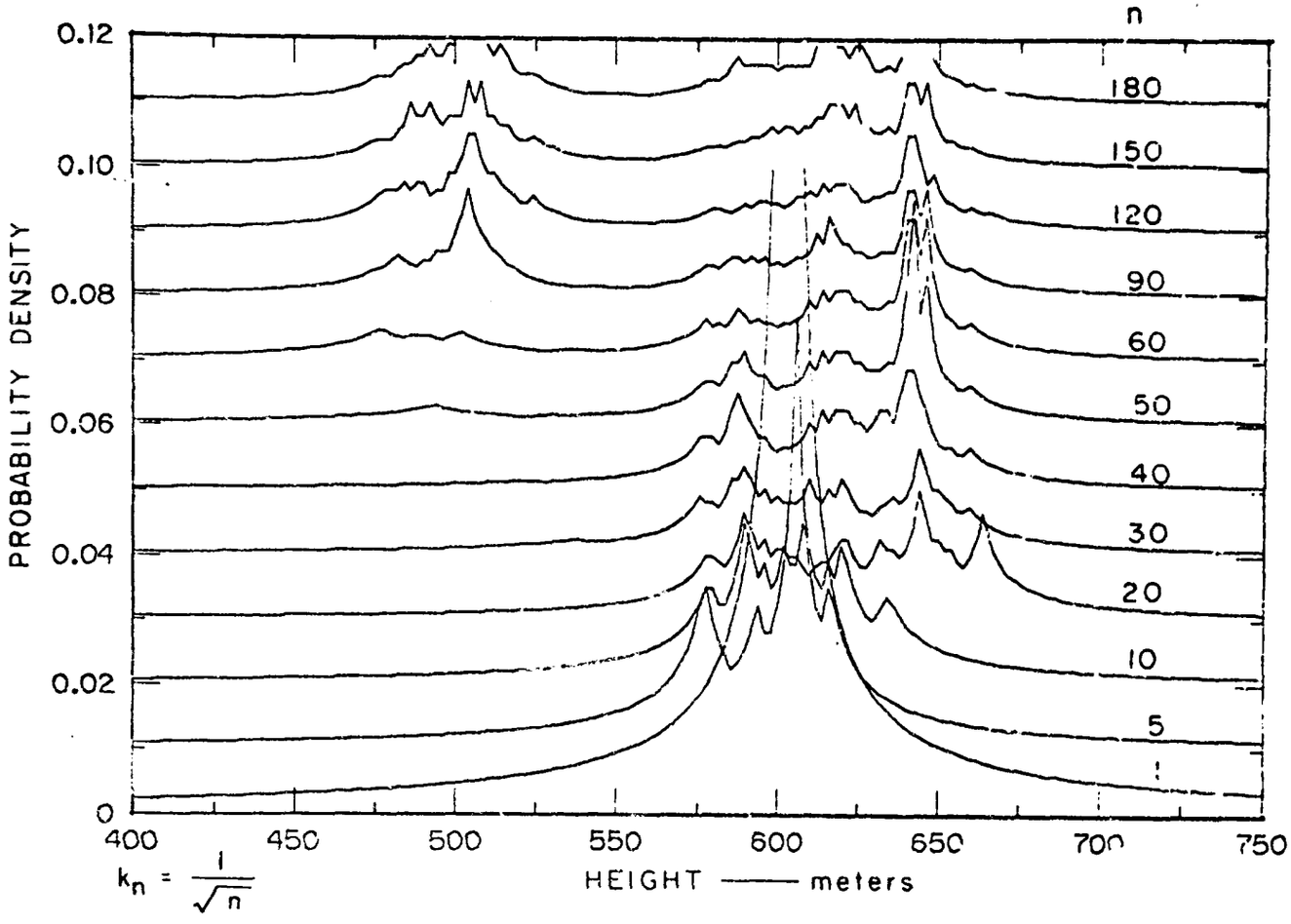

FIGURE 18 k_n-NEAREST NEIGHBOR ESTIMATE

C. Analysis of Normal Mixtures

In recent years, the problem of analyzing a mixture density

$$p(h) = \sum_{k=1}^{L} p_k(h)\, P_k \tag{29}$$

to find the component densities $p_k(h)$ and the mixing probabilities P_k has received considerable attention. Some authors have investigated the problem of extracting the component densities when the mixture density is known exactly (Medgyessy, 1961). Others have analyzed the more difficult problem where only samples drawn from p(h) are available (Stanat, 1968; Wolfe, 1970). Wolfe derives general equations for maximum likelihood estimates of the unknown parameters, assuming that the number L of components is known. In the special case where $p_k(h)$ is a normal density with mean $\bar{h}_k$ and variance σ_{bk}^2, his equations yield the following conditions on the estimates:

$$\hat{P}_k = \frac{1}{n} \sum_{i=1}^{n} \hat{P}(k|h_i) \tag{35}$$

$$\hat{h}_k = \frac{1}{n\hat{P}_k} \sum_{i=1}^{n} h_i\, \hat{P}(k|h_i) \tag{36}$$

$$\hat{\sigma}_{bk}^2 = \frac{1}{n\hat{P}_k} \sum_{i=1}^{n} (h_i - \hat{h}_k)^2 \hat{P}(k|h_i) \quad , \tag{37}$$

where $\hat{P}_k$ is the estimate of P_k, $\hat{h}_k$ is the estimate of $\bar{h}_k$, $\hat{\sigma}_{bk}^2$ is the estimate of σ_{bk}^2, and $\hat{P}(k|h)$ is given by

$$\hat{P}(k|h) = \frac{p_k(h)\, \hat{P}_k}{\sum_{j=1}^{L} p_j(h)\, \hat{P}_j} \quad . \tag{38}$$

These equations have a simple physical interpretation. $\hat{P}(k|h)$ is the probability that a height reading h came from sensing the k^{th} cloud layer. Roughly speaking, the estimate of P_k given by Eq. (35) is the fraction of readings coming from the k^{th} layer; since we never

know for sure which layer gave rise to reading h_i, the fraction is computed using the probabilities $\hat{P}(k|h_i)$. The quantity $n\hat{P}_k$ is essentially our estimate of the number of readings that came from the k^{th} layer. Thus Eqs. (36) and (37) can be interpreted as Eqs. (26) and (27) modified to account for our uncertainty as to the layer for reading h_i.

Unfortunately, the solution of these equations is complicated greatly by the fact that the unknown estimates are involved in the computation of $\hat{P}(k|h)$. Wolfe suggests some iterative procedures, but it is clear that their performance depends crucially on obtaining good initial values for the unknown quantities. If the means $\bar{h}_k$ are widely separated relative to the standard deviations σ_{bk}, then various clustering procedures can be used to obtain the initial estimates. Although these procedures are heuristic and lack demonstrably provable optimal properties, they may provide a complete practical solution to the problem.

D. Clustering

The literature on clustering is quite extensive, with a number of special procedures having been developed to meet the needs of particular problems. Excellent surveys of this work have been given by Ball (1965) and Sneath (1969). Many of these procedures can be described as iterative methods for partitioning the data to minimize a criterion function. We shall examine three such techniques that use the pooled sample variance as a criterion function.

1. The Pooled Sample Variance

Suppose that we partition our set of n samples $\{h_1,\ldots,h_n\}$ into g subsets or clusters $C_1,\ldots,C_g$. Let n_i be the number of elements in the i^{th} cluster, and define the sample mean $\hat{h}_i$ and the sample scatter $\hat{s}_i$ for the i^{th} cluster by

$$\hat{h}_i = \frac{1}{n_i} \sum_{h \in C_i} h \tag{39}$$

and

$$\hat{s}_i^2 = \sum_{h \in C_i} (h-\hat{h}_i)^2 \quad , \tag{40}$$

respectively. The pooled sample scatter $\hat{s}_p^2$ and the pooled sample variance $\hat{\sigma}_p^2$ for this partition of the data are defined as

$$\hat{s}_p^2 = \sum_{i=1}^{g} s_i^2 \tag{41}$$

and

$$\hat{\sigma}_p^2 = \frac{1}{n-1} \hat{s}_p^2 \quad , \tag{42}$$

respectively. The pooled sample variance is a measure of the variability associated with the partitioned data. A general goal is to find that partitioning that minimizes this criterion function.

It should be noted that the minimum value of $\hat{\sigma}_p^2$ depends on the number g of clusters. If g = n, i.e., if each measurement is a cluster, then $\hat{\sigma}_p^2 = 0$. If g = 1, then $\hat{\sigma}_p^2$ is merely the sample variance for all of the data. In general, it can be shown that the minimum value of $\hat{\sigma}_p^2$ is a monotonically nondecreasing function of the number of clusters.

2. Hierarchical Clustering

No computationally feasible solution is known for the problem of partitioning n samples into g clusters so that $\hat{\sigma}_p^2$ is minimized. (Exhaustive procedures that consider all possible groupings are not computationally feasible.) A number of heuristic methods have been suggested that seem to give good results, although the partitions obtained are not always optimal. Among the simplest of these are the so-called hierarchical clustering procedures (Sokal and Sneath, 1963; Johnson, 1967). These procedures form a sequence of clusterings starting with the original data viewed as a set of n clusters and ending with all the data in one cluster. The step from g clusters to g - 1 clusters is made by measuring a distance between all pairs of clusters and merging the closest pair. Once the members in two clusters are joined, they are never separated in subsequent steps. This greatly reduces the number of partitions that need to be considered, and leads to the hierarchical structure in the sequence of clusterings.

In the case of ceiling height data, the following hierarchical clustering scheme is very effective.

(1) Initially, order the samples so that $h_1 \leq h_2 \leq \ldots \leq h_n$. Let $g = n$, $C_i = \{h_i\}$, $n_i = 1$, and $\hat{h}_i = h_i$, $i = 1, \ldots, n$. This corresponds to n singleton clusters.

(2) Measure the $g - 1$ distances between pairs of adjacent sample means. Let $\hat{h}_j$ and $\hat{h}_k$ be the closest pair.

(3) Merge C_j and C_k. Mathematically, replace C_j by $C_j \cup C_k$ and delete C_k.

(4) Update the sample mean by replacing $\hat{h}_j$ by $(n_j \hat{h}_j + n_k \hat{h}_k)/(n_j + n_k)$.

(5) Update the counters by replacing g by $g - 1$, replacing n_j by $n_j + n_k$, and deleting n_k.

(6) If $g = 1$, stop. Otherwise, return to Step 2.

Here we have used the distance between sample means as a measure of the distance between clusters, and we have taken advantage of the one-dimensional character of the data to reduce the comparisons from the $g(g - 1)/2$ possible pairs of clusters to the $g - 1$ adjacent pairs. The computation required is very straightforward, with this description of the procedure amounting to a flow chart for the program.

Intuitively, it is clear that by combining closest clusters we are tending to partition the data so as to minimize the pooled sample variance. However, it is not hard to find examples for which the resulting clusters are not optimum. There is a simple modification of this procedure that selects clusters C_j and C_k so that the pooled sample variance after merging is minimized. If we let $\hat{\sigma}_p^2(g)$ denote the pooled sample variance before merging, then it is not hard to show that

$$\hat{\sigma}_p^2(g-1) = \hat{\sigma}_p^2(g) + \frac{1}{n-1} \frac{n_j n_k}{n_j + n_k} (\hat{h}_j - \hat{h}_k)^2 \quad . \tag{43}$$

Thus, no matter which pair of clusters we merge, $\hat{\sigma}_p^2(g-1) > \hat{\sigma}_p^2(g)$. However, we can minimize the increase in the pooled sample variance by selecting the pair of clusters for which the squared "distance"

$$d_{jk}^2 = \frac{n_j n_k}{n_j + n_k} (\hat{h}_j - \hat{h}_k)^2 \qquad (44)$$

is minimum. If all of the clusters had the same number of elements, this corresponds to selecting the pair whose sample means are closest. When the clusters have different sizes, this criterion favors the growth of the larger clusters.

To use this rule as stated, it is necessary to compute d_{jk}^2 for all $g(g-1)/2$ pairs of cluster. However, it is not hard to show that the sample means for which d_{jk}^2 is minimum are adjacent. Thus, our previous procedure will yield the minimum increase in $\hat{\sigma}_p^2$ at each step if the distances measured in Step 2 are computed by Eq. (44).

3. Hierarchical Splitting

Hierarchical clustering schemes have the disadvantage that even if one is only interested in partitioning the data into two clusters, it is necessary to consider n clusters, n-1 clusters, n-2 clusters, etc. Hierarchical splitting procedures attempt to achieve similar results by starting with the data as one cluster and repeatedly splitting clusters in two.

The first problem we face is the selection of the cluster to split. Since our goal is to partition the data so as to minimize the sum of the scatters s_i^2, it is reasonable to select the cluster for which s_i^2 is maximum. A computationally more costly alternative is to make trial splits of every cluster, selecting that cluster that ultimately yields the greatest reduction in the sum of scatters.

The second problem we face is the decision of how to split the cluster. With multivariate data, this problem is so severe that hierarchical splitting methods are rarely if ever used. However, with univariate data, such as that provided by ceiling-height measurements, an exhaustive approach can be considered. Let us consider only those partitions of clusters formed by picking a critical value h*. If the cluster to be split contains m members, then it can be partitioned into two clusters in m-1 ways. For each of these partitions we compute the sum of the two sample scatter values given by Eq. (40). The best partition is the one that minimizes this sum.

4. Nonhierarchical Splitting

With hierarchical splitting, once a boundary between two clusters is established, it is never changed. This prevents the procedure from finding the minimum-pooled-sample-variance solution when there are three or more clusters. Improved results can be obtained by readjusting all of the boundaries between clusters after each splitting. Let h_i^* be the boundary between cluster C_i and C_{i+1}, $i = 1, \ldots, g-1$. Then the splitting procedure that we investigated can be described as follows:

(1) Initially, let g*=1 and let C_1 be the entire data set.

(2) Make trial splits to find the cluster C_i for which $\hat{s}_{iL}^2 + \hat{s}_{iR}^2$ is minimum, where $\hat{s}_{iL}^2$ is the sample scatter for the left half and $\hat{s}_{iR}^2$ is the sample scatter for the right half of C_i. Let h* be the location of the boundary that best splits that cluster.

(3) Increase g* by 1 and insert h* in the sequence of boundaries.

(4) Starting at h* and working outward alternately to the left and right, adjust each boundary h_i^* to best split C_i and C_{i+1}.

(5) Repeat Step 4 until no further reduction in $\hat{\sigma}_p^2$ is obtained.

(6) If g* = g, stop. Otherwise, increase g* by one and return to Step 2.

Thus, with this procedure, all of the boundaries between clusters are adjusted until no further pairwise improvement in performance can be achieved. This still does not guarantee a minimum-pooled-sample-variance solution, but it usually results in better performance than can be obtained by hierarchical splitting.

5. Mode Seeking

Another popular class of clustering procedures is the so-called mode-seeking procedures. They include the k-means method (MacQueen, 1967), and Isodata method (Ball and Hall, 1967), and several related methods (Rogers and Tanimoto, 1960; Sebestyen, 1966). All of

these methods can be viewed as simplified versions of Wolfe's procedure for estimating the parameters of normal mixtures. The following is a typical mode-seeking procedure:

(1) Pick an initial set of g cluster centers $\hat{h}_1, \ldots, \hat{h}_g$.

(2) Partition the n samples into g clusters, with $h \in C_i$ if $|h-\hat{h}_i| \leq |h-\hat{h}_j|$ for j = 1 to g. Let n_j denote the number of samples in C_i.

(3) Recompute the $\hat{h}_i$ by Eq. (39).

(4) If the $\hat{h}_i$ are unchanged, stop. Otherwise, return to Step 2.

Compared to the hierarchical schemes described previously, this procedure has the advantage that it works with a fixed number of cluster centers. The iterative adjustment of the boundaries resulting from adjusting the sample means is much simpler than the exhaustive computation required by the nonhierarchical splitting method. However, the results obtained depend strongly on the initial set of cluster centers.

One of the best ways to find an initial set of cluster centers is to use the results of hierarchical clustering or splitting procedures. A simpler but poorer approach is to make a random selection from the set of n samples. A third approach involves the use of a parameter Δh, which is interpreted to mean the smallest allowed distance between distinct cloud layers. Letting g* denote the number of cluster centers selected at an intermediate stage, we can describe the process of finding g centers as follows:

(1) Initially set g* = 1, $\hat{h}_1 = h_1$, $n_1 = 1$, k = 1, and set $n_i = 0$ for i = 2 to g.

(2) Increase k by one. If k > n, stop; otherwise read h_k.

(3) Compute $e_i = h_k - \hat{h}_i$ for i = 1 to g*. Let $|e_m|$ be the smallest $|e_i|$.

(4) If $|e_m| < \Delta h$ or if g* = g, increase n_m by one, increase $\hat{h}_m$ by e_m/n_m, and return to Step 2.

(5) Otherwise, increase g* by one, set $\hat{h}_{g*} = h_k$, set $n_{g*} = 1$, and return to Step 2.

Clearly, this in itself is another clustering procedure. To describe it in words, it uses the first sample as a trial cluster center. As long as successive readings h_k are within Δh of the first cluster, they are just averaged in with previous readings. When a reading greater than Δh away is encountered, it forms a second cluster center. In general, a new cluster center is formed whenever a new reading is more than Δh away from all of the previous cluster centers.

One of the main advantages of this procedure is that it operates sequentially, and is well suited to processing data in real time. One can readily think of variants of this approach, in which, for example, cluster centers that have not been updated recently are deleted, or in which the updating in Step 4 is modified to give more weight to more recent readings. The chief disadvantage of this method is its dependence on the parameter Δh. If Δh is too small, too many clusters will be formed, whereas if Δh is too large the opposite will be true. When we generate data with the model, we know the value of Δh that will work. One is not so lucky with real data, and a valid evaluation of this method can only be done experimentally without foreknowledge of the data.

E. Experimental Results

To compare the density estimation and clustering techniques, a series of experiments were performed using data generated by the model and measured ceiling height data supplied to us by the National Weather Service Test and Evaluation Laboratory. The two clustering methods used were the nonhierarchical splitting method described in Section IV-D-4, and the hierarchical clustering method described in Section IV-D-2. The former was believed to represent an exhaustive method that should give the best results, while the latter was believed to represent a computationally simple method that would be an attractive candidate in practice.

1. Nonhierarchical Splitting

The nonhierarchical splitting procedure was programmed and applied to the same data used to demonstrate the Parzen window and k_n-nearest-neighbor procedures. This corresponded to a three-layer problem with layers at 500, 600 and 640 meters, each layer having a 20-meter standard deviation. The n samples were the 180 consecutive readings shown in Figure 13.

When the splitting procedure was applied, the results shown in Figure 19 were obtained. As expected, the pooled standard deviation $\hat{\sigma}_p$ decreased with the number of clusters. With all the data grouped in one cluster, the sample mean was at 572 meters and $\hat{\sigma}_p$ was 63 meters. With the data split into three clusters, the sample means were at 501, 598, and 644 meters, and $\hat{\sigma}_p$ was 16.3 meters. These sample means are quite close to the true means, but the pooled sample standard deviation is significantly less than the standard deviation for the individual layers; this is a common result of partitioning, which transfers samples far from the mean to another cluster. Of the 180 samples, 73 were in the first cluster, 53 in the second, and 54 in the third. Thus, the sample probabilities $\hat{P}_i$ for each layer were 0.406, 0.294, and 0.300. The deviations from the true values of 0.333 for each layer are not statistically significant.

While the results obtained by splitting the data into three clusters are in good agreement with the model, in practice one does not know a priori how many cloud layers exist. There are no generally accepted criteria for determining the number of clusters in a set of data. Wolfe suggests continuing the subdivision until a χ^2-test indicates that the reduction in pooled sample variance is not statistically significant (Wolfe, 1970). Ball and Hall observe that if a uniform probability density is divided into g clusters, then the pooled sample standard deviation will be reduced by a factor of g, so that one would expect at least this much improvement even in the absence of any structure in the data (Ball and Hall, 1970). They suggest that the optimum value for g is the one that minimizes $g\hat{\sigma}_p$.

This criterion fails with our data because the reduction in $\hat{\sigma}_p$ in going from one cluster to two is so great that the additional, significant improvement in going from two clusters to three is not detected. However, the criterion can also be applied incrementally by asking that the $\hat{\sigma}_p(g+1)$ obtained for g+1 clusters be less than $g\hat{\sigma}_p(g)/(g+1)$, the value one would obtain from a uniform density. Thus, to continue clustering, $\hat{\sigma}_p(2)$ must be less than $\frac{1}{2}\hat{\sigma}_p(1)$, $\hat{\sigma}_p(3)$ must be less than $\frac{2}{3}\hat{\sigma}_p(2)$, etc. An empirically derived modification of this

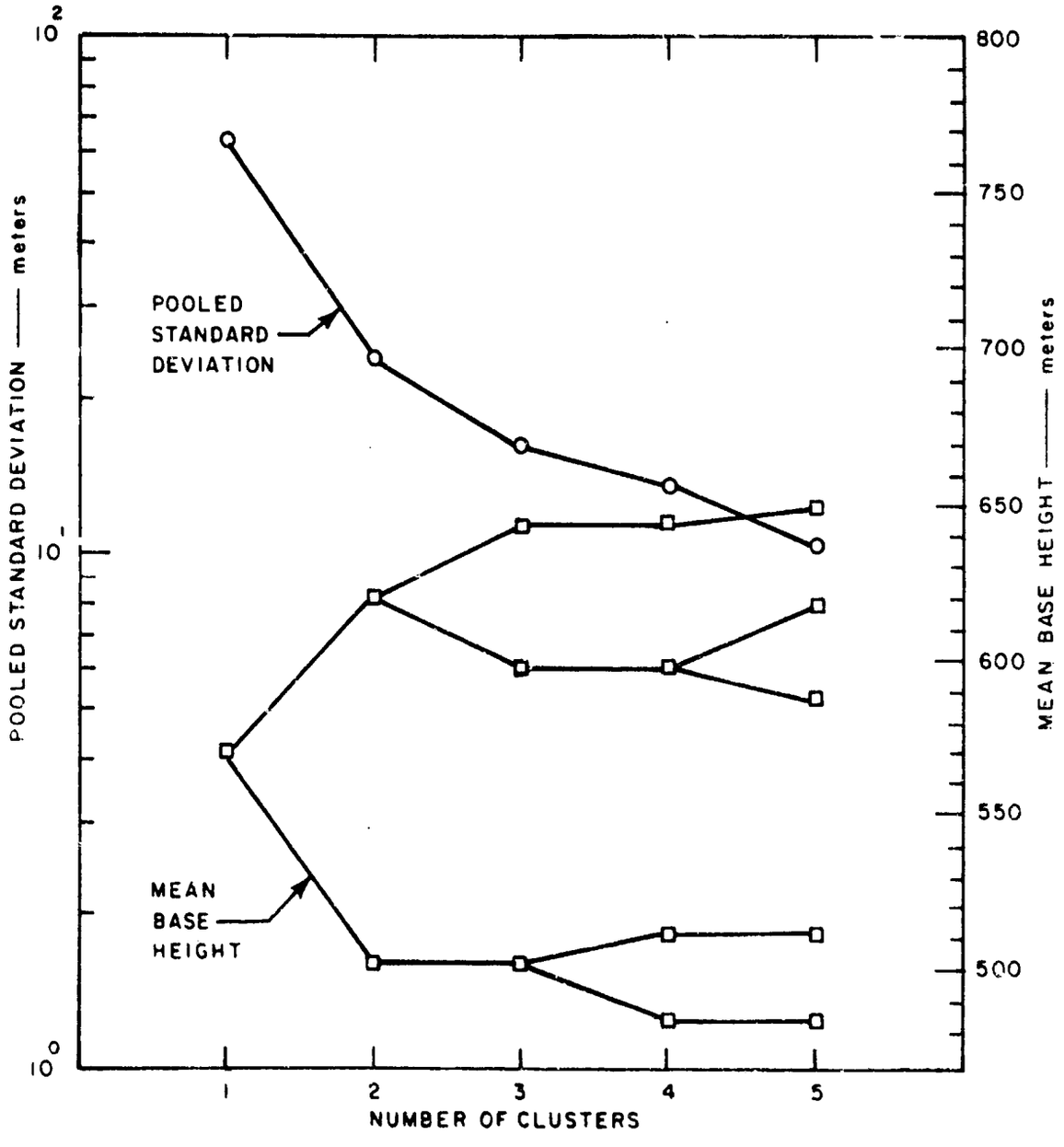

FIGURE 19 NONHIERARCHICAL SPLITTING

criterion is to ask that $\hat{\sigma}_p(g+1)$ be less than $g\,\hat{\sigma}_p(g)/(g+0.8)$. This latter criterion was successful in almost all of our experiments, and is the one we recommend.

However, it should be pointed out that in practice one might want to use other criteria, or to impose additional conditions. For example, one might insist on splitting a cluster if the sample standard deviation for samples in that cluster is too great. The simple criterion "keep splitting clusters until σ_p is less than 20 meters" also worked well with our data. Since angular inaccuracies will make ceilometer readings for high clouds more variable, one might want to make any such threshold a function of height. We mention these alternatives to point out that our study was not exhaustive, and further modifications may be needed for an actual automatic system.

2. Hierarchical Clustering

The hierarchical clustering procedure described in Section IV-D-2 was also programmed and applied to the model data. The results of this experiment are shown in Figure 20. Considering the simplicity of the technique, it is remarkable that the results are so similar to those obtained by the more exhaustive nonhierarchical splitting procedure. The pooled sample variance values are slightly higher and the sample means are slightly different, with a distinctly different four-cluster partitioning, but the overall results are essentially the same. The following table summarizes numerical values for the three-cluster solution.

i	$\hat{h}_i$(m)	n_i	$\hat{P}_i$	True Values	
				h_i(m)	P_i
1	501	73	.406	500	.333
2	604	69	.383	600	.333
3	650	38	.211	640	.333

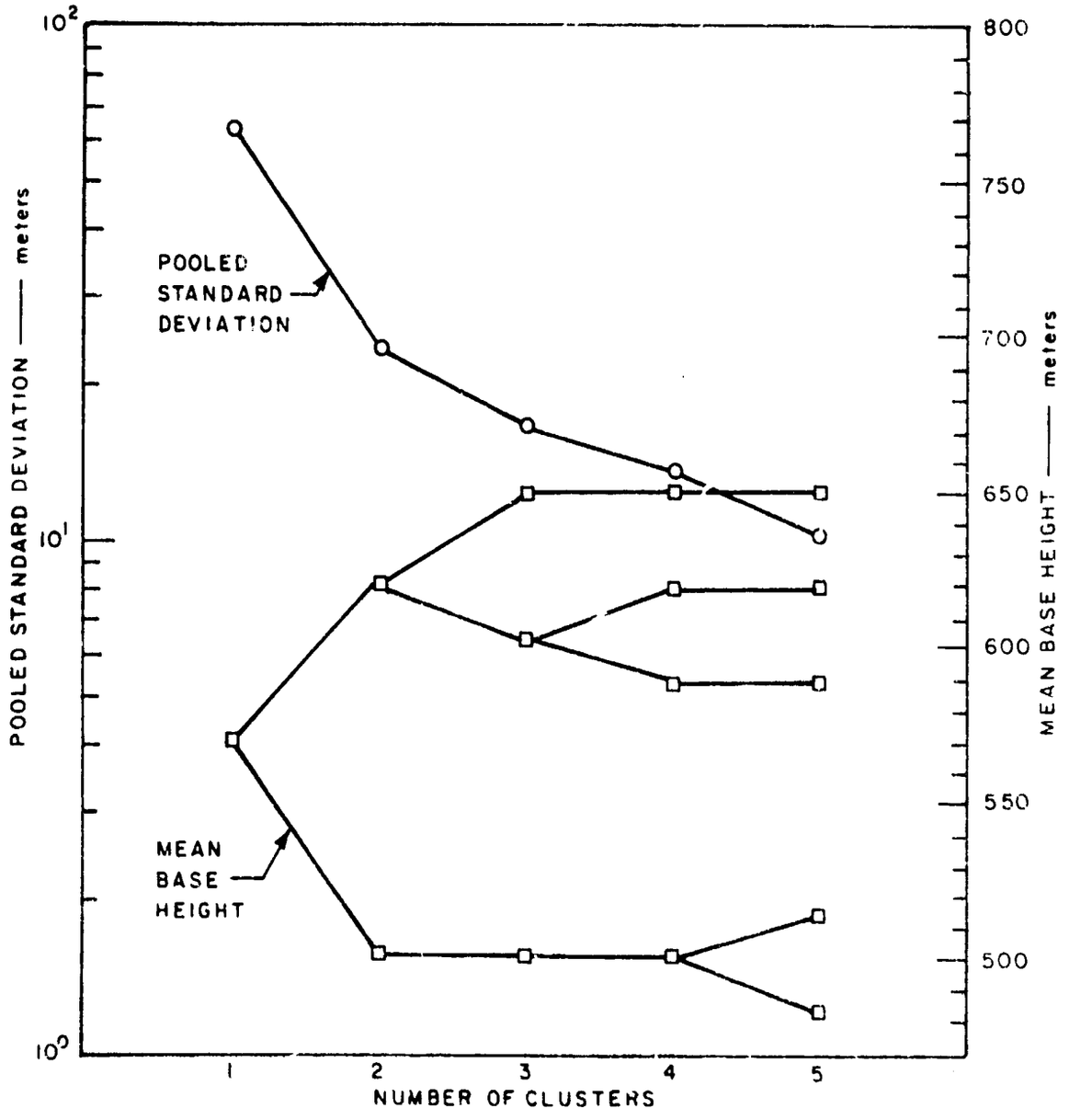

FIGURE 20 HIERARCHICAL CLUSTERING

As before, these results were obtained by clustering all 180 samples. To determine the effect of the sample size, the clustering procedure was repeated using the first 5, 10, 20, 40, 80, and 160 samples. Figure 21 shows that behavior stabilized when between 40 and 80 samples had been received. By the time 80 samples had been received, all three layers had been firmly detected. This agrees with the results of estimating the probability density function. It also makes sense with reference to Figure 13, which shows that until the twenty-fourth sample no data had been obtained from the lowest layer, and only four of the first 40 samples came from this layer.

The hierarchical clustering procedure was also applied to some measured ceiling-height data supplied to us by the National Weather Service Test and Evaluation Laboratory (Lefkowitz, 1970). We selected three data periods that seemed to show qualitatively different characteristics. Figure 22 shows the data from period 50-69 for RBC-1, a rotating-beam ceilometer with a 400-ft. baseline. Figure 23 shows more variable data from period 49-69 for RBC-3, which had an 800-ft. baseline. Figure 24 shows even more variable data from period 17-70 for RBC-1; only the primary returns, indicated by the circled data points, were used, although one might also want to consider the inclusion of secondary returns.

The results of clustering these data are shown in Figure 25. Using the criterion that $\hat{\sigma}_b(g+1)$ had to be less than $g\hat{\sigma}_b(c)/(g+0.8)$, we obtained the following results:

Data Period	No. of Layers	$\hat{h}_{i(ft.)}$	n_i	$\hat{P}_i$
50-69	1	799	65	1.000
49-69	1	1370	45	.693*
17-70	2	225	61	.642
		1542	34	.358

*A total of 65 readings were made during the period.

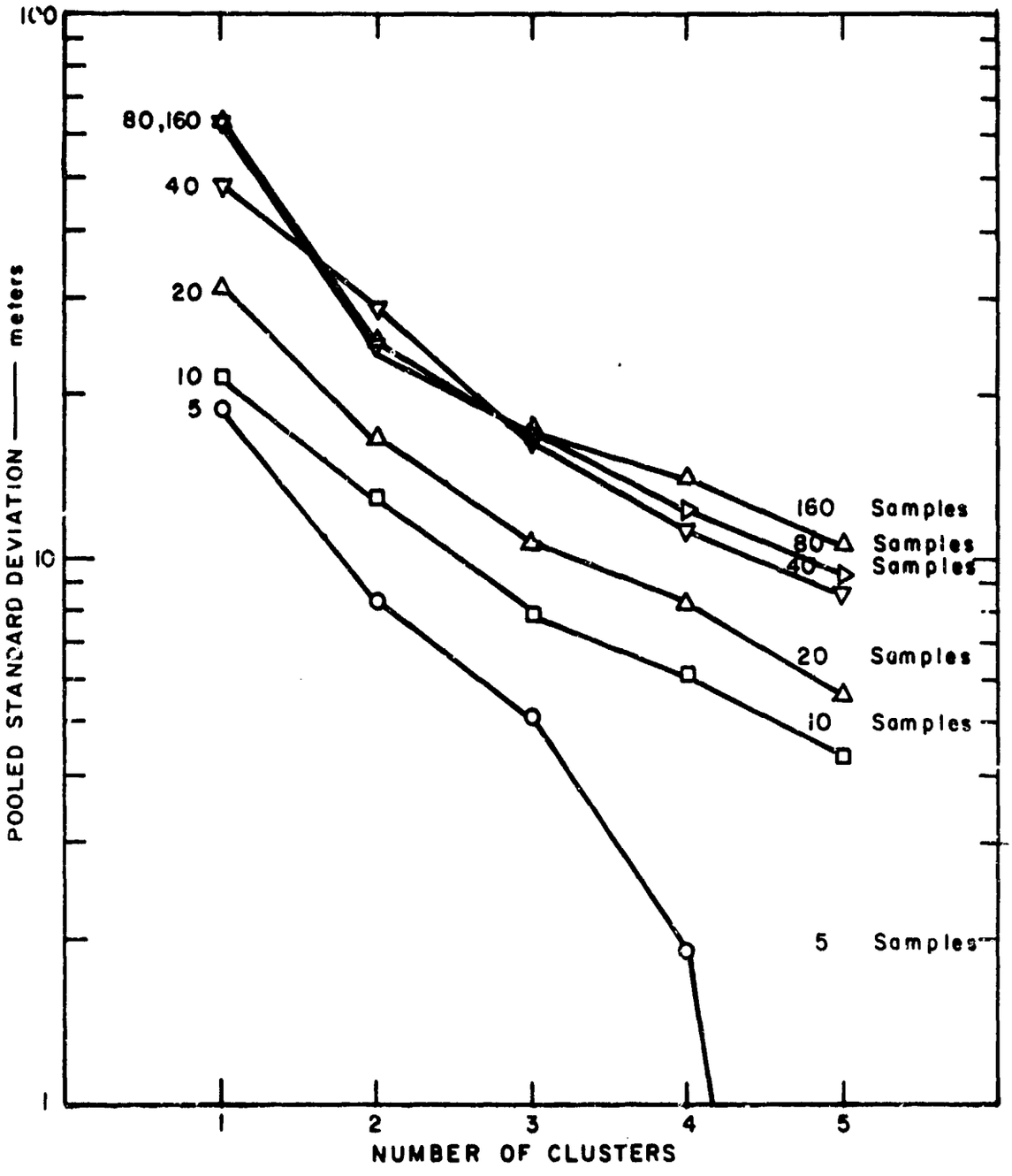

FIGURE 21 EFFECT OF SAMPLE SIZE ON CLUSTERING PERFORMANCE

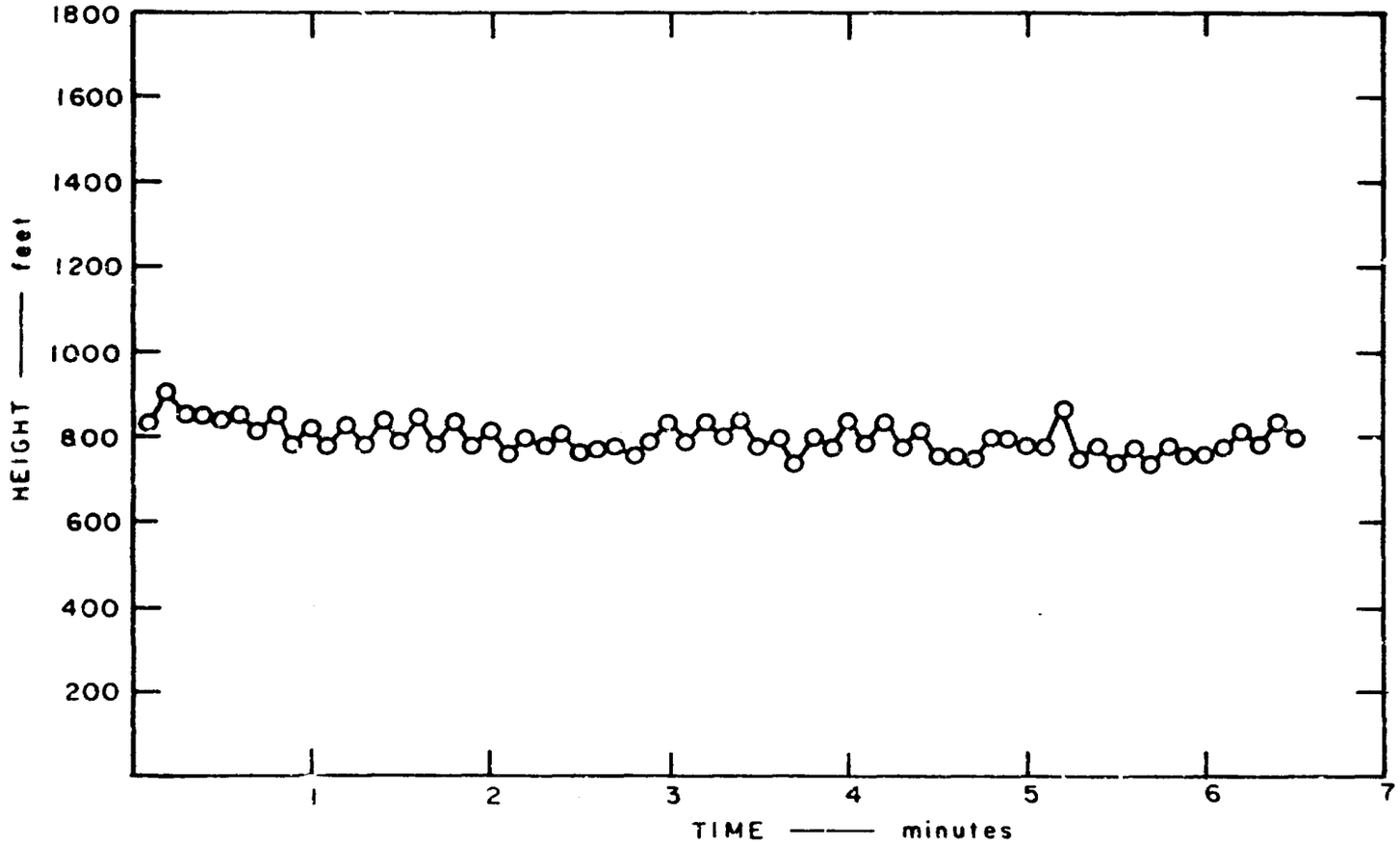

FIGURE 22 CEILING HEIGHT MEASUREMENTS FOR RBC-1, DATA PERIOD 50-69

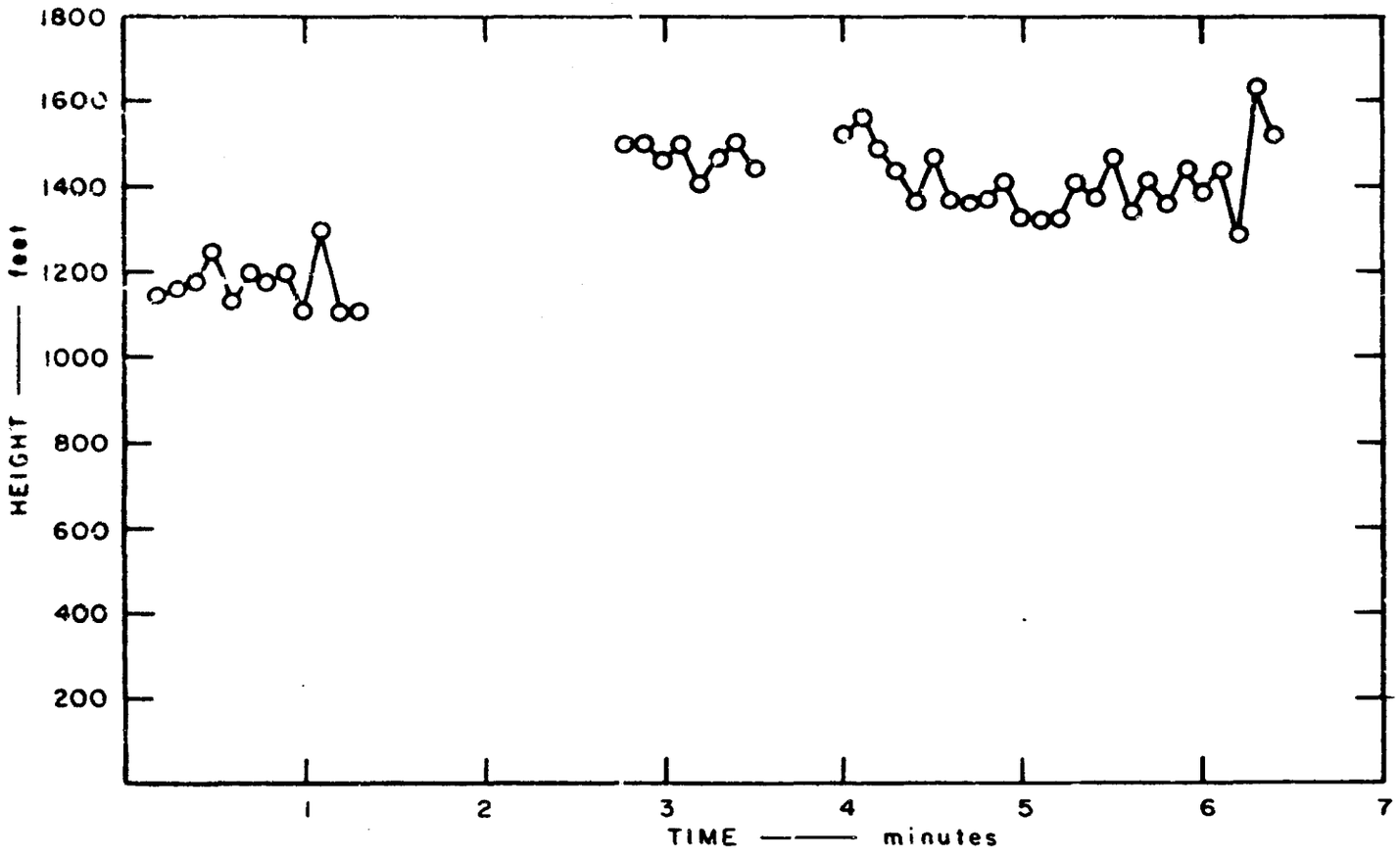

FIGURE 23 CEILING HEIGHT MEASUREMENTS FOR RBC-3, DATA PERIOD 49-69

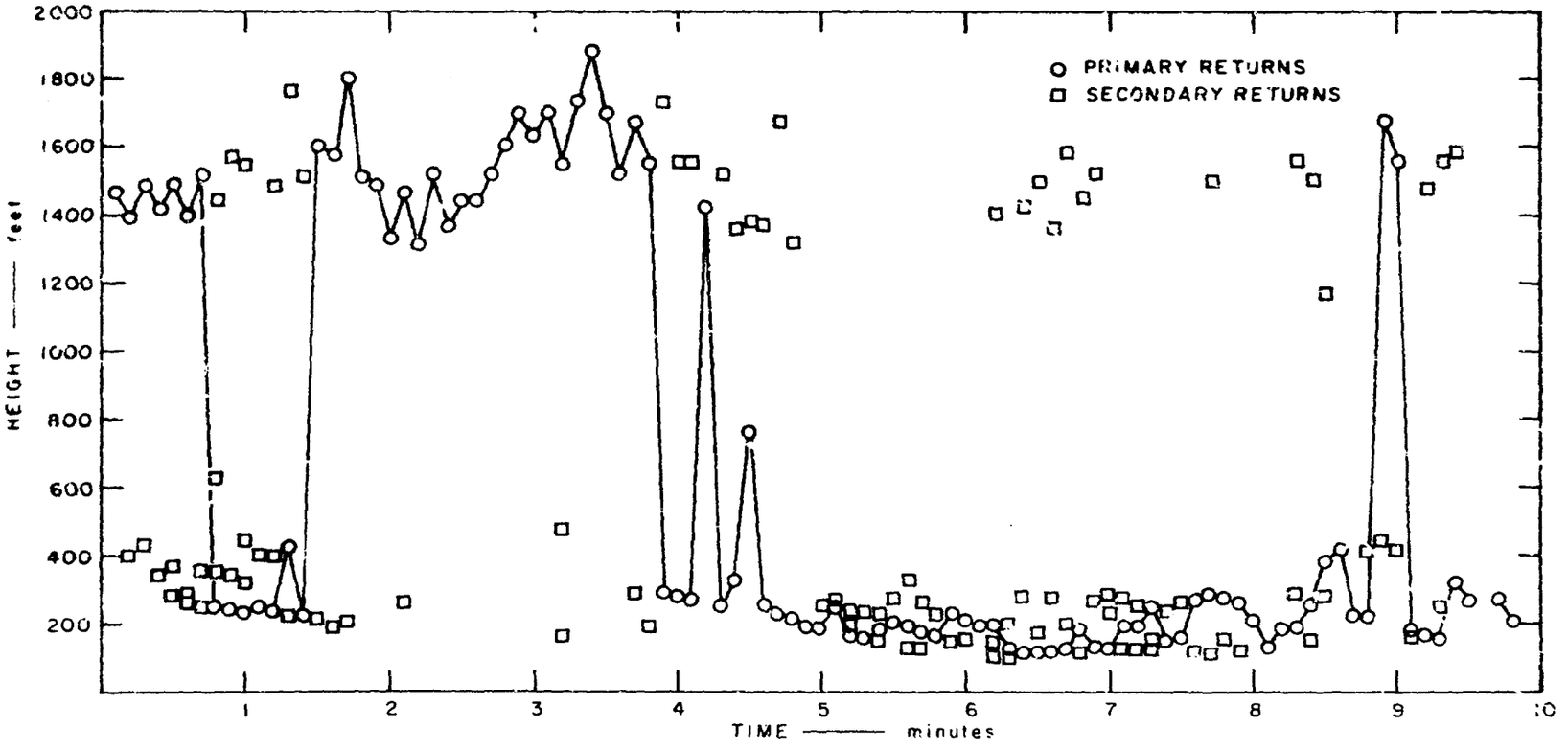

FIGURE 24 CEILING HEIGHT MEASUREMENTS FOR RBC-1, DATA PERIOD 17-70

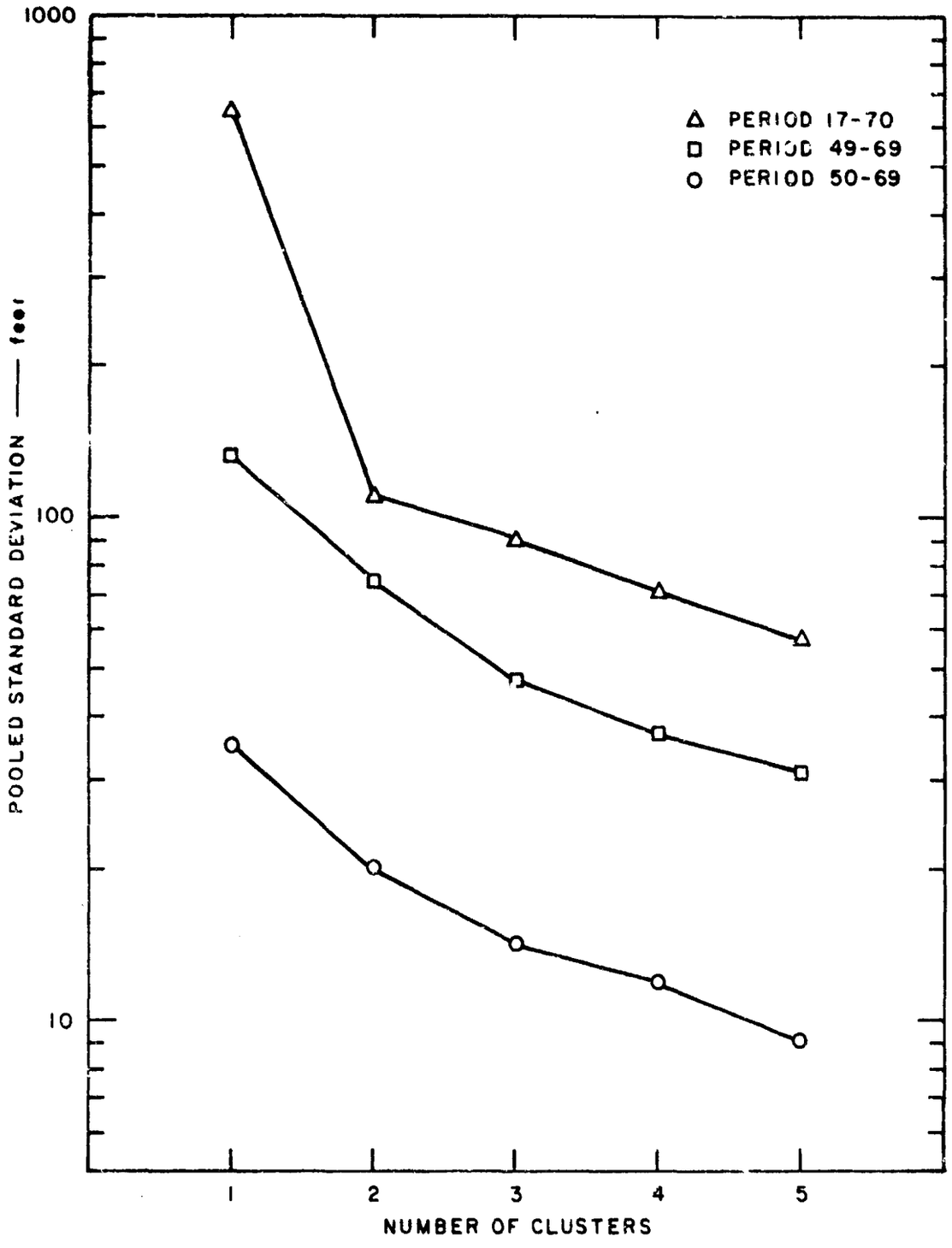

FIGURE 35 HIERARCHICAL CLUSTERING OF CEILING HEIGHT MEASUREMENTS

In the case of data period 49-69, the decision that there was only one layer was a marginal one; if two layers had been selected, they would have been located at 1165 ft. and 1429 ft. A longer data record would be needed to make a firm choice between these alternatives.

F. Remarks

This investigation of density estimation and clustering procedures was concerned with ways of processing ceilometer data to obtain information about the number of cloud layers, the average height of each layer, and the cloud amount in layers. The problem was shown to be one of analyzing a mixture distribution, a problem that has no computationally simple solution.

A simple hierarchical clustering procedure was shown to be quite effective on data generated by the model, and gave reasonable results for a small sample of real ceilometer data. Thus, the basic feasibility of this kind of objective data processing was established. However, a few problems must be solved before the technique can be used routinely in practice. These include the following:

(1) Verification that the criterion for determining the number of layers gives the desired results.

(2) Determination of the needed number of samples for valid clustering. The number needed for valid clustering may not be the same as the optimum number to average for cloud amount estimation.

(3) Possible modification of the procedure to ensure stable results as a function of time.

The first two problems require fairly extensive experimentation with actual ceilometer data, but are not expected to call for any major changes in the procedure. The third problem is potentially more difficult. Most of the clustering procedures ignore the fact that the data arrive in time sequence, and that it might be desirable to find and to track simple trends. Thus, in a period during which the cloud base height is becoming steadily lower, a clustering procedure might well describe the sky as containing two or more cloud layers. If the

time period for clustering is kept short enough to prevent this behavior, there is the danger that the sky description will become erratic as layers are seen, forgotten, and seen again. Serious problems of this sort could require additional research directed at solving this particular problem.

G. Instrument Limitations

Although the cloud/instrument model can simulate both the sky conditions and the physics of the instruments, the physics of the instruments were ignored in this study. In general, the physical limitations introduce systematic and random inaccuracies that reduce the performance that can be achieved. Three classes of problems can be distinguished:

(1) Measurement accuracy

(2) Failure to detect clouds

(3) Detection of false signals.

Measurement accuracy for a rotating-beam ceilometer is affected by several factors, such as the base line distance, the cone angles, and the levelling of the instrument. The problems of measuring the heights of high clouds by triangulation are well known. In general, an inaccuracy in measurement will introduct the same inaccuracy in the resulting calculation of cloud base height, whether it is calculcated by averaging or by clustering.

Failure to detect clouds and the detection of false clouds are both related to the problem of interpreting the waveform produced by the instrument. The basic problem is one of detecting a signal in the presence of noise. The physical design of the instrument can enhance the signal by increasing the power of the transmitted signal, increasing the sensitivity of the receiver, or modulating the signal to distinguish it from noise. Similarly, the instrument design can minimize noise through the use of filters, care to avoid vibration, etc. Nevertheless, thermal noise, photon noise, and interference of various kinds are always present, and any automatic system must be able to cope with detection errors of both kinds.

Failure to detect a cloud that is present has obvious effects: cloud amount estimates are too low, and cloud height estimates are more uncertain than they need be. However, a small percentage detection failure does not cause serious problems.

The "detection" of nonexistent clouds causes much more serious problems. These false alarms are commonly due to electrical interference, solar interference, or precipitation (e.g., the rainbow effect). To the extent that these causes yield typical patterns, it should be possible to program the automatic system to check for and eliminate them. For example, interference might lead to clustering producing an abnormally high number of clusters, or an abnormally high pooled sample standard deviation. Rainfall leads to a spurious response at a height corresponding to an elevation angle of 49° that a computer program can be alert for. Snow leads to strong responses down to near zero elevation angle. If temperature and rainfall information is also available to the processing program, many of these false responses can be eliminated. This suggests that the writing of the program for processing ceilometer data should be done in conjunction with people who are intimately familiar with the characteristics of the instrument, and have data illustrating its behavior.

V DETERMINATION OF INSTRUMENT CHARACTERISTICS

A. System Configuration

There are several ways to use the theoretical results of this report to determine instrument and data processing requirements for an automatic system for cloud-amount and ceiling-height measurement. These alternatives make it difficult to provide a summary that is both simple and complete. In this section the theoretical results are used to provide design curves for a system of multiple vertically-pointing instruments that uses adaptive time averaging and hierarchical clustering. While this is not the only kind of system to which the theory could be applied, it is an important one that illustrates the theory well.

The basic components of this system are illustrated in Figure 26. The n ceilometers are synchronized vertically-pointing instruments, each of which provides a ceiling-height reading every ΔT seconds. It is assumed that the output of each ceilometer is a voltage that gives the detector response as a function of time, and that by calibration, the relations between time, beam angle, and cloud height are known. The multiplexer samples each instrument in turn, returning to the first instrument in a small fraction of ΔT.* It also samples an anemometer that supplies wind speed values; these can be adjusted by theoretical means to give the cloud speeds used in determining the averaging time for cloud amount and cloud height determination. Cloud speeds may also be obtained by inference from the wind data obtained from upper air soundings.

---

*Consider a rotating-beam ceilometer that sweeps 180° in time ΔT and has a baseline "a." To obtain P_h percent accuracy at height h the multiplexer must return in time (ΔT_m)

$$\Delta T_m = \frac{P_h}{100\pi} \frac{ha}{h^2 + a^2} \Delta T \quad .$$

For five percent accuracy at h = 5000 ft. with a = 400 ft., ΔT_m = 0.0013 ΔT.

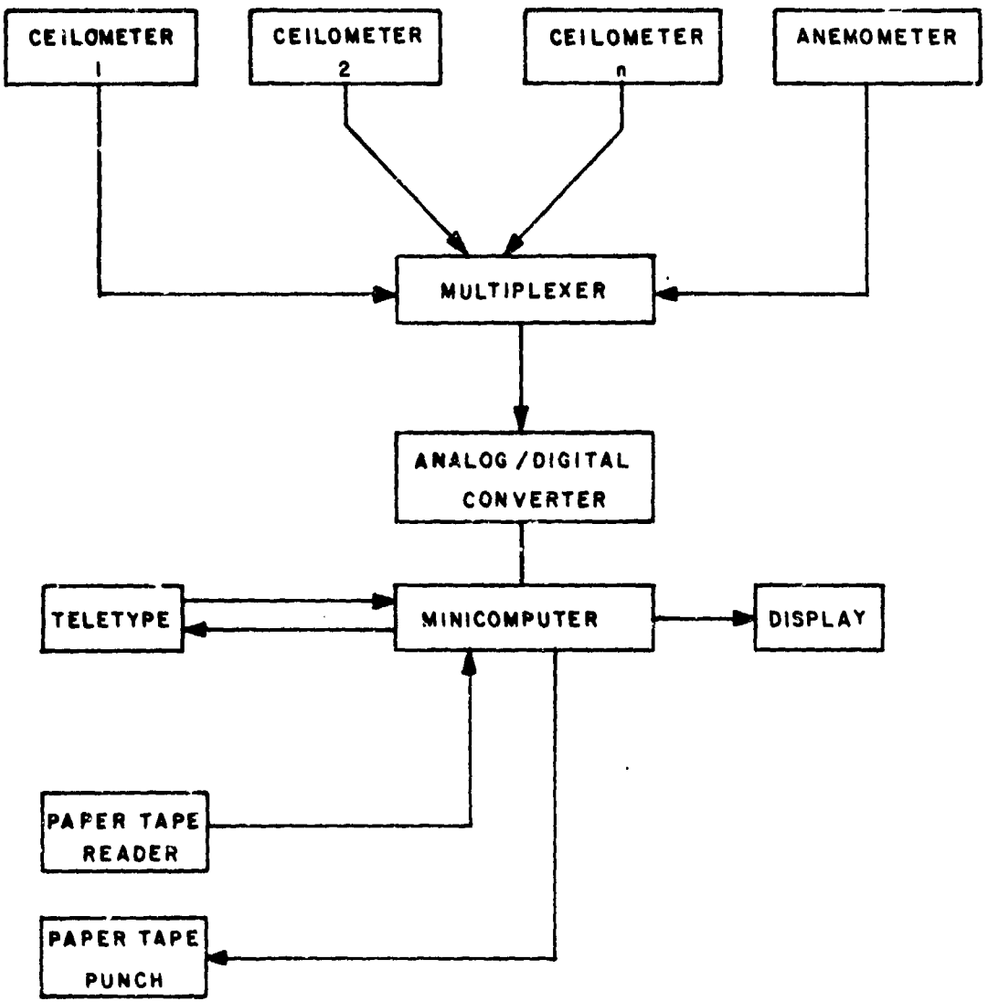

FIGURE 26 COMPONENTS OF AN AUTOMATIC SYSTEM FOR MEASURING CLOUD AMOUNT AND CEILING HEIGHT

The minicomputer has several tasks. For each instrument it maintains a table (or, to be more exact, a circular list) of the ceiling height readings for the last T seconds. It uses these tables to compute, record, and display the results of averaging to obtain cloud amount, and the results of clustering to determine the number of layers, the cloud amount in layers, and the base height of each layer. Each time (ΔT_m) the minicomputer is interrupted by a ceilometer reading, it checks that reading to see if a maximum response (presence of clouds) has been obtained. Every ΔT seconds it updates the tables for each instrument, replacing the oldest readings with the newest ones. Each time it is interrupted by the anemometer, it updates the wind speed record. This is corrected to estimate cloud speed and periodically used to adjust the averaging time for cloud-amount and base-height determination. Finally, the minicomputer may be called upon to provide permanent records and summary statistics as desired. These can be listed on the teletype and/or punched on paper tape for processing elsewhere.

It should be emphasized that this report is concerned with theoretical requirements, not system design, and other system configurations should be considered. In particular, the computer hardware requirements can be very sensitive to the display and output requirements, the procedures for servicing interrupts, and the way that the computational programs are coded. However, the theory does provide absolute minimum computational requirements needed to achieve a specified level of performance.

B. Specifications, Characteristics, and Parameters

The theory developed in this report relates three sets of quantities: performance specifications, instrument and processing parameters, and cloud parameters. These are listed explicitly below:

(1) Performance specifications

(a) Root-mean-square error in estimating cloud amount $\hat{\sigma}_c$

(b) Root-mean-square error in estimating cloud base height $\hat{\sigma}_h$

(c) Area to be covered A

(2) Instrument and processing requirements

(a)	Number of instruments	n
(b)	Instrument configuration	-
(c)	Sampling interval	ΔT
(d)	Averaging time	T
(e)	Data processing requirements	-

(3) Cloud parameters

(a)	Mean cloud length	ℓ_m
(b)	Cloud amount	c_a
(c)	Cloud speed	v
(d)	Mean base height	$\bar{h}$
(e)	Base-height standard deviation	σ_b
(f)	Base-height correlation distance	d

In the remainder of this section we will show how the performance specifications and the cloud parameters together determine the instrument and processing requirements. Although we restrict our attention to the specific system illustrated in Figure 26, the more general applicability of our results should be clear. We will show how different decisions regarding performance specifications and cloud parameters lead to different instrument and processing requirements. We now consider each of these requirements in turn.

C. Number of Instruments

If no time averaging is employed, the number (n) of instruments needed to achieve a specified error in estimating cloud amount ($\hat{\sigma}_c$) depends on the cloud amount (c_a), the area (A), and the mean cloud length (ℓ_m). We will only consider the worst case, where c_a = 0.5, keeping in mind that better performance will be achieved if c_a is near zero or one. Figure 6 shows the relation between n, $\hat{\sigma}_c$ ($\hat{\sigma}$ on this figure), and $\sqrt{A}/\ell_m$. In general, this figure indicates the need for either a large number of instruments or time averaging.

To simplify the consideration of time averaging, we assume that the cloud speed (v) can be measured and used to determine the averaging time. Although Eq. (18) indicates the existence of an optimum averaging time, it can call for a long period if v is small. This

can prevent the system from being able to respond to sudden changes in conditions. To accommodate this problem, we introduce a new parameter, the maximum allowed averaging time T_{max}. We assume that the actual averaging time is computed according to

$$\left.\begin{aligned} T &= \frac{\sqrt{A}}{v} \quad \text{if} \quad v > \frac{\sqrt{A}}{T_{max}} \\ \text{or} \\ T &= T_{max} \quad \text{if} \quad v \leq \frac{\sqrt{A}}{T_{max}} \quad , \end{aligned}\right\} \tag{45}$$

so that the averaging time never exceeds T_{max}.

The choice of a value for T_{max} is basically a trade off between the desired time of response and cost for a given performance. This in turn involves how rapidly ceiling conditions can deteriorate at a given airport and how important this is. Too short a T_{max} time may yield unrepresentative results, or may require an increased number of instruments to achieve representative results. Our graphs show the effects of different choices for T_{max} on instrument requirements; in our examples we use T_{max} = 0.1 hr., which seems to be a reasonable choice.

Figure 7 shows how averaging reduces the RMS error $\hat{\sigma}_m(n)$. Note that the case T = 0 corresponds to no averaging, and the resulting RMS error is exactly the $\hat{\sigma}$ of Figure 6. With the use of time averaging, $\hat{\sigma}_m(n) = \hat{\sigma}_c$, the specified RMS error. For simplicity, in the range $vT/\sqrt{A} \leq 1$, we approximate the curves in Figure 7 by

$$\hat{\sigma}_c \approx \frac{\hat{\sigma}}{2}\left[\left(1 - \frac{vT}{\sqrt{A}}\right)^2 + 1\right] \quad . \tag{46}$$

The procedure for finding the number of instruments is then straightforward, and involves the following steps:

(1) Select a value for the maximum allowed RMS error $\hat{\sigma}_c$.

(2) Select a value for the maximum allowed averaging time T_{max}.

(3) Select a value for the area A to be covered.

(4) Determine the minimum cloud speed v and the minimum cloud length ℓ_m of interest at the particular area.

(5) Compute vT_{max}.

(6) If $vT_{max} > \sqrt{A}$, let $\hat{\sigma} = 2\hat{\sigma}_c$; otherwise use the formula

$$\hat{\sigma} = \frac{2\hat{\sigma}_c}{1 + \left(1 - \frac{vT_{max}}{\sqrt{A}}\right)^2} \qquad (47)$$

(7) Use this $\hat{\sigma}$ and the value of $\sqrt{A}/\ell_m$ to obtain n from Figure 6.

To illustrate the results of this computation, a series of design curves were obtained in this way. A value of 0.15 was selected for $\hat{\sigma}_c$, since this corresponds fairly well to the performance of human observers (Galligan, 1953). Ranges of values were used for the other parameters, leading to the results shown in Figure 27. For a specific case, consider an 800 ft. by 4000 ft. area ($\sqrt{A}$ = 0.34 mi.) located in a region where time averaging should be limited to T_{max} = 0.1 hr. and clouds as small as ℓ_m = 0.05 mi. are important. Thus vT_{max} = 0.5 mi., and for $\sqrt{A}$ = 0.34 mi. Figure 27(b) shows that for this case two instruments would be adequate. From these curves one can see how changes in any of the parameters other than σ_c influence this conclusion. The formulas allow similar curves to be obtained for any desired RMS error in cloud amount $\hat{\sigma}_c$.

D. Instrument Configuration

All of these theoretical results were obtained under the assumption that the instruments are located as far from one another and the boundary of the area as possible. This had the purpose of obtaining readings from each instrument that were as independent as possible. Furthermore, for reasonably large values of n, this made the behavior of the system insensitive to the cloud direction. Particular configurations that meet these requirements for a square area are shown in Figure 4.

In practice, various constraints usually prevent the use of an optimum configuration. In addition, climatological considerations

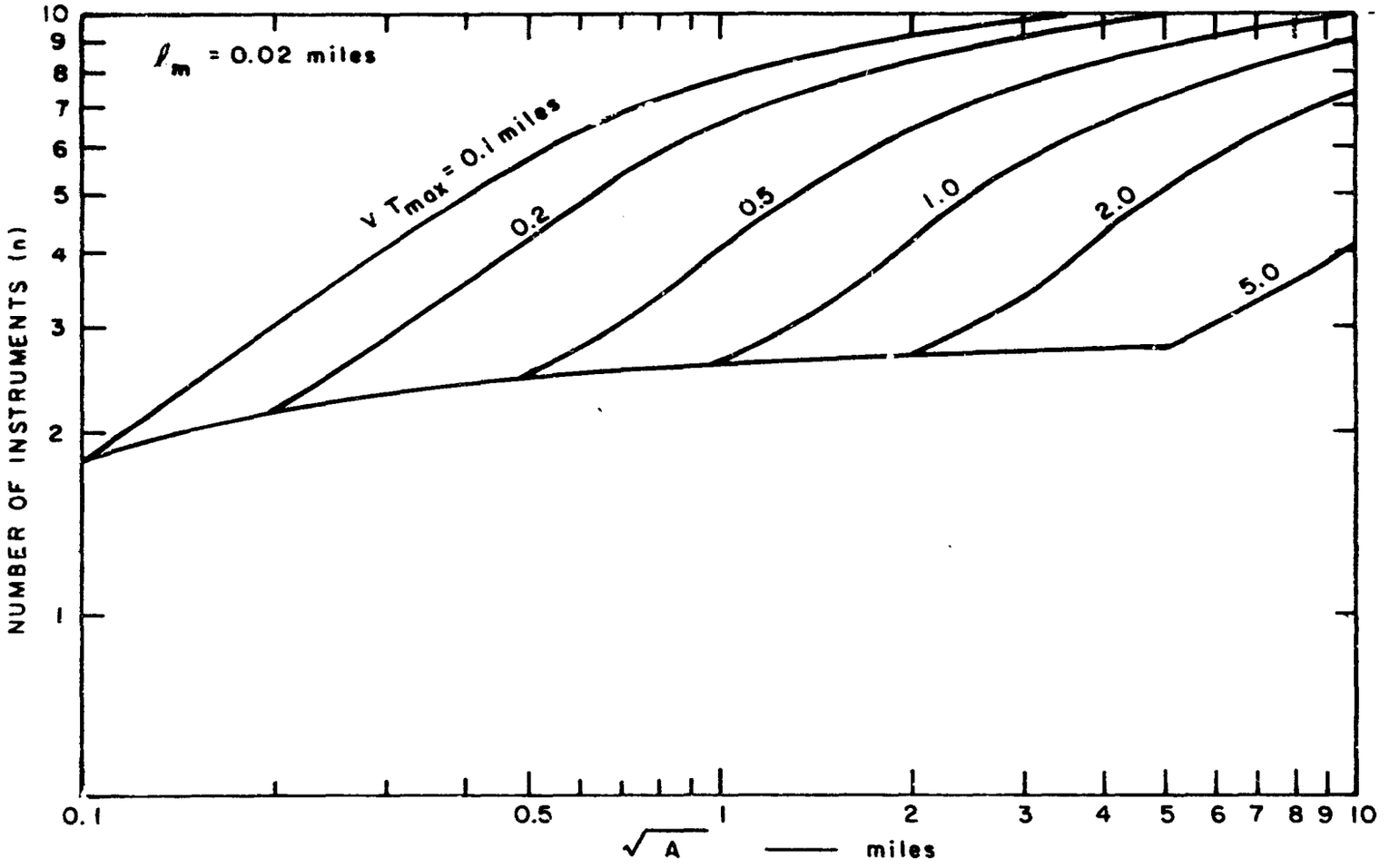

FIGURE 27 NUMBER OF INSTRUMENTS REQUIRED
(a) ℓ_m = 0.02 MILES

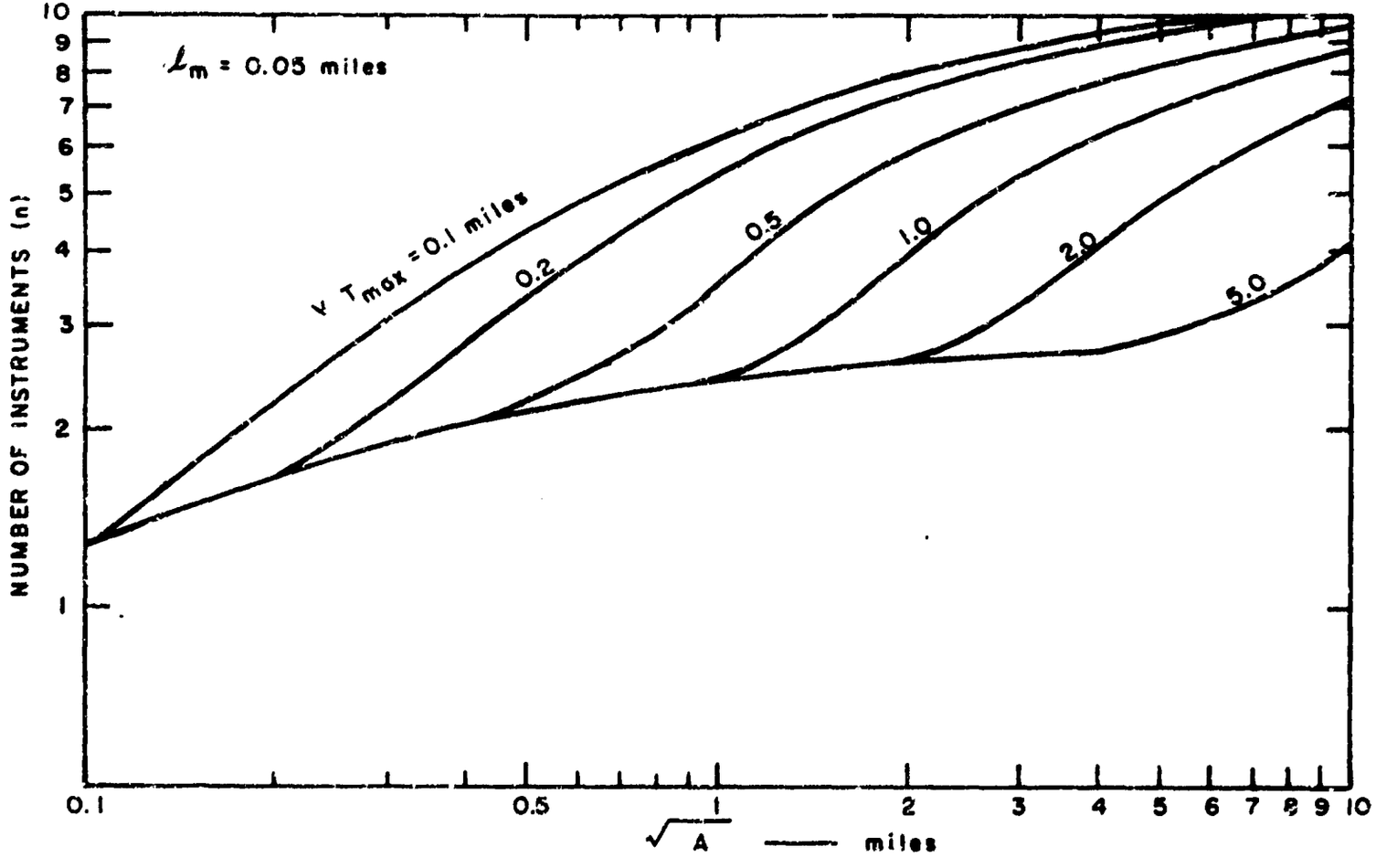

FIGURE 27 NUMBER OF INSTRUMENTS REQUIRED
(b) ℓ_m = 0.05 MILES

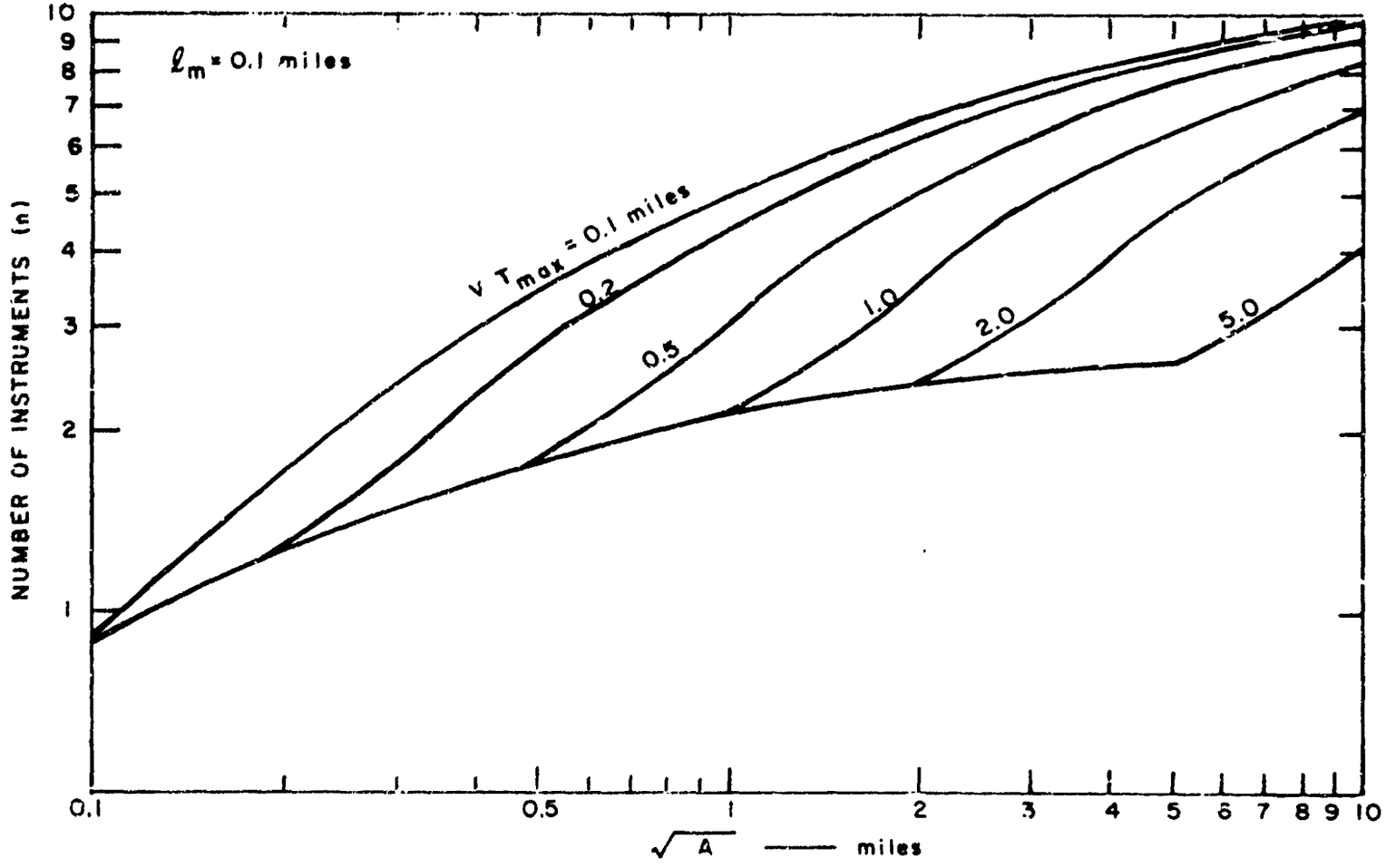

FIGURE 27 NUMBER OF INSTRUMENTS REQUIRED
(c) ℓ_m = 0.1 MILES

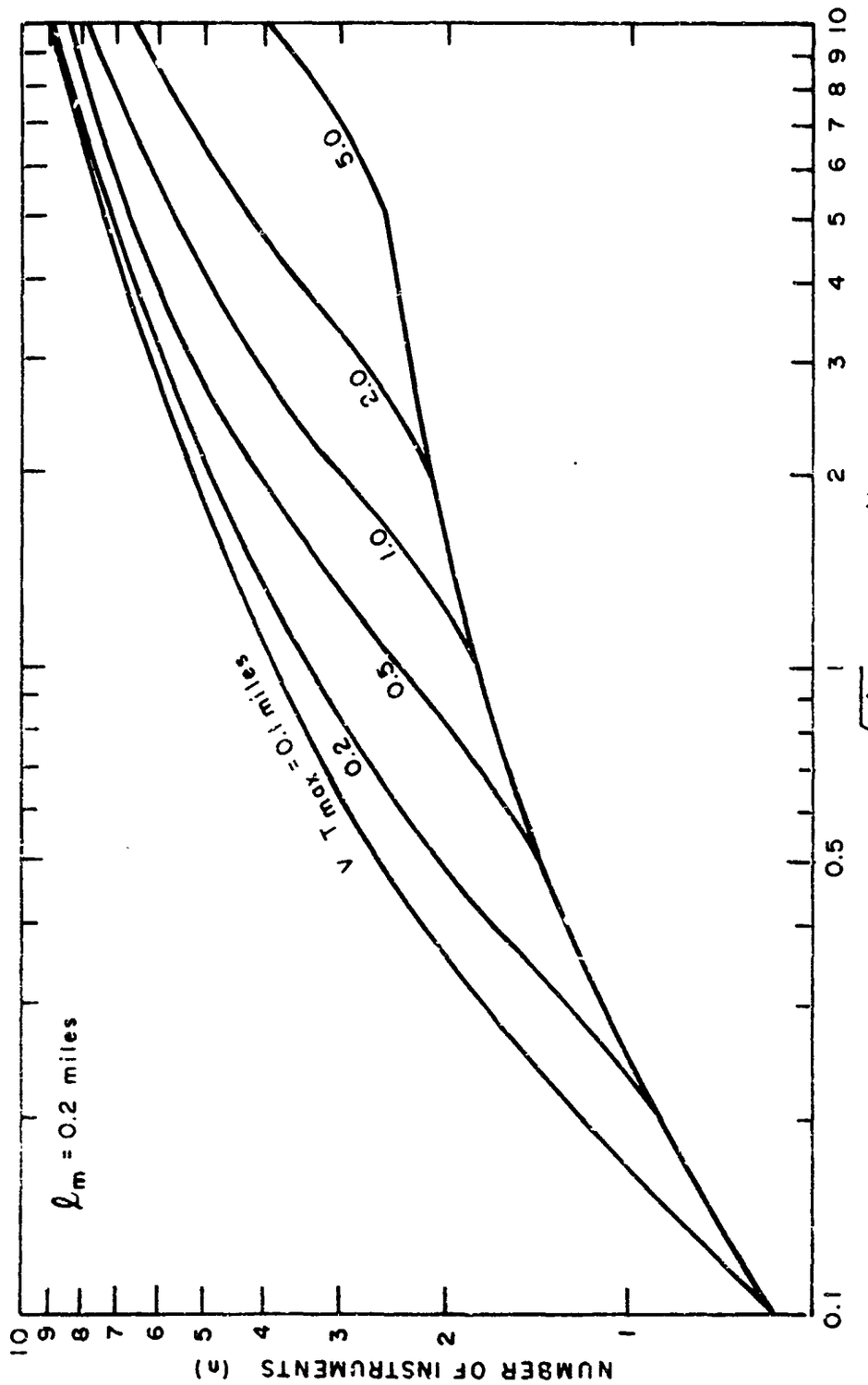

FIGURE 27 NUMBER OF INSTRUMENTS REQUIRED
(d) ℓ_m = 0.2 MILES

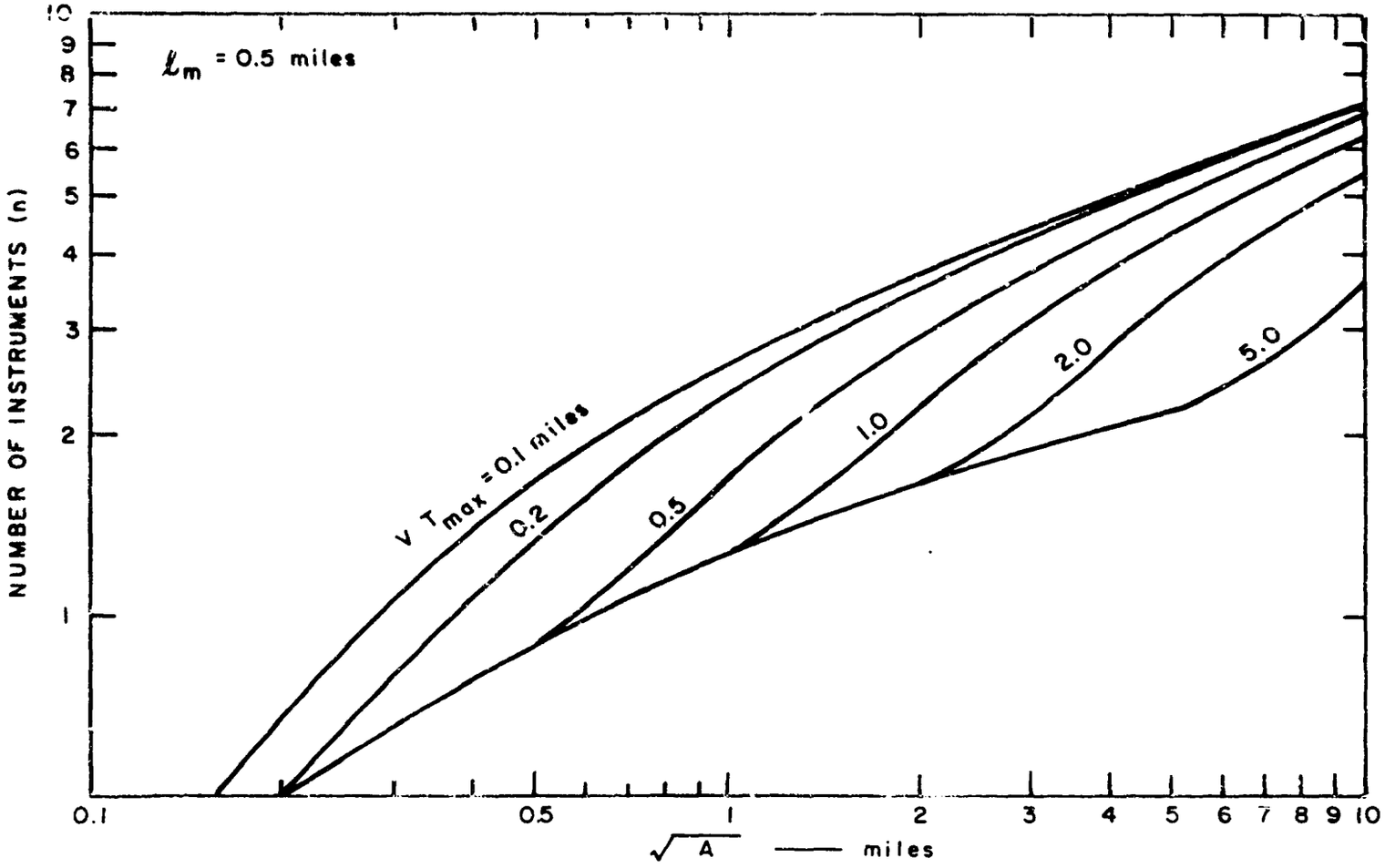

FIGURE 27 NUMBER OF INSTRUMENTS REQUIRED
(e) ℓ_m = 0.5 MILES

may dictate a nonisotropic configuration to take advantage of common weather patterns. For example, suppose that it is known that at a particular location the clouds almost always come in from the west. Then the instruments should be arranged equally spaced in a line along the west edge of the area. Although the theory does not specify compromise solutions, a general rule is that the instruments should be located to obtain readings that are as independent as possible, as quickly as possible.

E. Sampling Interval

The sampling interval ΔT affects the accuracy with which the cloud amount and the mean cloud base height can be determined. In Section II-C-2 it is shown that little additional accuracy can be obtained if the sampling interval ΔT is smaller than $0.25\ \ell_m/v$ or $0.5\ d/v$, where ℓ_m is the mean cloud length, v is the cloud speed, and d is the base-height correlation distance. In addition, of course, ΔT must be smaller than the averaging time T, which in turn is less than $\sqrt{A}/v$. Thus, ΔT is fixed by the requirement

$$\Delta T = \frac{\min\left\{\frac{\ell_m}{4}, \frac{d}{2}, \sqrt{A}\right\}}{v} \quad . \tag{48}$$

To determine numerical values for ΔT, one must have knowledge of the worst possible conditions at which specified performance is to be achieved. Specifically, this means knowing the shortest mean cloud length, highest cloud speed, and shortest correlation distance (which measures how rapidly a given base height fluctuates). Figures 28 and 29 show how the required sampling interval varies with these parameters. As expected, the requirements are most severe when the cloud speed is large and when any of the lengths ℓ_m, d, or $\sqrt{A}$ are small. In most cases of interest the area A is not the limiting factor. Lack of data on the correlation distance makes it difficult to decide whether or not it is more significant than ℓ_m in determining ΔT. If d is less than $0.5\ \ell_m$, then d is the more important factor. That is certainly the case for large clouds, but it may not be true for the smallest clouds of interest.

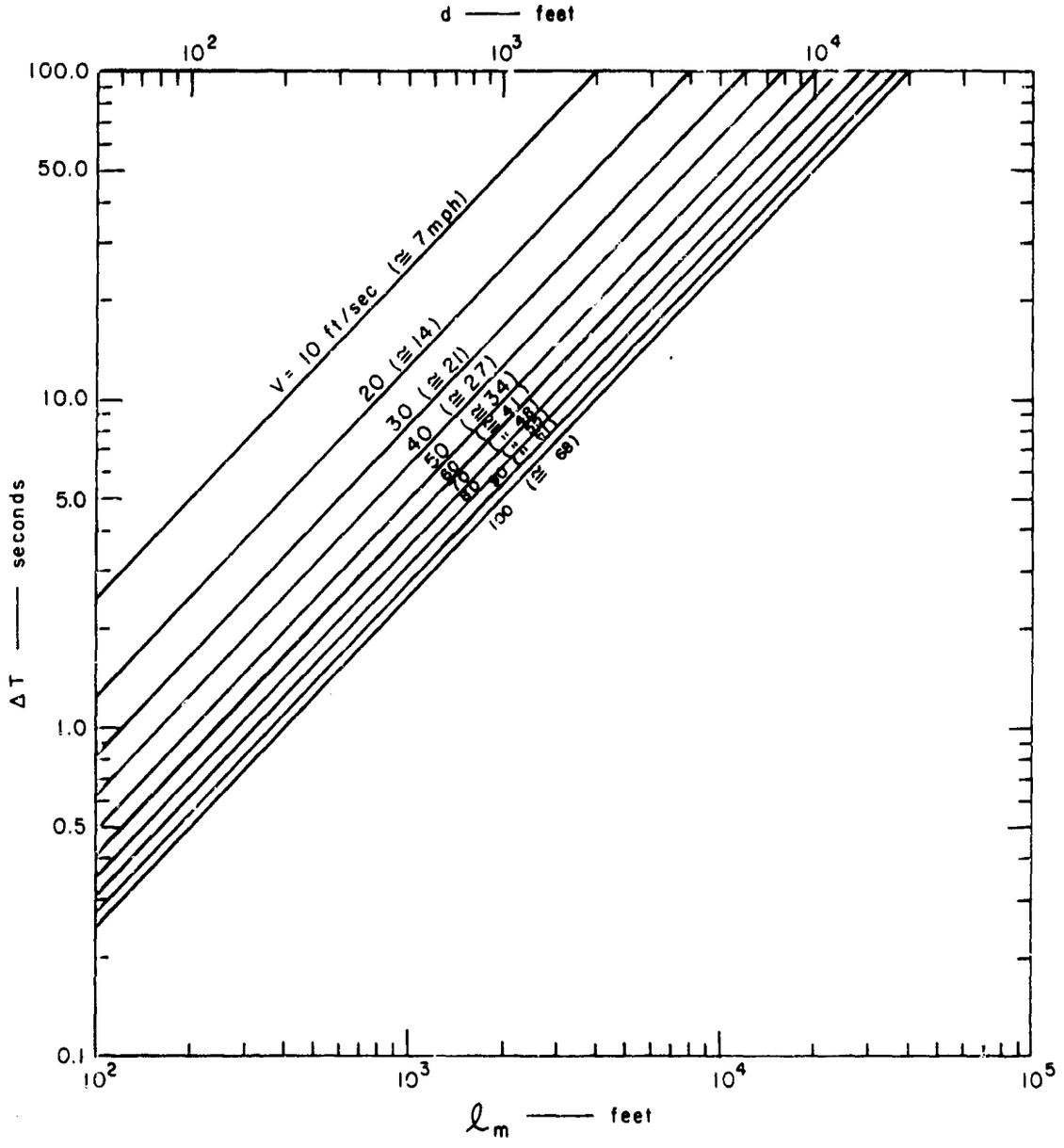

FIGURE 28 SAMPLING INTERVAL VERSUS CORRELATION DISTANCE AND MEAN CLOUD LENGTH

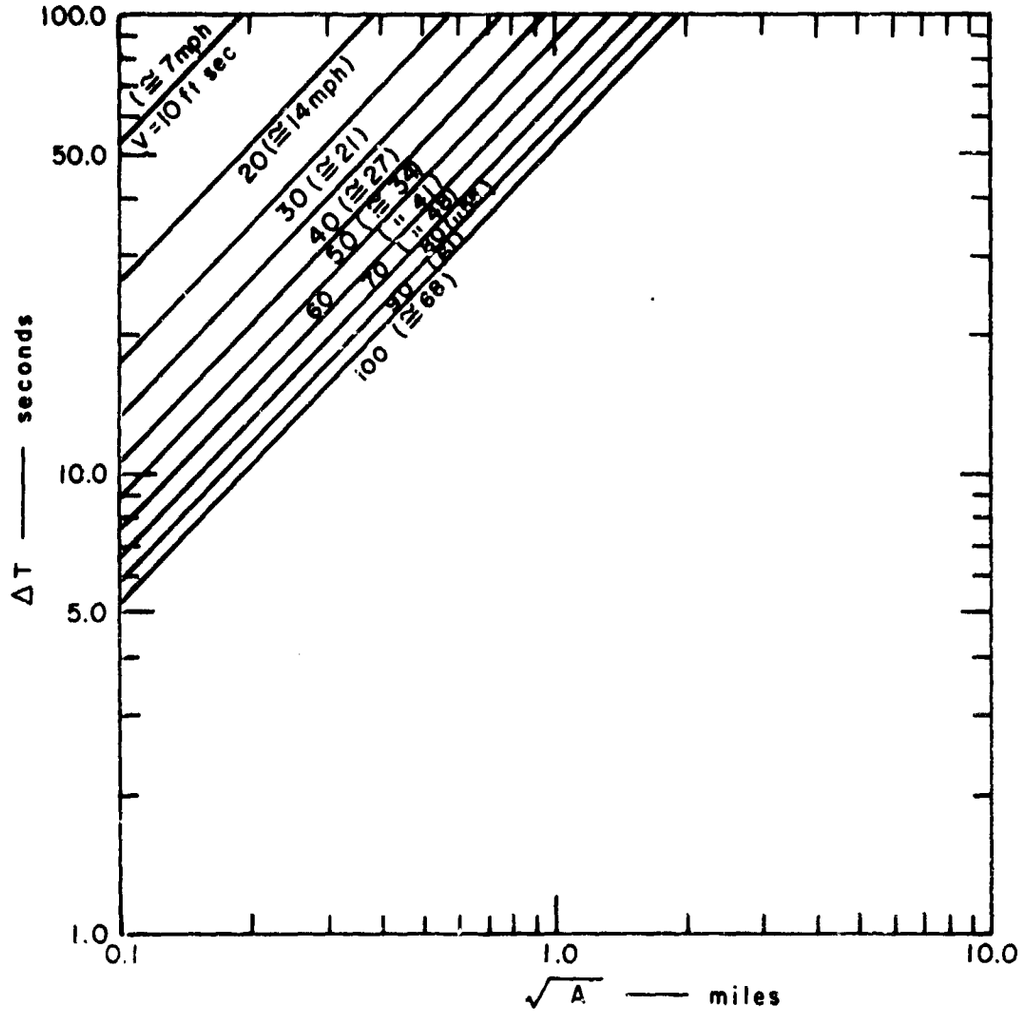

FIGURE 29 SAMPLING INTERVAL VERSUS AREA COVERED

In any case, once the largest value of v and the smallest values of ℓ_m, d, and $\sqrt{A}$ are selected, ΔT can be determined from Figures 28 and 29.

F. Averaging Time

Eq. (45) gives the averaging time for the determination of cloud amount. In addition, an averaging time is needed for determining the cloud base height, and these two times need not be the same. This latter time is determined primarily by the specified RMS error $\hat{\sigma}_h$ in estimating the cloud base height, or, alternatively, by the percentage error in estimating the cloud base height (P_h)

$$P_h = \frac{100\hat{\sigma}_h}{\bar{h}} \quad , \tag{49}$$

where $\hat{\sigma}_h$ is the RMS error in estimating cloud base height and $\bar{h}$ is the mean base height.

For simplicity, we consider only the single-layer case in determining the averaging time. Appendix E contains a derivation of the RMS error for a single instrument. For n widely separated instruments the corresponding results are

$$\hat{\sigma}_h = \frac{\sigma_b}{\sqrt{nvT/2d}} \left[1 - \frac{1-e^{-vT/d}}{vT/d}\right]^{\frac{1}{2}}, \tag{50}$$

where σ_b is the base-height standard deviation, v is the cloud speed, T is the averaging time, d is the base-height correlation distance, and n is the number of instruments.

This result can be simplified further by assuming that σ_b is proportional to $\bar{h}$. To give specific results, we used the 10-minute data in Table VII of Davis (1969) to obtain the approximate relation $\sigma_b = 0.1\,\bar{h}$. This leads to the formula

$$P_h = \frac{10}{\sqrt{nvT/2d}} \left[1 - \frac{1-e^{-vT/d}}{vT/d}\right]^{\frac{1}{2}}. \tag{51}$$

Figure 30 shows the resulting relation between P_h and vT/d for different values of n when $\sigma_b = 0.1\bar{h}$; other values of σ_b could yield other curves. By specifying P_h and n, one can determine vT/d, and hence T. Note that as in the case of cloud amount estimation, T will vary with v and will be large if v is small. Once again it is

necessary to set a maximum averaging time T_{max} to allow the system to respond to sudden changes. When v is so small that T reaches this maximum, Figure 30 can be used to obtain the resulting percentage error P_h.

Example:

Suppose n = 4 and a percentage error of no more than P_h = 3% is desired. From Figure 30, vT/d = 4.2. Thus, if this performance is desired for v as small as 5 mi/hr and d as large as 0.5 mile, T must be at least 0.42 hr. If T cannot exceed T_{max} = 0.1 hr, we cannot achieve 3% error with four instruments. However, under these same conditions, an averaging time T of 0.1 hours gives vT/d = 1, and our graphs show that the percentage error (P_h) will be 4.3%.

In general, the reader should be cautioned against setting specifications that call for extreme accuracy in determining the mean base height. If the mean height is 1000 ft. and the standard deviation is 100 ft., it is rather meaningless to ask, say, for one percent accuracy in determining the mean. While in theory this accuracy can be achieved, it is obtained at the cost of excessively long averaging times, and from an operational viewpoint the 100 ft. fluctuations reduce the usefulness of knowing the mean to within 10 ft.

It should also be noted that we have used the mean height $\bar{h}$ of the clouds in a given layer to define the height of that layer. For aviation applications, it may be desirable to modify this definition. For example, if the effective base height is defined as $\bar{h} - 2\sigma_h$, then the instantaneous cloud height will be below the effective base height less than five percent of the time. Such alternative definitions do not affect any of the results we have presented, since they merely make changes in the way that the effective base height is obtained from the results of clustering.

G. Computational Requirements

The two basic computations to be performed by the mini-computer are the cloud-amount calculation and the cloud-base-height calculation. The former is much simpler than the latter, involving merely the counting of the number of hits obtained during the averaging period. This can be done in little more than the time required to service the interrupts from the multiplexer.

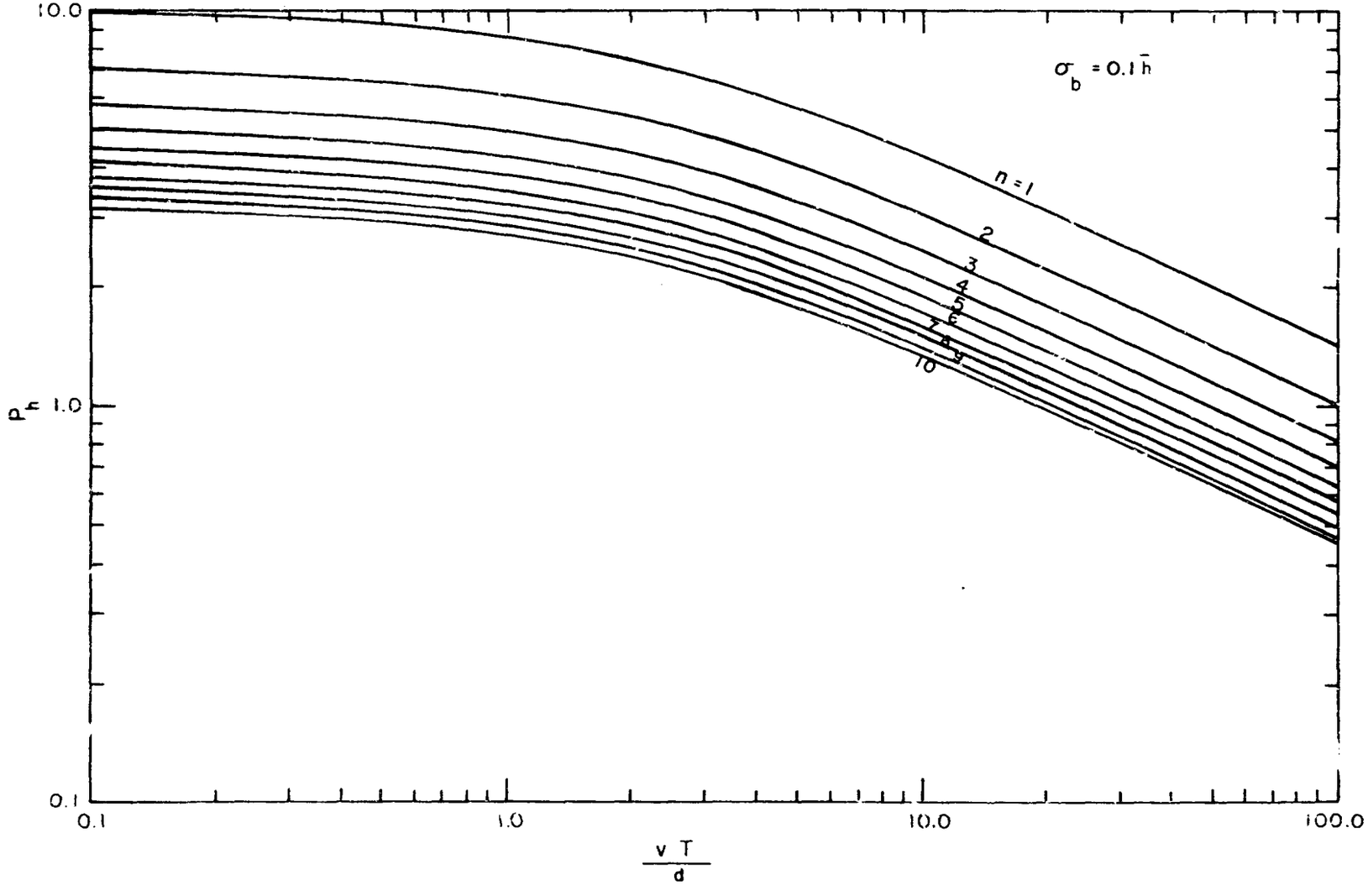

FIGURE 30 PERCENTAGE ERROR FOR CLOUD BASE HEIGHT ESTIMATION

Were it not for the possibility of multiple cloud layers, the cloud-base-height calculation would also be simple, involving merely the averaging of the ceilometer readings obtained during the averaging period. However, when multiple layers are possible and clustering is required, the computational requirements can rise significantly. Our study of clustering indicated that simple hierarchical clustering can be very effective, but it also exposed some questions (discussed in Section IV-F) that should be answered before the exact computational procedure can be established. Despite this problem, this simple procedure can be used to establish minimum computational requirements.

A particular version of the modified hierarchical clustering procedure described in Section IV-D-2 and used in Section IV-E-2 is analyzed in Appendix F. This procedure analyzes ceilometer readings to give the number of cloud layers, the mean height of each layer, and the cloud amount in layers. The minicomputer used to implement this procedure is assumed to require time t_{add} for an addition or subtraction and time t_{mul} for a multiplication or a division. The results of the analysis lead to the following minimum computer requirements:

$$\text{High-speed memory:} \quad \frac{3nT}{\Delta T} \text{ words}$$

$$\text{Operation speed:} \quad 7t_{add} + t_{mul} \leq \frac{\Delta T^2}{n^2 T} .$$

Here n is the number of instruments, T is the averaging time, and ΔT is the sampling interval.

For example, suppose that to meet other performance specifications we must have n = 4 instruments, an averaging time as long as T = 0.1 hr, and a sampling interval of ΔT = 2 sec. Then the minicomputer must have at least 2160 words of high-speed memory, and must take no longer than 694 microseconds to perform seven additions and a multiplication.

These results show that the computer requirements grow rapidly with the ratio $nT/\Delta T$, the total number of measurements taken during the averaging period. Of the two, the speed requirements are

more severe, since they grow approximately as the square of that ratio. Figure 31 shows the speed requirements graphically.

Again, it should be emphasized that these requirements have been derived for a particular data processing procedure coded in a particular way. Although they should serve as a useful guide for minimum requirements, the limitations of this analysis should be remembered.

By directly relating the specific climatology of a given airport and its environs to the parameters of the model described in this study, one could specify the exact system requirements to automatically specify the cloud amount and base height at a given airport. Such a system could be an advantage at those airports where manpower is at a minimum.

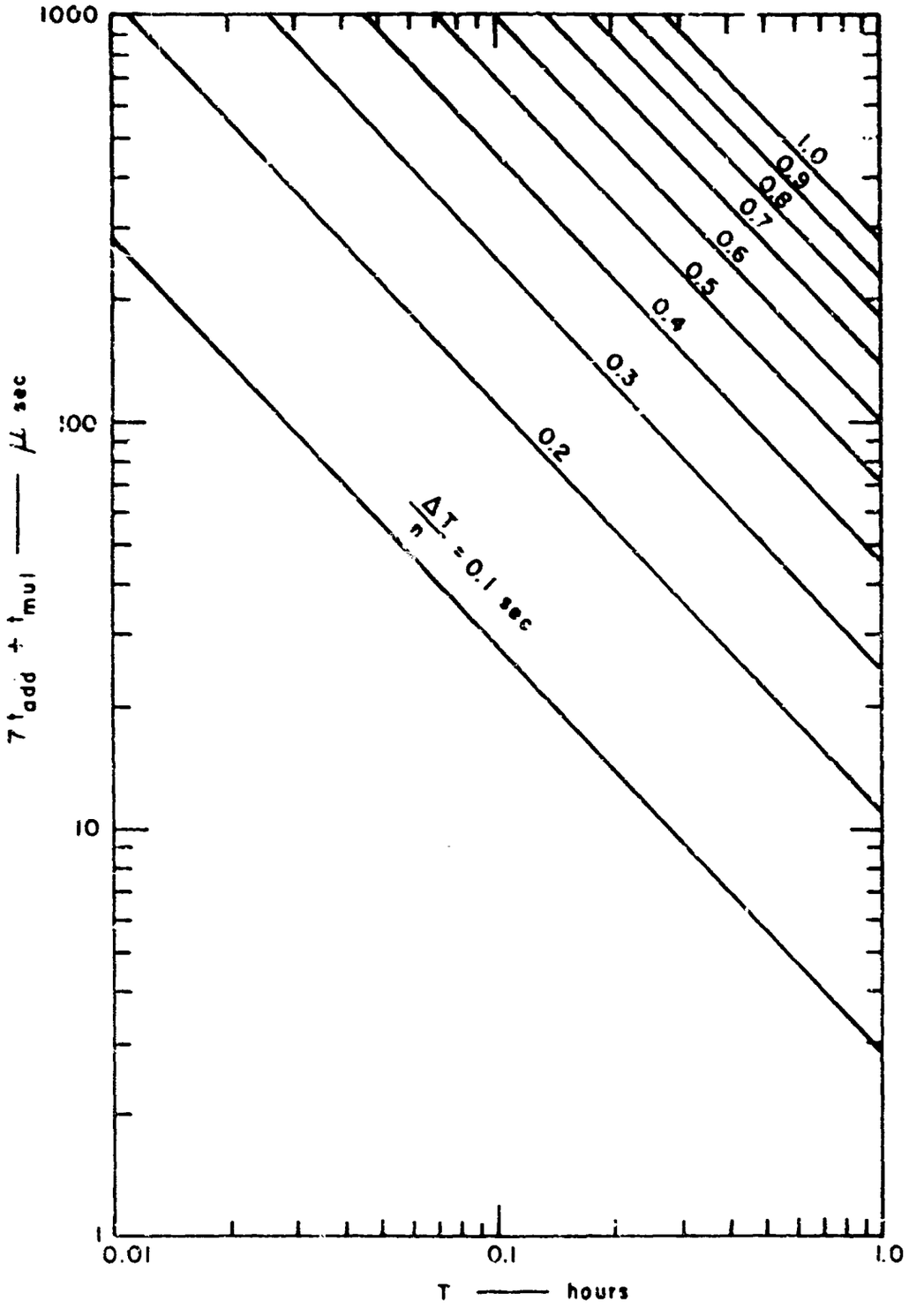

FIGURE 31 COMPUTER OPERATION SPEED REQUIREMENTS

VI COST COMPARISONS

A. Introduction

An automated system for measuring cloud amount and ceiling height has the potential advantage of making, recording, and communicating objective observations frequently and reliably. However, the cost for such a system can be quite high, particularly when a large number of instruments must be used. This section compares the cost of an automated system using n instruments with the cost of the present manual system. For simplicity, our comparison involves costs only, and tacitly assumes that the systems being compared provide results of equal value or benefit. The question of benefit must also be considered in the eventual selection of the method to be used.

The results of the cost analysis depend upon the assumptions used for the various costs involved. The Federal Aviation Administration has provided salary, installation, and maintenance support costs, and values for the time involved in making weather observations. It should be noted that these data and other data used in the following analysis do not necessarily reflect the experience or mission of the National Weather Service.

In the course of the study, it was found that the frequency of taking readings was the most important factor affecting the least-cost choice. The current method provides one report per hour at each airport, with more frequent reports in critical situations. Assuming that more frequent reports might be required merely by the projected future volume of aviation operations, we also considered manual methods that would provide more frequent reports routinely.

It is important to note that under certain conditions the observer may have to make a number of instrument readings to obtain one recorded report. Thus, we have given the cost comparison in terms of the number of instruments and the frequency of making readings. The reader should be cautioned that the number of readings per hour is generally greater than the number of reports per hour.

Scope of the Comparison

Current methods of obtaining ceiling information are assumed to consist of a person operating a rotating beam ceilometer, performing calculations, making visual observations, performing judgment, and then recording results. The cost for obtaining measurements is thus assumed to consist of the cost of the ceilometer plus the cost of a person's time for the time involved. It also is assumed that the persons involved are provided cost-free facilities by the larger establishment (e.g., the airport weather office) and that this larger establishment can absorb usefully the remaining fraction of the observer's time (nonintegral number of persons) left over after obtaining ceiling measurements. In short, only the cost of the ceilometer and the fractional man-hour cost of the observations (cost of a possibly nonintegral number of persons) is included in the comparison.

For the automated system there is assumed to be no cost for operating personnel. The equipment is turned on by the cost-free larger establishment and the equipment then produces results.

For both methods there is no cost included for what is done with the results. The manual system has done its job when it has produced handwritten data in on a sheet of paper. For the automated system, the job is done when a punched tape or teletypewriter printout has been produced.

For both methods the costs included are:

(1) Amortization of original equipment cost

(2) Amortization of initial spare-parts inventory

(3) Labor involved in maintenance of equipment

(4) Parts costs in maintenance of equipment

(5) Amortization of equipment installation costs.

For both methods the costs not included are:

(1) The overall management function

(2) Utilities

(3) Office space

(4) Training

(5) Initial engineering studies.

Labor and equipment costs are as of 1971, and no inflation is assumed.

With the exception of the ceilometer, the equipment to be used has not yet been selected, and therefore it has been necessary to arrive at costs as a function of rough definitions. For this reason the use of judgment is necessary. To better bracket this judgment, high, medium, and low equipment costs have been used.

In the case of personnel costs and utilization, it is also not clear as to the exact amounts to be considered. The personnel cost given by the Federal Aviation Administration appears to be salary only, whereas there is usually about 100 percent overhead and/or payroll burden on most salaries. Also, the personnel utilization factor given by the Federal Aviation Administration is not definitive. For these reasons, it has been found necessary to use judgment. As will be seen below, the judgment is bracketed by using high, medium, and low cost estimates.

C. Cost Assumptions and Data for the Current Manual Method

Though one can assume that there already is a rotating beam ceilometer at each airport, it is also true that they will eventually wear out or become obsolete. Therefore, it was decided to amortize the ceilometer to obtain the most equitable comparison.

1. Cost and Installation

From Weather Measure Corporation (undated), the purchase cost of the ceilometer is $20,000. However, its installation cost will vary. Weather Measure Corporation (undated) gives evidence to support an average of $2,000 for installation. In keeping with our plan to provide a spectrum of cost estimates, $1,000, $2,000, and $3,000 have been used as low, medium, and high installation costs respectively.

2. Initial Spare-Parts Inventory

For electronic equipment, an often used, and usually reliable factor for the cost of initial spare parts is 33 percent of original cost. For the low estimate this cost was left out, and for the high estimate it was doubled.

3. Maintenance

Maintenance of the ceilometer consists of purchased labor plus replacements to the stock of spare parts. Values of 10 percent,

20 percent, and 30 percent of the initial cost have been used as historically valid factors for low, medium, and high maintenance costs, respectively.

4. Personnel

The Federal Aviation Administration gives $11,700 per year as the cost of a man, and states that considerably less than 1/5 of his utilization is for the ceiling measurement function. The $11,700 does not, but ought to, include overhead. One would be inclined to double the $11,700 to include overhead, and multiply the 1/5 by $\frac{2}{3}$ or $\frac{1}{2}$; this assumes that the time required for a weather observation is about 1/5 of the observer's time, and about two-thirds or one-half of this is used in making the ceiling observation. We have chosen the latter, and arrive at $\$11{,}700 \times 2 \times \frac{1}{5} \times \frac{1}{2} \simeq \$2{,}400$ as the medium manpower cost for obtaining and recording ceiling measurements hourly. Other combinations of overhead rate and utilization multiplier could arrive at the same figure. For low and high costs, we use half and one-and-a-half of this amount, respectively, resulting in $1,200, $2,400, and $3,600 per reading per hour per year.

When readings are to be taken more frequently than hourly, we assume that the one ceilometer is adequate but that the manpower must increase in direct proportion to the number of readings per hour. The resulting cost spectrum for the current manual method is given in Table 1.

D. Assumptions and Data for the Proposed Automated Method

1. Cost and Installation

The proposed automated method would use from one to six ceilometers, and all of these possibilities are analyzed herein. The cost assumptions for the ceilometer are the same as stated in the previous section.

The ceilometers are activated by and give analog results to a "multiplexer," which, in turn, is driven by a minicomputer. The multiplexer gives digital information to the computer. For multiplexer described in Weather Measure Corporation (undated) and by the $500-$1,000 cost of analog-to-digital conversion when there is no multiplexing

Table 1

COST TABLES AND FORMULAS FOR THE CURRENT MANUAL METHOD

K	L	M*	N*	P*	Q*	P + Q*
				N × 5	Five-Year Cost of One Ceilometer (see page 102)	
Readings per Hour	Time Between Readings (Min.)	Cost per Reading per Hour per Year (labor)	K × M Yearly Cost of Readings (labor)	Five-Year Reading Cost (labor)	Lo 1.00 B + E + 5x.1B Med 1.33 B + E + 5x.2B Hi 1.66 B + E + 5x.3B	Five-Year Cost
			Low Cost			
1	60	1.2	1.2	6.0	31	37
3	20	1.2	3.6	18.0	31	49
5	12	1.2	6.0	30.0	31	61
6	10	1.2	7.2	36.0	31	67
12	5	1.2	14.4	72.0	31	103
60	1	1.2	72.0	360.0	31	391
			Medium Cost			
1	60	2.4	2.4	12.0	48	60
3	20	2.4	7.2	36.0	48	86
5	12	2.4	12.0	60.0	48	108
6	10	2.4	14.4	72.0	48	120
12	5	2.4	28.8	144.0	48	192
60	1	2.4	144.0	720.0	48	768
			High Cost			
1	60	3.6	3.6	18.0	66	84
3	20	3.6	10.8	54.0	66	120
5	12	3.6	18.0	90.0	66	156
6	10	3.6	21.6	108.0	66	174
12	5	3.6	43.2	216.0	66	286
60	1	3.6	216.0	1,080.0	66	1,146

*In thousands of dollars

function. Various multiplexers are on the market costing from $2,000 to $15,000, the variation being due to many things, including the multiplex number. For low, medium, and high costs for the multiplexer we have assumed an initial cost of $500, $1,000, and $2,000 per ceilometer, respectively.

The minicomputer maintains the clock function and drives the multiplexer. It then obtains digital information, and computes and states results. An examination of the relative costs showed a minicomputer to be much less costly than the possible use of a shared-time computer. This is especially true as the desired readout frequency increases. Minicomputer costs run from $5,000 to in excess of $25,000. Those costs in excess of $25,000 are usually for complex output devices. It is assumed here, however, that the output is a punched paper tape and/or a teletype printout. Values of $10,000, $15,000, and $25,000 have been assumed to indicate low, medium, and high costs, respectively.

2. Initial Spare Parts and Maintenance

For the multiplexer and the minicomputer, the same assumptions are made as for the ceilometer concerning cost of initial parts, stocks, and maintenance costs. It is assumed that each item of equipment has an average expected life of 10 years.

3. Personnel

No personnel costs are involved. The cost spectrum for the proposed automated method is given in Table 2.

E. Findings

Figures 32, 33, and 34 show the numerical results in graphic form as obtained from Tables 1 and 2. The diagonal lines on these figures represent the five-year cost of ceiling readings using the present method. Near the right-hand edge of this graph, at 60 minutes between readings, the current costs can be read. Low, medium, and high are about 37, 60, and 84 thousand dollars, respectively, as can be verified in Table 1. If readings are to be taken at intervals shorter than 60 minutes, then more manpower will be required. Moving left across the graph, as the reading interval decreases the cost increases. On the graphs it can be seen that if readings are to be taken every two minutes with the present method, then the five-year costs--low, medium,

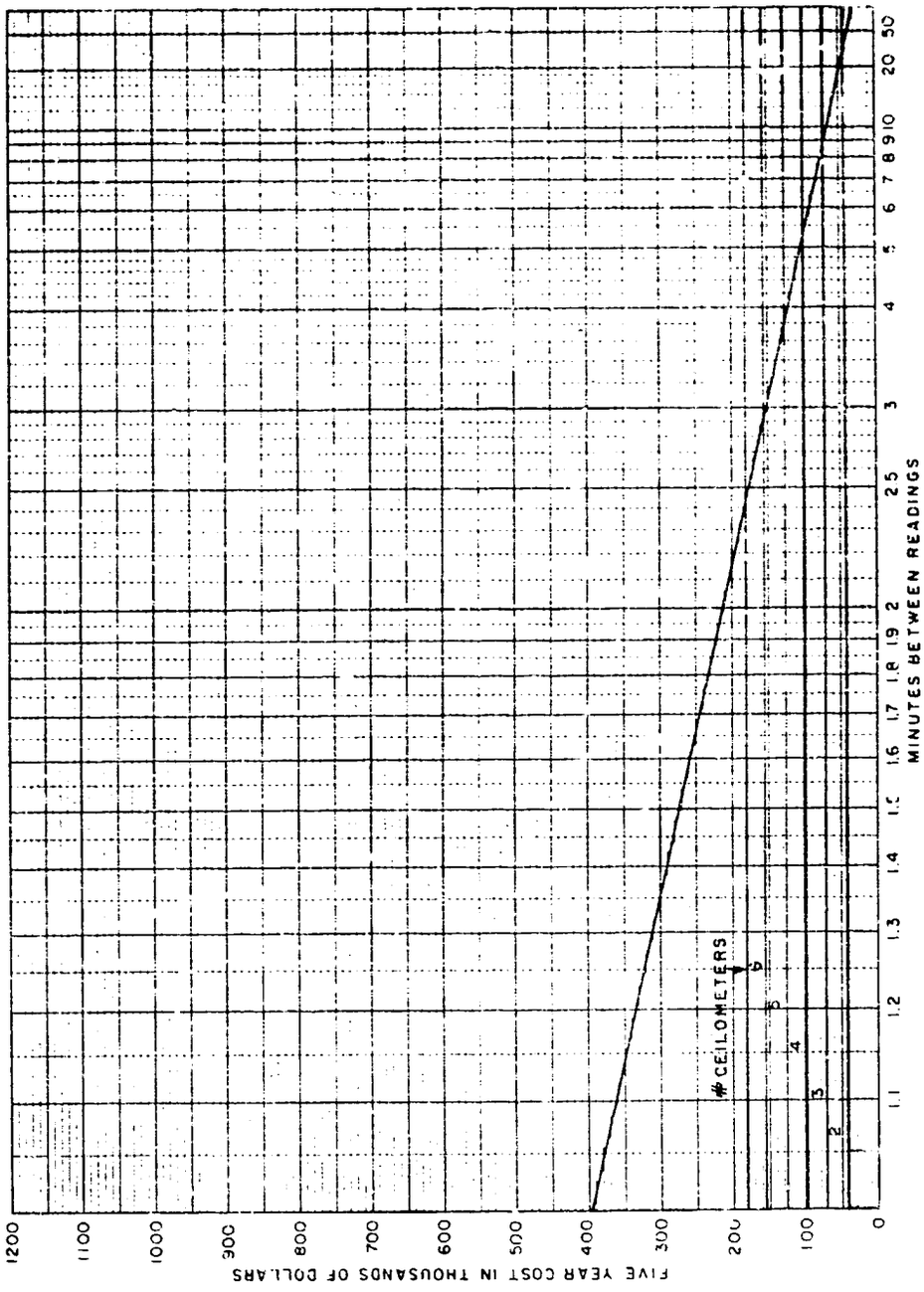

FIGURE 32 COST OF MANUAL AND AUTOMATED SYSTEMS: LOW COST CASE

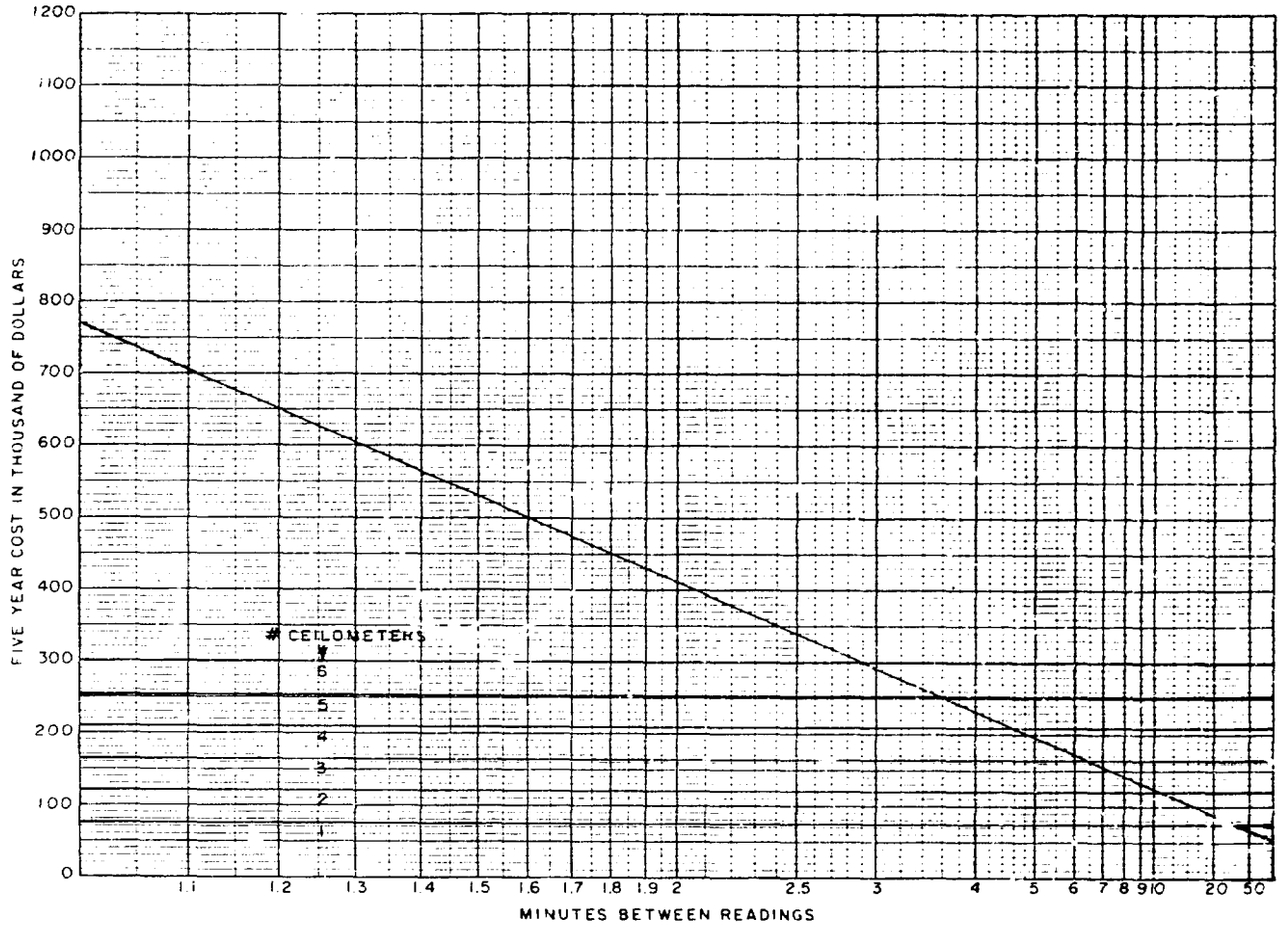

FIGURE 33 COST OF MANUAL AND AUTOMATED SYSTEMS: MEDIUM COST CASE

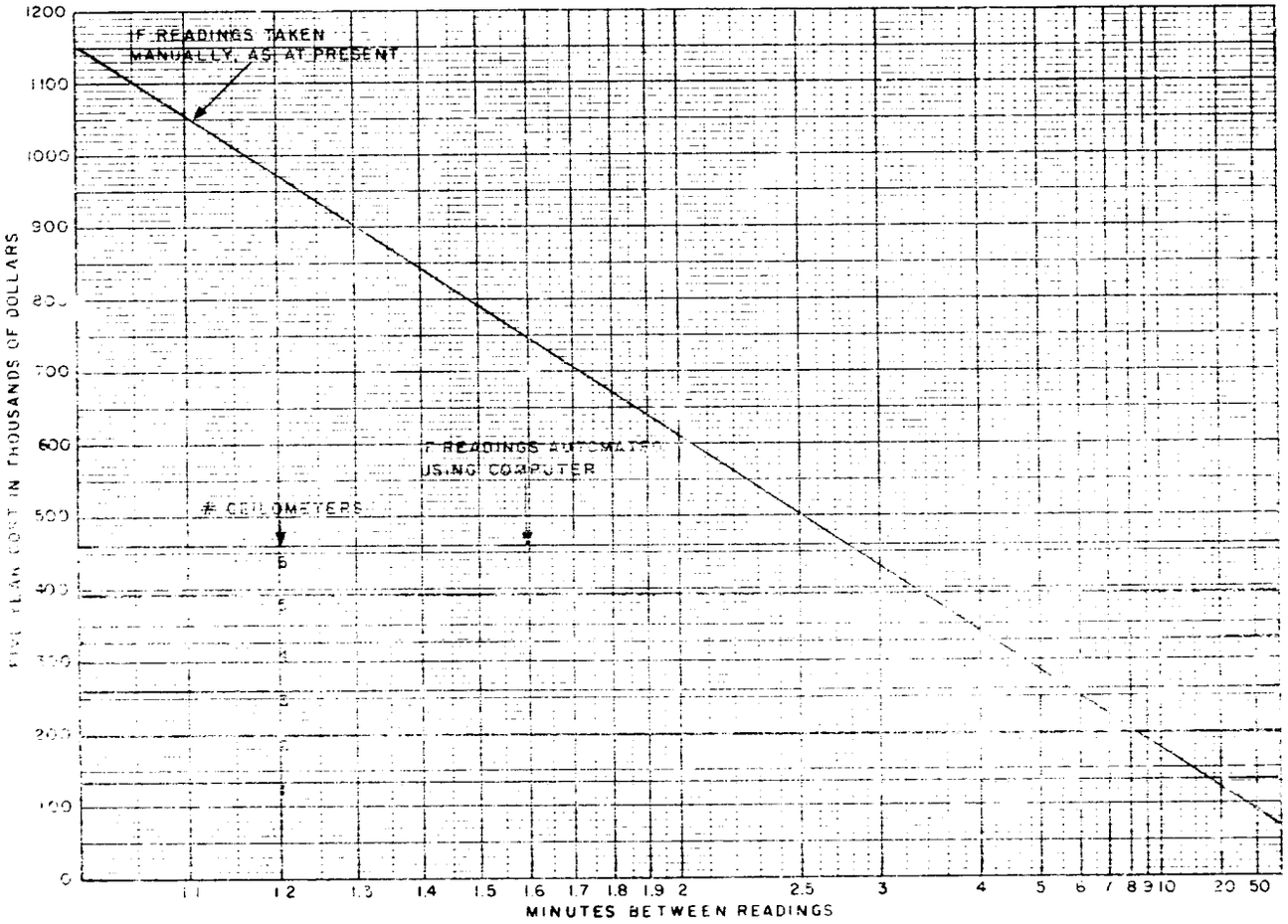

FIGURE 34 COST OF MANUAL AND AUTOMATED SYSTEMS: HIGH COST CASE

Table 2

COST TABLES AND FORMULAS FOR THE PROPOSED AUTOMATED METHOD

No. of Ceilometers	A* Minicomputer	B* Ceilometer	C* Multiplexer	D* .33(A+B+C) Initial Stocks	E* Ceilo. Install.	F* A+B+C+D+E Tot. Init. Cost	G* $\frac{F}{10} \times 5$ Five-Yr. Amort.	H* Lo: F × .1 Med: F × .2 Hi: F × .3 Yearly Maint.	I* H × 5 5-Yr. Maint.	J* Lo: F Med: $\frac{3F}{2}$ Hi: 2F Five-Year Cost
Low Cost										
1	10	20	.5	10.2	1	41.7				41.7
2	10	40	1	17	2	70				70
3	10	60	1.5	23.8	3	98.3				98.3
4	10	80	2	30.7	4	126.7				126.7
5	10	100	2.5	37.5	5	145				145
6	10	120	3	44.3	6	183.3				183.3
Medium Cost										
1	15	20	1	12	2	50				75
2	15	40	2	19	4	80				120
3	15	60	3	26	6	110				165
4	15	80	4	33	8	140				210
5	15	100	5	40	10	170				255
6	15	120	6	47	12	200				300
High Cost										
1	25	20	2	15.7	3	65.7				131.4
2	25	40	4	23	6	98				196
3	25	60	6	30.3	9	130.3				260.6
4	25	80	8	37.7	12	162.7				325.4
5	25	100	10	45	15	185				390
6	25	120	12	52.3	18	227.3				454.6

*In thousands of dollars

and high respectively--are 210, 410, and 610 thousand dollars. This represents about a fivefold increase in cost. Using the diagonal line, costs can be read for the present method for any reading interval down to one minute.

The automated systems have the capability of giving readings as frequently as desired above about 15 seconds. Thus, on the graphs they lead to horizontal lines. Their costs are fixed by the number of ceilometers that they use, and can be read directly on the graphs. The medium costs for one through six ceilometer systems respectively are: 75, 120, 165, 210, 255, and 300 thousand dollars (as can be verified in Table 2) regardless of the time interval between readings. Because they use more equipment, it can be seen that at readings of 60-minute intervals they are always more costly than the present method; but if readings are to be taken every two minutes, then all of the automated methods are better than the manual method.

Thus, using the graphs it is possible in a number of ways to compare the present method to the proposed method. Some examples follow.

Suppose that it has been decided a priori that the reading interval ought to be five minutes. Then Table 3 can be obtained from the graphs.

Table 3

COST COMPARISON WITH READING INTERVAL OF FIVE MINUTES

Cost Estimate	5-Year Cost (thousands of dollars)						
	Present Method	Number of Ceilometers in Automatic System					
		1	2	3	4	5	6
Low cost	102	42	70	98	127	145	183
Medium cost	195	75	120	165	210	255	300
High cost	273	131	196	261	325	390	455

From Table 3 it can be seen that for a 5-minute interval airports using 1, 2, or 3 ceilometers with the automated method would achieve lower

cost than will airports with the present method. But the opposite would be true for airports using 4, 5, or 6 ceilometers with the automated method.

Another way of using the charts would be to hypothesize a situation in which a maximum of $250,000 were available for each airport and it would be used to minimize the time interval between readings. Table 4 shows the results of such a comparison.

Table 4

SPEND UP TO $250,000 AT EACH AIRPORT AND MINIMIZE THE TIME INTERVAL BETWEEN READINGS

Cost Estimate	Present method ($250,000 is spent) time interval achieved	Proposed method (time interval <1 minute)
Low cost	1.67 min.	all airports <$250,000
Medium cost	3.5 min.	1-4 ceilometer airports <$250,000
High cost	5.2 min.	1-2 ceilometer airports <$250,000

In Table 4 it can be seen that airports requiring 1 or 2 ceilometers in the automated method would spend less money and achieve better results than the present methods. For airports requiring more than 2 ceilometers for the automated method a more careful cost study is needed before the decision could be made.

A number of other interesting relationships can be found in the graphs, but the one proposed here as the most meaningful is shown in Table 5. This table was constructed from the graphical findings to show those reading intervals for which one method is superior to the other, regardless of cost uncertainty. Note in Table 5 that for reading intervals greater than 45 minutes the current manual method is superior (costs less). For reading intervals of 2 minutes or less the automated method is superior, even at 6-ceilometer airports. In between these limits the choice is a function of the number of ceilometers required by the automated system. When the number of ceilometers is known, then the uncertainty band, due to cost uncertainty, is small.

Table 5

COMPARISON OF MANUAL AND AUTOMATED SYSTEMS, REGARDLESS OF COST UNCERTAINTY

Interval between readings (minutes)	Number of Ceilometers					
	1	2	3	4	5	6
1	A	A	A	A	A	A
2	A	A	A	A	A	A
3	A	A	A	A	A	U
4	A	A	A	U	M	M
5	A	A	A	M	M	M
10	A	U	M	M	M	M
12	U	M	M	M	M	M
15	U	M	M	M	M	M
20	U	M	M	M	M	M
30	U	M	M	M	M	M
45	M	M	M	M	M	M
60	M	M	M	M	M	M

A = Proposed automated better than current manual regardless of cost uncertainty.

M = Current manual better than proposed automated regardless of cost uncertainty.

U = Uncertain.

The overwhelming importance of the reading interval is clear. If it is not to be reduced, then present systems are adequate. If it is to be reduced, then the proposed automated system becomes increasingly desirable.

VII CONCLUSIONS

The research effort described in this report was a theoretical study of the problem of automatically describing cloud amount and cloud base height. The study was based on the analysis and computer simulation of a theoretical cloud model. To the extent that this model gives an adequate representation of actual cloud conditions, this study demonstrated the theoretical feasibility of automation. It was shown that cloud amount estimates more accurate than those of human observers can be obtained by properly averaging the responses of an appropriate number of conventional vertically-pointing instruments. It was also shown that clustering techniques can determine the number of cloud layers, the mean height of each layer, and the cloud amount in layers.

The definitions of cloud amount and cloud base height used in this work corresponded to the way these quantities were defined in the cloud model. Thus, the cloud amount in a given layer was defined as the fraction of the ground area covered by clouds in that layer and not covered by clouds in lower layers. The cloud base height for a given layer was defined as the average height of the base of the clouds in that layer. When the distance between two layers is small relative to the standard deviation for the cloud base, the clustering procedures may not be able to resolve the two layers. In such cases, it may ultimately be preferable to adopt the operational definition that the number of layers and the mean base heights for each layer are defined by the results of clustering. However, this is not recommended until more experience with the characteristics of the clustering procedures has been obtained.

The number and characteristics of the instruments required for an automatic system depend on the performance specifications. A number of theoretically and experimentally determined relations between the accuracy, number of instruments, sampling interval, area covered, cloud parameters, and averaging time were presented. Design curves were given to show how these relations can be used to establish some of the more important instrument and computational requirements. This report did not address the question of how the performance specifications

should be determined, or the question of how the cloud parameter data should be obtained. These are important topics that must be treated with care in the design of an actual automated system.

A simple cost comparison of the present manual and possible automatic systems was made to address the question of economic feasibility. In making a comparison, it was assumed that the systems gave equivalent performances, and other possible benefits of either system were not considered. The results were found to depend heavily on the frequency with which instruments must be read and the number of instruments required for an automatic system. If a frequency of one reading per hour is satisfactory, then the manual system is definitely less expensive. The crossover point occurs in the frequency range of six to twelve readings per hour, the exact results depending on the number of instruments required and the effects of cost uncertainties.

Appendix A

CLOUD DETECTION BY SCANNING MICROWAVE RADARS

by R. H. Blackmer, Jr.

1. Introduction

Microwave radars operate in the frequency range between 100 Mhz and 100 GHz. Within this frequency range, many meteorological targets including clouds are detectable. Interest in cloud detection led to the design, testing, and operational use of radars specifically for cloud detection. Because of the nature of cloud cover, the end result to date has been radar sets with short wavelengths, say 0.86 cm, a transmitting and receiver antenna oriented in a fixed position directed toward the zenith, and a short pulse length, narrow beam, and low power output.

While radars with the above characteristics have evolved as the optimum systems to meet old requirements, i.e., as an instrumental aid to human observers, they are not necessarily the optimum answer in a fully automated system. Parallel to the development of these "radar ceilometers," there have been developments in other types of radar systems for other purposes that could aid or even replace the radar ceilometers, depending on various trade-offs in cost and type of data desired.

If three-dimensional data on cloud cover at frequent intervals are desired, then a narrow, fixed vertical beam is obviously not acceptable, and a scanning antenna system must be employed. The problems of attempting to scan with one of the radars designed as a vertically pointing cloud ceilometer were discussed at length by Blackmer and Ligda (1963). Cogent points from their report will be presented later in this report.

If accurate cloud base measurements (especially when low clouds prevail) are desired for airport operations, the types of currently available radars capable of scanning in three dimensions may not suffice since they have some severe limitations in the detection of clouds at short ranges and low elevation angles. These systems and their limitations will be discussed later.

The problem then is to:

(1) Specify the operational requirements

(2) Examine the characteristics of current equipment to see how well it meets these requirements, and

(3) Make recommendations for either new equipment or new use of old equipment to result in a system that will meet operational requirements.

This Appendix will touch briefly on Items 1 and 3 and will consider Item 2 in detail.

2. Operational Requirements

Since the objective is an automated system to provide cloud amount and height over an area the size of an airport (or larger), some sort of scanning instrumentation is required. To meet this general requirement it is necessary to scan the volume rapidly enough so that clouds do not change substantially during the period required and to feed the results of the scan into some computation system that can convert the frequency of target detection into percent of cloud cover at various levels. Further, it will be necessary to eliminate noncloud targets that are radar-detectable. Depending on the characteristics of the radar, such targets as insects, birds, aircraft, refractice index gradients, chaff, lightning, balloons, smoke, dust, and ground targets in sidelobes may be detected. A radar capable of detecting all clouds would undoubtedly detect many of the above-listed noncloud targets, so there must be some trade-offs between the amount of cloud detected and the number of noncloud targets detected.

3. Cloud Measurement Using Current Radars

One of the more widely used radar ceilometers is the AN/TPQ-11 vertically pointing radar. Table A-1 lists the characteristics of this radar together with the characteristics of radars used for long range precipitation detection or for research purposes.

The table shows that the Wallops Island radar, except for the longer wavelengths, is in some respects superior to the TPQ-11, e.g., the transmitted power is much higher, the antenna is larger, and the minimum detectable signal is lower. The longer pulse length would, of

Table A-1

RADAR CHARACTERISTICS

Radar	Wallops Island			AN/CPS-9	WSR-57	AN/TPQ-11
	X Band	S Band	UHF	X Band	S Band	Ka Band
Wavelength, cm	3.2	10.7	71.5	3.2	10.3	0.86
Antenna diameter, m	10.4	18.4	18.3	2.8	3.7	2.2
Beamwidth, degree	0.21	0.48	2.9	1.0	2.0	0.25
Pulse length, μ sec	2	2	2	0.5 and 5	0.5 and 4	0.5
Antenna gain (dB > isotropic radiator)	58 3.8×10^5	51	35	42	39	56
Peak transmitted power (10^6 watts)	0.9	3.0	6.0	0.25	0.5	0.14
Minimum detectable signal (dBm)*	- 101	- 111	- 112	- 104	- 109	- 99
Minimum detectable cross section at 10 km, cm^2	6.0×10^{-4}	2.5×10^{-5}	3.4×10^{-5}			
Corresponding water sphere diameter for above, cm	0.26	0.33	1.3			
Minimum detectable reflectivity at 10 km, cm^{-1}	2.6×10^{-15}	2.0×10^{-17}	7.6×10^{-19}			

*Decibels relative to a milliwatt

course, be a detriment to the accurate determination of cloud base height when the beam was pointed vertically.

All the radars listed except the AN/TPQ-11 scan either horizontally or vertically or can be operated as a vertically pointing instrument. The AN/TPQ-11 is designed only for operation in the fixed, vertically pointing position.

The AN/CPS-9, because of its relatively low power output, and the WSR-57, because of its long wavelength, do not detect many clouds until the particles within them become quite large. The relatively broad beamwidths of these radars would make it impossible to measure accurately the altitudes of clouds, and low clouds would merge with ground targets.

The Wallops Island Radar has been used widely in the study of clear air echoes, but little has been published about the detection of clouds by this radar. In some instances, however, cirrus cloud has been present or convection has proceeded to the point that visible convective clouds were forming. On these occasions the cloud cover presents a solid target that is distinguishable from noncloud targets.

During periods when the atmosphere is visually clear the radar may show a number of layers of refractive index discontinuity between the surface and the tropopause. The level of the tropopause itself is often evident in the radar return. In illustrated examples of the clear air radar returns, presented by Mather and Hardy (1970), the problem of detection of ground targets and aircraft is obvious. Detection of these targets in sidelobes of the beam results in the presentation over a broad altitude range when the antenna is scanned in the vertical. The same would be true on a horizontal scan, so without some method of eliminating these noncloud returns these "super-sensitive" radars would not be useful as part of an automatic cloud-reporting system.

The possibility of scanning these sensitive radars at reduced gain for cloud detection could be considered, but instead of operating these radars in such a manner it might be more economical to build a less sensitive radar for cloud detection. However, in the event that such radars were brought into widespread use for such tasks as detection of clear air turbulence, for example, joint use at reduced sensitivity for cloud

detection might be feasible. This possibility is considered in more detail in the next section.

4. Modification of Present Radar Systems

Atlas (1968) discusses in detail methods of clear air turbulence detection. He concludes that sensitive radars, because of their size and cost, would be of questionable economic feasibility unless they can be time-shared for other purposes. However, he states that a radar suitable for clear air turbulence detection "would also be an effective cloud base and top indicator as well." In his discussion of adapting surplus military radars for clear air turbulence, he estimates a modification cost of $39,000 per unit. Presumably this is with a fixed, vertically pointing antenna, and a mount for a rotatable antenna would add to the expense. Such expense would probably be justified, since scanning would probably be necessary to give the required aerial coverage.

Blackmer and Ligda (1963) made a study of the increased cloud detection possible with a radar with a fixed scanning angle. The angle chosen by considering the size of the vertical component of the pulse volume was 53 degrees from the vertical. A scanning rate of one revolution in 12 minutes was chosen on the basis of the radar data recording system. At this scan rate one degree is 10 recorder sweeps. With this angle the altitude at which clouds are detected varies from the surface at the antenna to 60,000 feet at 13 nautical miles. Clouds around 1,000 feet would be detected at a distance of two nautical miles. Such operation would not fulfill the requirement for a scanning radar covering all altitude intervals over an airport. A series of elevation angles would be required to cover a broad altitude range.

At the fixed altitude scan of 53 degrees the presentation of the clouds on the display scope suffered serious distortion. The report by Blackmer and Ligda gives several examples of what the cloud cover would look like when scanned vertically and would look like when scanned at 53 degrees. Scanning would obviously require some type of constant altitude presentation to make order from the chaos that scanning at a single angle would give. Data processing of scans at multiple angles would

be very complex even with only a simple "yes" or "no" as to whether or not there was echo at a given slant range on each scan. To quantify echo intensity at a number of ranges at a number of elevation angles and to convert these numbers to percent of cloud cover at various heights would be very complicated. The problem arises when the beam intercepts the base of the clouds at one range and the sides of the clouds at a greater range when there is one layer of clouds. When there are multiple layers, one can never be sure whether the beam is intercepting the base of the clouds with a single scan angle. Multiple scan angles must be rapid enough so that clouds do not move or change much between scans so that a given cloud element can be identified on subsequent scans. Modification of present radar ceilometers for rapid scanning over a sector containing an airport should be considered. Scanning a sector would be simpler than a 360-degree scan and, if only the lowest clouds were of interest, the radar could be located so that the range of elevation angles required would be limited. There would be some trade-off required between distance from the airport and range of elevation angles. If the radar was close to the airport, the range of elevation angles required would be greater. If the radar was far from the airport, the range of elevations would be smaller, but the greater distance from radar to clouds might reduce the chances of detecting some clouds.

Present weather radars could undoubtedly be modified in the manner Atlas suggested for surplus military radars at a cost of about $40,000 each. Better still, current ultrasensitive cloud radars could be used to study clouds, a determination made of how much the sensitivity could be reduced, and a new radar built incorporating the results of the study.

5. Summation

There are in use today fixed vertically pointing radar ceilometers and precipitation-detecting scanning weather radars. Neither of these two types of equipment can provide three-dimensional information on cloud distribution over an airport either for aviation purposes or for general meteorology. Either type of equipment could be modified: the radar ceilometer by devising some type of rotatable antenna mount, although

the limitations in cloud detection capability would still exist; the weather radars by adding larger antennas, parametric amplifiers, and an integrator.

In addition to the two types of operational radars, there are ultrasensitive research radars used for the study of clear air phenomena. Such radars can also detect clouds but would probably be too expensive for widespread operational use as cloud detection sets. Such radars could serve, however, as prototype units and studies made of how much the sensitivity could be reduced, and from such studies a new scanning cloud radar could be designed and built.

Whatever radar is finally used will require elaborate auxiliary equipment to filter out birds, insects, clear air returns, etc., and convert the received signal into useful cloud information. Design of such equipment may be more difficult than design of the radar and will certainly require extensive study.

Appendix B

LIDAR MEASUREMENTS OF CLOUD BASE

by R. T. H. Collis

1. Introduction

The use of the radar principle to measure cloud base with pulsed light was first employed in France in 1939 (Bureau, 1946). Developments of this approach using flash lamp light sources have been used routinely for many years (Perlat and Petit, 1961). The advent of the pulsed laser in the early 1960's, however, marked the beginning of a series of major improvements that are still in progress. Initially using giant-pulsed "Q-switched" ruby lasers, a number of workers demonstrated the facility with which "lidar," as the technique has become known, could make observations of clouds and measure the heights of their base (Collis, 1965; Andermo et al., 1965).

Although these developments were largely concerned with research, either into the lidar technique or with atmospheric phenomena (e.g., Collis et al., 1968), some attempts have been made to develop lidars for use in routine cloud base measurement (ASEA, 1968; Bird and Rider, 1968) and to explore their use in this role (Viezee et al., 1969). The problems involved in this application were discussed further by Collis (1969), who gave particular note to safety considerations. The safety problem as well as various technical factors has led to the exploration of lasers operating outside the visual range, and low-peak-power systems using solid-state lasers are under development (e.g., Sperry Rand, 1971).

Although there can hardly be any doubt that the lidar technique of cloud observation is preeminent for research applications, considerable problems remain to be solved before its full potential can be realized in practical operational systems intended for untended routine use at meteorological observing stations.

2. Basic Lidar Concept

In its basic form, lidar employs a laser simply as a source of pulsed energy. In typical high-peak-power systems, Q-switched ruby or neodymium doped glass lasers are used to generate light pulses having peak powers of tens of megawatts and durations of 10-20 nanoseconds.

These pulses are directed in highly collimated beams by suitable optical systems. Energy backscattered by the atmosphere is detected by a photomultiplier after collection by a lens or reflector system. The resulting signal is evaluated as a function of time from the transmission of the pulse. It is typically displayed on an oscilloscope, either directly or after storage in a magnetic-disc video recorder. Polaroid or other photographs may be used to record the displayed data.

Taking advantage of the monochromatic nature of the laser energy, narrow-band optical filters may be used in the receiver system to minimize "noise" caused by extraneous light and thus make daytime use readily possible. The nature of the received signal, P_r, is given by the equation:

$$P_r(R) = P_t \, \ell \, \beta(R) \, A_r R^{-2} \exp\left\{-2 \int_0^R \sigma(r)dr\right\} \qquad (B\text{-}1)$$

where

P_r	is instantaneous recived power	(watts)
P_t	is transmitted power	(watts)
ℓ	is effective pulse length ($\ell = c\tau/2$ where c is the velocity of light and τ is pulse duration; it is the range interval from which signals are simultaneously received at time t.)	(m)
β	is the volume backscattering coefficient of the atmosphere	$(ster^{-1} m^{-1})$
R	is range ($R = c(t-t_0)/2$, where t_0 is the time of transmission of pulse	(m)
σ	is the volume extinction coefficient, and	(m^{-1})
A_r	is the effective receiver aperture.	(m^2)

The magnitude of β and σ depend upon the wavelength of the incident enery, and the number, size, shape, and refractive properties of the illuminated particles per unit volume. These range from the hydrometeors of precipitation, cloud, or fog, through the particulate components of the "clear" aerosol, to the molecules of the gaseous atmosphere.

In relatively clear atmospheres both the backscattering coefficient and the extinction coefficient are small, and increases in backscattering as a function of range can readily be interpreted. For example, the presence of a sudden increase in scattering due to a cloud layer is obvious and unequivocal. In strongly scattering conditions, however, marked attenuation occurs, and in observing a cloud, for example, the lidar return rapidly diminishes as the penetration of the cloud increases. The evaluation of lidar signals in such circumstances thus presents certain difficulties and imposes the need for care in making qualitative interpretations. Typical values of β and σ are indicated in Figure B-1.

A single lidar observation provides information on atmospheric scattering in a specified direction in terms of scattering intensity as a function of range. Series of such observations may be made by scanning at angular intervals within a plane. If this plane is vertical, a cross section may be derived that corresponds to a radar RHI (Range Height Indicator) display. By making successive observations in the zenith at a single location, a time/height display can be generated representing a form of vertical section parallel to the wind direction, or showing how the vertical conditions change with time.

3. Realization of Practical Cloud-Base-Measuring Systems

A. General

The application of the lidar concept in a practical operational form for cloud-base measurement involves two major technical problems and the ever-present problem of achieving technical solutions at an acceptable cost. The first technical problem is concerned with the acquisition of the basic raw data, and is essentially an engineering problem in which performance must be balanced against the time factor, complexity, safety requirements, etc. The second technical problem is the recovery of the wanted information from the raw data. The interrelations of these problems and their further involvement with the economics of the situation present a very complicated task to anyone considering how best to meet operational requirements that have themselves not been fully defined.

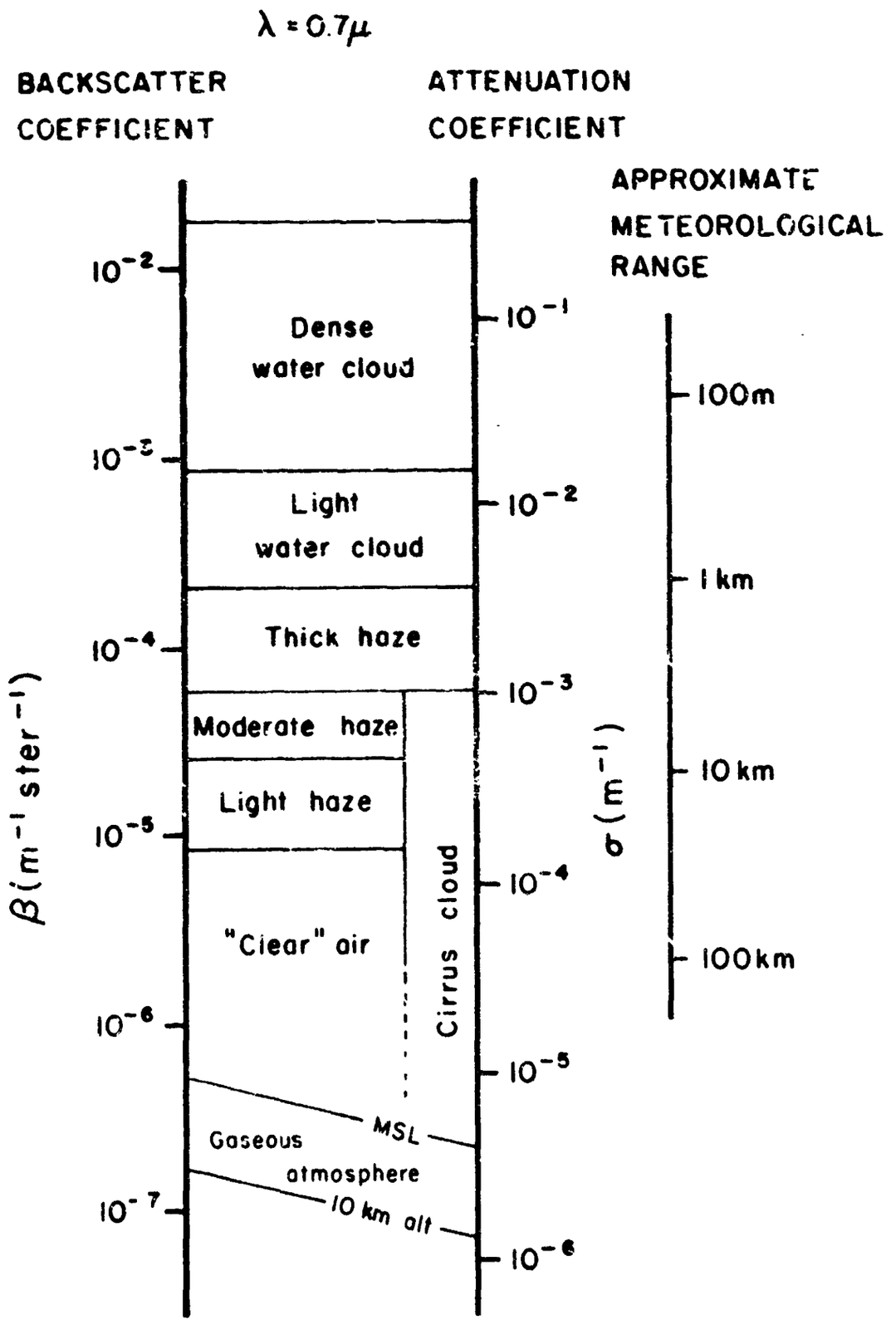

FIGURE B-1 VOLUME BACKSCATTERING AND ATTENUATION COEFFICIENTS CALCULATED FOR RUBY LIDAR WAVELENGTHS (0.7 μ)

The individual aspects of the problems are now considered separately, from which will be apparent the main uncertainties that must be resolved if lidar is to play a role in making routine cloud base measurements. In general, as would be expected, the solution appears the more feasible as the requirement becomes simpler. Difficulties grow rapidly as the fuller realization of lidar's potential is attempted.

B. Data Acquisition

The acquisition of signals of adequate intensity for evaluation depends upon the optical properties of the clouds and the intervening "clear" atmosphere, and upon the characteristics of the lidar. In the simplest case, where a well-defined cloud base is encountered above clear conditions with good visibility, the problem is simply one of optimizing the engineering variables so that the energy transmitted is sufficient to produce a signal larger than the minimum detectable signal from the range in question. The interrelation of the engineering variables will be apparent from a consideration of Eq.(B-1). The matter is discussed in greater detail by Northend et al. (1966) (see also Sperry Rand, 1971). With high-peak-power pulsed ruby or neodymium lasers, sufficient performance can readily be obtained with a single pulse. With such lasers, however, the question of eye safety arises. The immediate solution would be to use lasers that operate well outside the visual hazard range, i.e., at wavelengths longer than 1.4 microns (Wyman, 1969). Another solution is to reduce the energy transmitted in a single pulse and use a series of less intense pulses, integrating the returned signals to achieve detectable levels. The ultimate in this approach is to use very-low-intensity transmitted pulses from solid-state lasers. For example, gallium arsenide lasers operating at 0.91 micron wavelength can produce useful power levels at repetition rates of the order of 1,000 pulses per second. In the Sperry Rand Ga As lidar system, in fact, pulses of 1,000 watts peak power are used at repetition rates of 500 pps. With these, integration of as few as five pulses is adequate to yield workable signal levels from typical cloud bases under optimum conditions.

Intermediate solutions could employ neodymium YAG lasers (1.06 micron wavelength) operating at low to moderate peak powers at repetition rates of some tens per second.

Other steps can also be taken to reduce hazards further. Transmitted beam divergence can be increased to reduce energy density levels without serious loss of resolution (beam widths of the order of 1 or 2 degrees would be quite adequate, sampling areas some 500-100 ft in diameter at an altitude of 3,000 ft). However, this approach leads to an increase of the minimum detectable signal level, because of the greater background noise that will result from increasing the receiver beam divergence to correspond to that of the transmitter. Again, the peak power can be reduced by increasing the pulse length. Only a small benefit can be gained in this way before range resolution is seriously affected.

On the question of range resolution, Q-switched lasers typically produce pulse lengths of 20 nanoseconds or so--i.e., an effective range resolution of 1.5 m. With gallium arsenide lasers, pulse lengths are of the order of 100 nanoseconds (7.5 m effective range resolution). The technical problems of increasing these pulse lengths by substantial amounts have no ready solutions however.

Another technical problem of some difficulty is the dynamic range involved. This is particularly acute with the single pulse approach, for in strongly scattering atmospheres, energy scattered from very close ranges can saturate the detector system. This system has to be sensitive enough to handle very weak signals that are returned from more distant cloud [note the effect of the inverse range squared term in Eq.(B-1)], particularly after attenuation due to the turbidity of the intervening path. The use of integration to achieve adequate signal levels from multiple low-intensity pulses goes far to overcoming the problem of overloading the receiver, for a single pulse return will be small, even in strongly scattering atmospheres at close range. (If considerable time is needed to achieve adequate signal levels, however, this can result in a limitation of data rate.) The question of nearest possible detection range is important. Because of dynamic range problems,

and also considerations of the geometry of the optical systems involved that make it difficult to achieve adequate beam overlap at short ranges, the minimum range at which cloud may be detected can be restricted in any particular system. In typical research lidars of the type used at SRI, this range is of the order of 50 to 100 m unless special adjustments are made. The Sperry Rand Ga As lidar is designed to make measurements as close as 30 m.

Thus, as will be seen, the design of a lidar capable of acquiring the basic raw data for the determination of cloud information is very much a question of selection and compromise. As demonstrated with high-performance research equipment, virtually any information required can be gathered at any one time. The problem lies in deciding what a general-purpose practical system should be capable of doing.

C. Recovery of Cloud Information from Basic Data

The discussion of data acquisition above has mainly considered the case of clearly defined cloud bases encountered above relatively clear atmospheres. A lidar observation of such conditions is shown in A-scope form (signal amplitude versus range) in Figure B-2. However, when the cloud base is diffuse or low visual range conditions exist below the cloud, the interpretation of the lidar signature is much more complicated and becomes a sophisticated problem in pattern recognition. The same is true where heavy rain or snow is falling. (Figure B-3 shows extreme cases of this type.) The point is important, for although it may be relatively easy for a human observer to interpret one or other forms of lidar data display that are possible, the automatic determination of information by an inanimate system may be surprisingly difficult.

For example, Figure B-4 shows an RHI type of display in which data of the type shown in Figure B-2 are presented in a range-corrected intensity-modulated form, derived from a series of shots made by scanning the lidar in a vertical plane (Viezee, 1971). The nature of the cloud cover, particularly the height of the cloud base, is apparent at a glance. In contrast, the problem posed to a "black box", even in the relatively straightforward conditions illustrated, are considerable. (Note how the eye can readily perceive the base of the cloud at the left of the section,

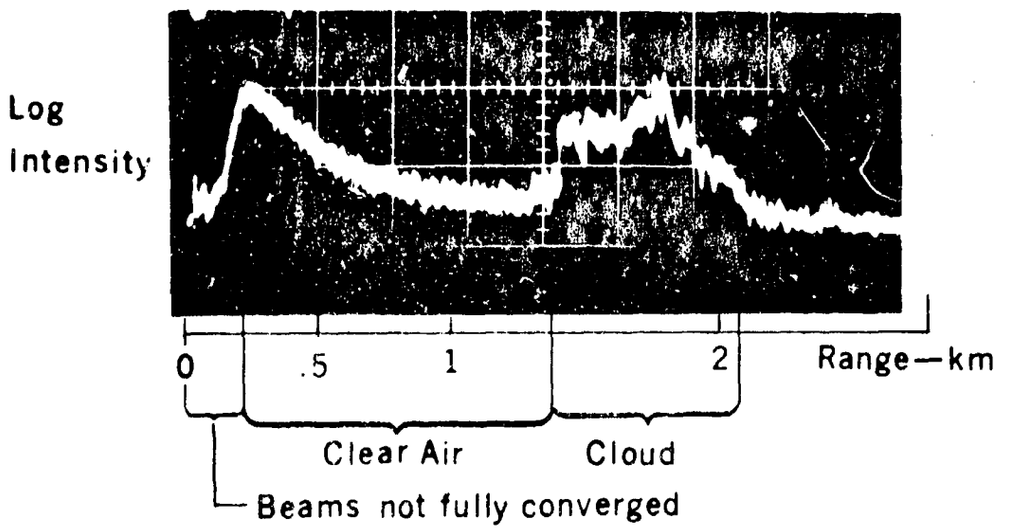

FIGURE B-2 OSCILLOGRAM OF TYPICAL LIDAR OBSERVATION OF CLOUD. Note how the signal from the clear air beneath the cloud decreases as an inverse function of range squared, and note also the attenuation within the cloud.

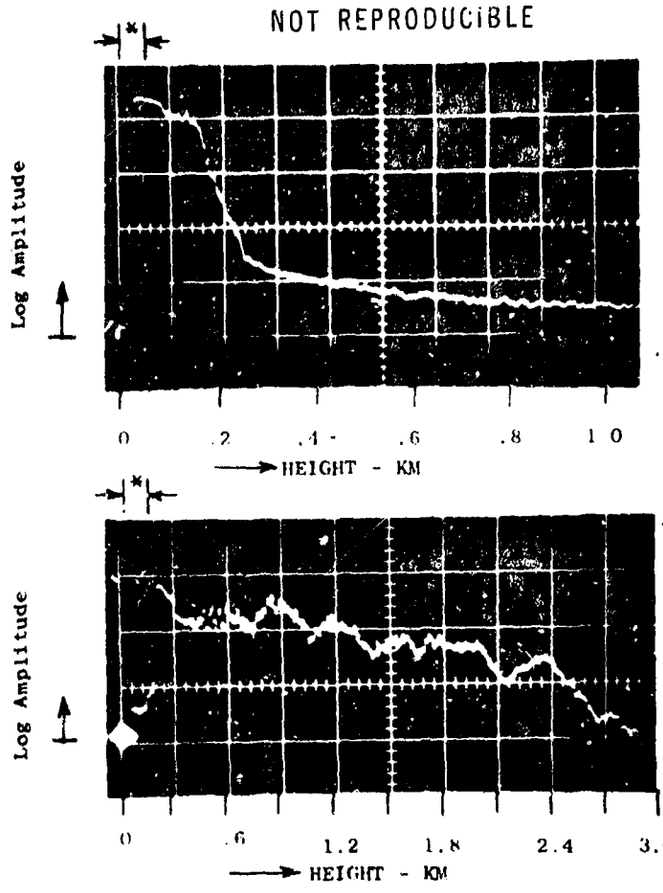

a

Hamilton AFB Elev. 47°
9 Jan. '68

Overcast, stratus with light drizzle and fog.

(Surface visibility 800 m)

150 m per range division

b

Menlo Park Elev. 90°
21 Aug. '68

Overcast, cumulonimbus with stratocumulus and intermittent very light rain.

(Surface visibility 10 km)

300 m per range division

* Region before full overlap of transmitter and receiver beams.

FIGURE B-3 OSCILLOGRAMS OF RUBY LIDAR OBSERVATIONS OF CLOUD BASE.
(a) Low stratus with light drizzle and fog at the surface.
(b) Cumulonimbus with stratocumulus; intermittent very light rain, surface visibility moderate

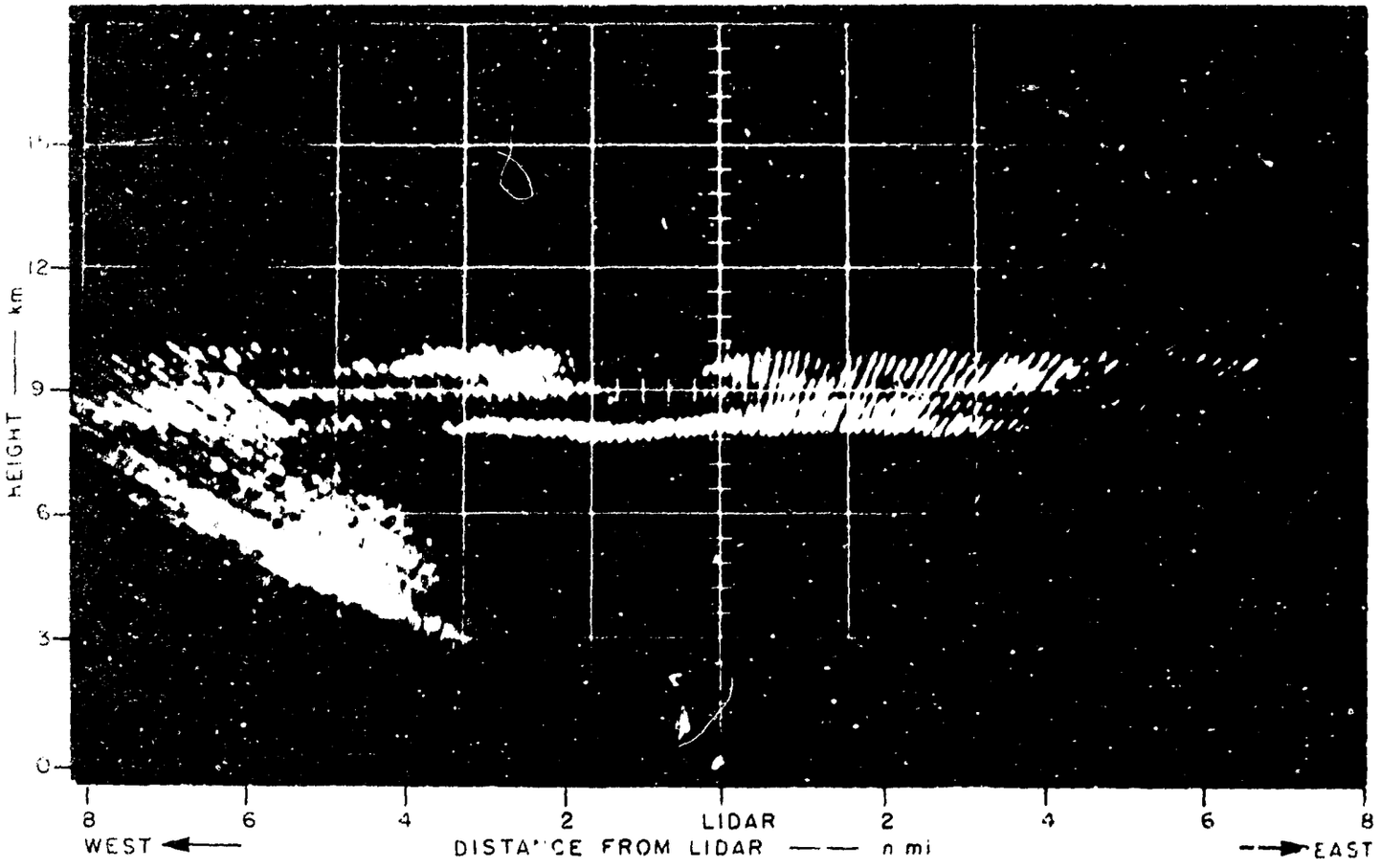

FIGURE B-4 VERTICAL CROSS SECTION MADE WITH SCANNING RUBY LIDAR SHOWING CIRRUS CLOUD LAYERS [from Viezee (1971)]. The display is from an intensity modulated CRT. Note that at the left of the picture where the lidar is pointed in the direction of the sun the forward scattering of solar energy causes an enhancement of the background noise. Because of slight nonlinearity in the range correction circuit, this noise is not uniformly displayed, and has the appearance of being a diffuse echo from above the surface. However, note how readily the cirrus layer can be perceived amid such noise.

even in the presence of considerable background noise.) In conditions such as those of Figure B-3 the task is essentially impossible. Even the relatively simple question of determining cloud base height requires that criteria be established for distinguishing what constitutes cloud base. As noted, this presents little difficulty when the base is well defined. Such automatic ranging devices that have been applied to this problem work very well in such circumstances. A timing device is triggered at the firing of the pulse and stopped when a significant signal is received from the cloud. The elapsed time may then be displayed or reported in digital form with some precision (electronic timing devices can readily provide the necessary accuracy, even at light velocities, for very precise measurement of distance). The first problem arises if the cloud base is diffuse. The returned signal increases as the pulse penetrates into the cloud but is simultaneously reduced by attenuation. In certain gradients of cloud density this will result in anything but the well defined sharp edged signatures that are appropriate for simple timing devices. Again, fluctuating signals due to variations in the turbid "clear" air below the cloud base can be confusing. The setting of arbitrary criteria as to what constitutes "cloud base" can thus lead to uncertainty and inaccuracy. (It should be remembered that the same problem is present with conventional, rotating beam ceilometers--and that the current definition of "cloud base height" is the height that the rotating beam ceilometer says it is.) Any simplified method of assessing and reporting "cloud base" suffers the further disadvantage of discarding some of the most valuable data that the lidar technique of cloud observation can provide--namely, a report on the nature of diffuse and ragged cloud bases, including information on the nature of conditions in the underlying layer, particularly when multiple layers are involved or where patches of diffuse cloud are present at various levels.

Mention of the latter condition raises the question of the spatial resolution required from a lidar ceilometer. Observations made in a single direction such as the zenith will provide samples of conditions at that point. Such samples can be made continuously or at intervals determined by the engineering aspects of the system. How well such

observations can represent the general conditions, even overhead, will depend upon the spatial and temporal variability of conditions and any motion that is present. In principle, of course, the lidar technique offers the possibility of scanning in two or three dimensions to derive much more complete information on the cloud cover situation. In practice, the engineering performance readily attainable will set a limit to this approach, and it is unlikely that more than two cross sections (derived at right angles) of the type shown in Figure B-4 could be achieved. An attractive alternative would be to make a circular scan at a fixed angle of, say, 60-70°. In this way conditions at each height level would be sampled around the circumference of a circle, the diameter of which would increase with height.

A further possibility is also available. If the beam is scanned in any systematic manner--for example, in a conical or circular scan or in one or more planes, the data acquired could be integrated before interpretation and presentation. In this way average or representative determinations of cloud-base heights, etc., could be more readily derived than by considering the data in basic form. While this has attractions, particularly where the acquisition of the raw data involves integration of many pulses, the resulting information would have serious deficiencies for many purposes for which cloud base-data are reported, and would again fail to offer the real benefit of lidar-acquired data.

This aspect of the problem is closely related to the method of presenting or reporting the information derived. Whether integration is performed before or after interpretation, or whether sampling in space and time is carried out, all involve the rate at which the raw data are acquired, and this in turn affects the complexity and sophistication required in the final display or reporting device. This is particularly so if the maximum recovery of data or utilization of the raw data is sought. For example, if it is sufficient to determine a single value of cloud height when a clear cut base exists, a very elegant slow-response digital range-evaluating system can be achieved by discarding all other data--which are redundant by definition. This is the course followed in the Sperry Rand Ca As system, in which a traveling range

gate scans through the total effective range of 3,000 ft. in 6 seconds. The range at which significant signals occur in the gate (i.e., above a predetermined threshold that varies with range) is thus readily determined as the "cloud base height." More complex systems with broad-band capability are needed to handle more complete information if comprehensive information on cloud-base conditions are required, or if the system is to produce accurate information in many types of weather condition encountered.

In summary, as with the acquisition of the raw data, the lidar technique offers very wide capability to make any type of presentation required. However, the cost and complexity of achieving any given degree of sophistication, especially if the system is to work on an untended, automatic basis, mount rapidly as any but the simplest ceiling measurement is attempted.

4. Safety

The question of safety has been alluded to above. Although the matter has often been exaggerated, the fact remains that laser energy improperly or injudiciously used can be hazardous to sight. Certainly, giant pulsed systems operating in the visible and near-infrared spectrum cannot be acceptable for automatic, untended use in the vicinity of airports because of the high peak power of the energy they produce. Although highly constrained in direction, there is always the chance that their transmitted beam will be viewed from above, and the possibility also exists that aluminum or other aircraft surfaces will reflect the energy back to the surface. The most certain way of avoiding any such risks is to operate either at sufficiently low peak powers as to leave an adequate margin of safety in terms of generating energy densities that can cause eye damage, or to operate well away from any frequency that can penetrate the outer surface of the eye and thus be focussed, however imperfectly, on the sensitive retinal surface, or worse still, on the critical fundus (Wyman, 1969; Vassiliadis, et al., 1969; Johnson, et al., 1970).

5. Conclusion

The lidar technique offers considerable potential and flexibility for the measurement of cloud base for operational purposes. However, the early realization of this potential depends upon overcoming the engineering and economic constraints imposed by the nature and complexity of the current technology. In particular, eye safety considerations indicate that low-peak-power systems should be used, but presently available low-peak-power lasers cannot achieve adequate performance fully to exploit lidar's capability for obtaining information over extended angles by scanning, or for that matter for achieving adequate range of detection in a fixed zenith pointing system. Even if adequate performance can be achieved with sufficiently high data acquisition rates, there remains the problem of integrating and processing the data. In this (as, of course, in other systems) the cost of sophisticated data processing could be considerable.

These are yet early days, however, in the development of lidar technology, and considerable progress can confidently be expected. The promise for the lidar technique may thus be considered to be very real, and exploration and definition of the expected requirements of a lidar cloud-ceiling monitoring system appears to be wholly justified at the present time, for no less reason than that a clearer understanding of the requirement will undoubtedly stimulate the appropriate technical development.

Appendix C

OPTIMUM SAMPLING INTERVAL FOR SINGLE-INSTRUMENT CLOUD AMOUNT ESTIMATION

In this appendix we derive the expected squared error for a single-instrument cloud-amount estimate and show how it depends on the time ΔT between samples. The analysis is for the special case of a single layer of nonoverlapping clouds, and only large-area cloud amount estimation is considered.

Without loss in generality, let the x-axis be aligned with the direction of cloud motion, and let the instrument be located at $x = 0$. Let $c(x + vt)$ indicate the presence or absence of a cloud over point x at time t, where v is the cloud speed. If ΔT is the time between samples, then the k^{th} instrument reading is given by

$$c_k = c(kv\Delta T) \quad . \tag{C-1}$$

We estimate the cloud amount by the average

$$\hat{c}_m = \frac{1}{m} \sum_{k=1}^{m} c_k \quad , \tag{C-2}$$

where m is the number of samples in the average. Defining the averaging time T by $m\Delta T$, we have

$$m = \frac{T}{\Delta T} \quad . \tag{C-3}$$

Let c_a be the large-area cloud amount, so that c_a is the expected value of c. It follows from Eq. (C-2) that

$$E[\hat{c}_m] = c_a \tag{C-4}$$

and

$$\sigma_m^2 = E[(\hat{c}_m - c_a)^2] = \frac{1}{m^2} \sum_{j=1}^{m} \sum_{k=1}^{m} E[(c_j - c_a)(c_k - c_a)] \quad . \tag{C-5}$$

In order to evaluate the expected error $\hat{\sigma}_m^2$, we must know the autocorrelation function for c(x). We assume that $c_a = 0.5$ and that*

$$E[(c(x)-c_a)(c(x+\zeta)-c_a)] = c_a^2 e^{-2|\zeta|/\ell_m} \quad , \tag{C-6}$$

where ζ is the correlation displacement and ℓ_m is the mean cloud length. From Eqs. (C-1) and (C-5),

$$\hat{\sigma}_m^2 = \frac{c_a^2}{m^2} \sum_{j=1}^{m} \sum_{k=1}^{m} e^{-2v\Delta T|j-k|/\ell_m} \quad . \tag{C-7}$$

From this and the formula

$$\sum_{i=0}^{m-1} \theta^i = \frac{1-\theta^m}{1-\theta} \tag{C-8}$$

we obtain

$$\hat{\sigma}_m^2 = \frac{c_a^2}{m(1-\theta)} \left[1 + \theta - \frac{2\theta(1-\theta^m)}{m(1-\theta)}\right] \quad , \tag{C-9}$$

where

$$\theta = e^{-2v\Delta T/\ell_m} \quad . \tag{C-10}$$

Note that $v\Delta T/\ell_m$ is the normalized cloud speed. As v/ℓ_m approaches infinity, the readings become uncorrelated, θ approaches zero, and $\hat{\sigma}_m^2$ approaches c_a^2/m. In this case we can make the expected squared error as small as we wish by letting m approach infinity. However, suppose instead that we fix the averaging time $T = m\Delta T$ and let m increase by

*This is equivalent to the assumption made in Appendix D, and discussed in greater detail there. If there were no overlap of clouds, it would be in complete agreement with our cloud model for five-tenths cover.

letting ΔT approach zero. In this case we obtain

$$\hat{\sigma}^2_{min} = \lim_{\Delta T \to 0} \sigma_m^2$$

$$= \frac{c_a^2}{vT/\ell_m} \left[1 - \frac{1 - e^{-2vT/\ell_m}}{2vT/\ell_m} \right] \quad . \tag{C-11}$$

This is the smallest value of $\hat{\sigma}_m^2$ that can be obtained merely by sampling faster. If ΔT is not zero, $\hat{\sigma}_m^2$ is greater than $\hat{\sigma}^2_{min}$, but it may not be much greater. We can derive the percentage increase in $\hat{\sigma}_m^2$ from Eqs. (C-9) and (C-11) as a function of $v\Delta T/\ell_m$ and vT/ℓ_m. These results are plotted in Figure C-1. Since the percentage increase is a monotonically decreasing function of vT/ℓ_m, it is bounded by the cases $T = \Delta T$ and $T = \infty$. This leads at once to the following bounds, which are also shown on Figure C-1:

$$\frac{\hat{\sigma}_m^2 - \hat{\sigma}^2_{min}}{\hat{\sigma}^2_{min}} \leq \frac{v\Delta T/\ell_m}{1 - \dfrac{1 - e^{-2v\Delta T/\ell_m}}{2v\Delta T/\ell_m}} - 1 \tag{C-12}$$

$$\frac{\hat{\sigma}_m^2 - \hat{\sigma}^2_{min}}{\hat{\sigma}^2_{min}} \geq \frac{v\Delta T}{\ell_m} \frac{1 + e^{-2v\Delta T/\ell_m}}{1 - e^{-2v\Delta T/\ell_m}} - 1 \quad . \tag{C-13}$$

Note that in the worst case $\hat{\sigma}_m^2$ is less than 20 percent greater than $\hat{\sigma}^2_{min}$ if $\Delta T = 0.25\ell_m/v$, and a further reduction in ΔT does not yield much further benefit. Thus, for example, if the mean cloud length is 200 ft. and the cloud speed is 10 ft./sec., there is little value in sampling faster than once every five seconds.

In theory, the minimum expected squared error $\hat{\sigma}^2_{min}$ can be reduced by increasing the averaging time T. In particular, if T is large relative to ℓ_m/v, σ_m^2 is approximately $c_a^2 \ell_m/vT$, which approaches zero as T approaches infinity. In practice, one can not allow T to become too large without losing the ability to respond to changes in c_a. Thus,

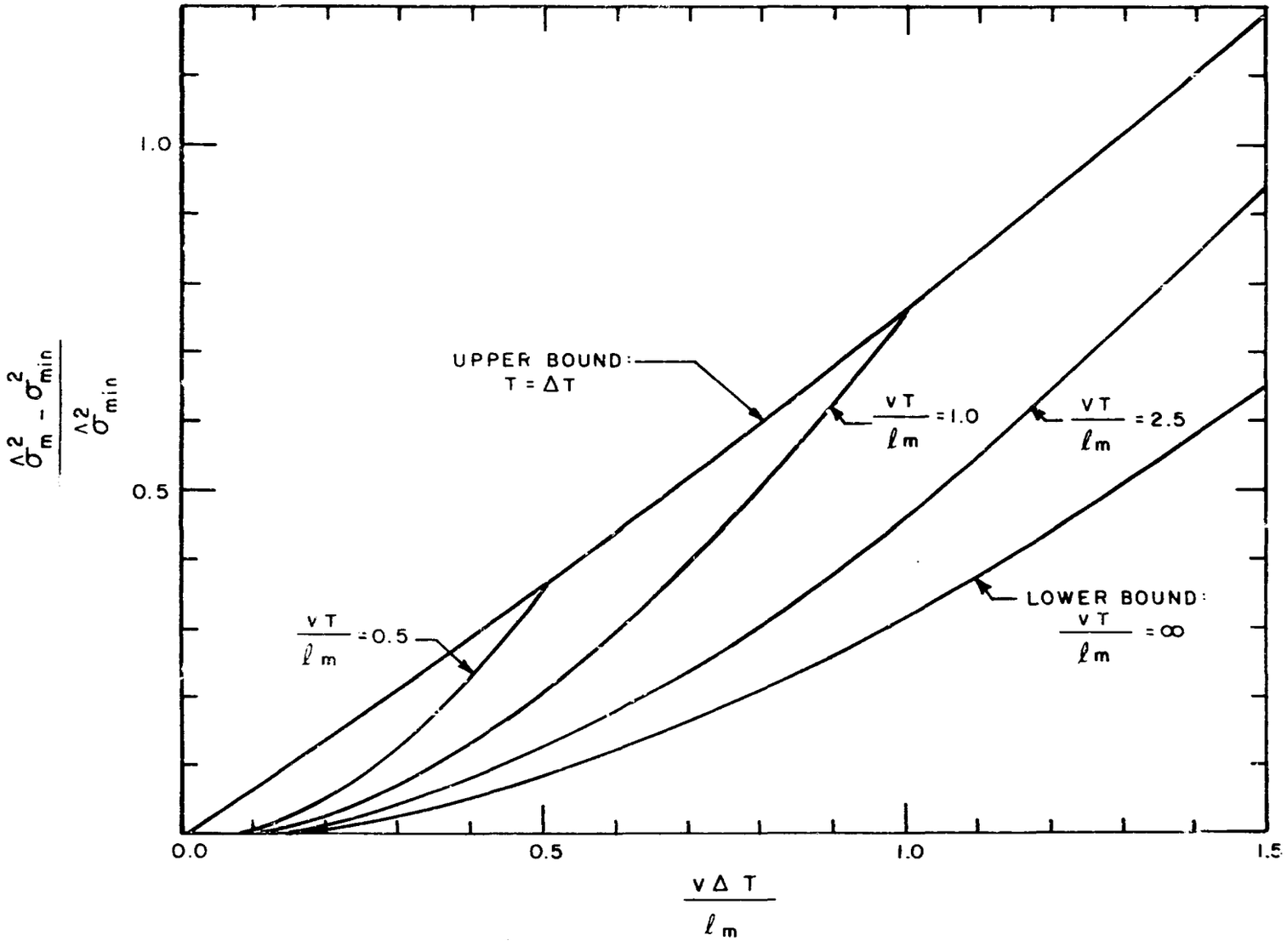

FIGURE C-1 THE FRACTIONAL INCREASE IN EXPECTED SQUARED ERROR DUE TO SAMPLING

one should probably select the largest T that is acceptable as far as response to systematic change in c_a is concerned, and see whether or not the resulting $\hat{\sigma}^2_{min}$ given by Eq. (C-11) is acceptable. If it is not, a single vertically-pointing instrument will not be adequate, no matter how small ΔT is made.

Appendix D

ANALYSIS OF CLOUD-AMOUNT VARIANCE

1. Introduction

In this appendix the problem of estimating cloud amount is analyzed for the case where the instruments are located along a straight line and the clouds are moving very rapidly. The restriction of the instrument locations reduces the problem to a one-dimensional analysis in which the exponentially distributed clouds form a Poisson process.

The analysis proceeds as follows. First we establish the statistical characteristics of the cloud amount $c(x)$ over a given point x. Then we use this to obtain the autocorrelation function for the cloud amount $\tilde{c}(x)$ over an airport centered at x, and the cross-correlation function for $c(x)$ and $\tilde{c}(x)$. Finally, letting $\hat{c}$ be the estimate of $\tilde{c}$ obtained by sampling at n fixed points, we derive an expression for the expected squared error in terms of these autocorrelation and cross-correlation functions.

2. The One-Dimensional Case as a Poisson Process

Let $c(x)$ indicate the presence or absence of a cloud above a given point x, with $c = 1$ if a cloud is present and $c = 0$ if a cloud is absent. Then $c(x)$ is a discontinuous function, switching back and forth from 0 to 1 at various transition points. We assume that these transition points have a Poisson distribution; that is, we assume that the probability of finding n transition points in an interval of length ζ is

$$P(n;\zeta) = \frac{(a\zeta)^n}{n!} e^{-a\zeta} \quad , \qquad (D\text{-}1)$$

where a is the average number of transition points per unit interval. If we are to assume further that transitions in nonoverlapping intervals are statistically independent, then it is well known* that the autocorrelation function for $c(x)$,

*Our result is a simple modification of that given by Lee (Lee, 1960, p. 223).

$$\varphi_{cc}(\zeta) = E[c(x)c(x-\zeta)] \quad , \tag{B-2}$$

is given by

$$\varphi_{cc}(\zeta) = \frac{1}{4}\left(1 + e^{-2a|\zeta|}\right) \quad . \tag{D-3}$$

This result has a simple interpretation. The independent Poisson assumption leads to an exponential distribution of the lengths of the intervals between transitions, with the mean interval being $\ell_m = 1/a$. Since a transition can be from cloudy to clear or from clear to cloudy, this mean interval ℓ_m is both the mean cloud length and the mean hole length. Thus, we are tacitly assuming that the large-area cloud amount is 0.5, which is a worst case from the standpoint of estimating cloud amount. If the correlation shift ζ is small relative to the mean length ℓ_m, φ_{cc} approaches the mean squared value of c(x), 0.5. If ζ is large relative to ℓ_m, φ_{cc} approaches the square of the mean value of c(x), $(0.5)^2$. In general, the correlation between $c(x_1)$ and $c(x_2)$ is high if $|x_1 - x_2| < \ell_m/2$ and low if $|x_1 - x_2| > \ell_m/2$.

3. Limited-Area Cloud Amount

Let $\tilde{c}(x)$ denote the cloud amount over an interval of width w centered at x. Then $\tilde{c}$ is related to c by

$$\tilde{c}(x) = \frac{1}{w}\int_{x-\frac{w}{2}}^{x+\frac{w}{2}} c(u)\,du \quad . \tag{D-4}$$

The autocorrelation function for $\tilde{c}$ is given by

$$\begin{aligned}\varphi_{\tilde{c}\tilde{c}}(\zeta) &= E[\tilde{c}(x)\,\tilde{c}(x-\zeta)] \\ &= \frac{1}{w^2}\int_{x-\frac{w}{2}}^{x+\frac{w}{2}}\int_{x+\zeta-\frac{w}{2}}^{x+\zeta+\frac{w}{2}} E[c(u)\,c(v)]\,du\,dv \\ &= \frac{1}{w^2}\int_{-\frac{w}{2}}^{\frac{w}{2}}\int_{\zeta-\frac{w}{2}}^{\zeta+\frac{w}{2}} \varphi_{cc}(u-v)\,du\,dv \quad ,\end{aligned} \tag{D-5}$$

where φ_{cc} is given by Eq. (D-3). Substituting for φ_{cc} and performing the integration, we obtain

$$\varphi_{\tilde{c}\tilde{c}}(\zeta) = \begin{cases} \frac{1}{4} + \frac{w - |\zeta|}{4a w^2} + \frac{e^{-2aw}\cosh 2a\zeta - e^{-2a|\zeta|}}{8a^2 w^2} & |\zeta| < w \\ \frac{1}{4} + \frac{1}{4}\left(\frac{\sinh aw}{aw}\right)^2 e^{-2a|\zeta|} & |\zeta| \geq w \end{cases} \quad . \tag{D-6}$$

Note that $\varphi_{\tilde{c}\tilde{c}}(\zeta) \to \varphi_{cc}(\zeta)$ as $w \to 0$ and $\varphi_{\tilde{c}\tilde{c}}(\zeta) \to \frac{1}{4}$ as $w \to \infty$. These two extremes correspond to airports of zero and infinite extent, respectively. As a special case of this result, we obtain the following expression for the mean squared value of $\tilde{c}$:

$$\begin{aligned} E[\tilde{c}^2] &= \varphi_{\tilde{c}\tilde{c}}(0) \\ &= \frac{1}{4} + \frac{1}{4aw}\left[1 - e^{-aw}\frac{\sinh aw}{aw}\right] \quad . \end{aligned} \tag{D-7}$$

4. The Cross-Correlation Function

The cross-correlation function between c and $\tilde{c}$ is defined by

$$\varphi_{c\tilde{c}}(\zeta) = E[c(x)\ \tilde{c}(x + \zeta)] \quad . \tag{D-8}$$

Using Eq. (D-4) for $\tilde{c}$ and Eq. (D-3) for φ_{cc}, we obtain

$$\begin{aligned} \varphi_{c\tilde{c}}(\zeta) &= \frac{1}{w}\int_{x+\zeta-\frac{w}{2}}^{x+\zeta+\frac{w}{2}} E[c(x)\ c(u)]\, du \\ &= \frac{1}{w}\int_{\zeta-\frac{w}{2}}^{\zeta+\frac{w}{2}} \varphi_{cc}(u)\, du \\ &= \frac{1}{4} + \frac{1}{4w}\int_{\zeta-\frac{w}{2}}^{\zeta+\frac{w}{2}} e^{-2a|u|} du \quad . \end{aligned} \tag{D-9}$$

Performing the integration, we obtain the final result

$$\varphi_{c\tilde{c}}(\zeta) = \begin{cases} \frac{1}{4} + \frac{1 - e^{-aw}\cosh 2a\zeta}{4aw} & |\zeta| < \frac{w}{2} \\ \frac{1}{4} + \frac{1}{4} e^{-2a|\zeta|}\frac{\sinh aw}{aw} & |\zeta| \geq \frac{w}{2} \end{cases} \quad . \tag{D-10}$$

It will turn out that we only need the result for $|\zeta| < w/2$, where c and $\tilde{c}$ are strongly correlated.

5. Cloud Amount Estimation

Let n ideal vertically-pointing instruments be located at $x_1, \ldots, x_n$. Then the k^{th} instrument reports a cloud if $c(x_k) = 1$ and reports clear conditions if $c(x_k) = 0$. Let $\hat{c}$ be a linear estimate of $\tilde{c}$ obtained by the relation

$$\hat{c} = \sum_{k=1}^{n} a_k c(x_k) \quad , \tag{D-11}$$

where a_k are constant coefficients. In general, the mean squared error for any estimate $\hat{c}$ is given by

$$\begin{aligned} \hat{\sigma}^2 &= E[(\hat{c} - \tilde{c}(x))^2] \\ &= E[\hat{c}^2] - 2E[\hat{c}\tilde{c}] + E[\tilde{c}^2] \quad . \end{aligned} \tag{D-12}$$

The third term in this sum is merely $\varphi_{\tilde{c}\tilde{c}}(0)$, and is given by Eq. (D-7). We now evaluate the other two terms for the case of uniform sampling.

5.1 $E[\hat{c}\,\tilde{c}]$

By Eq. (D-11) and Eq. (D-8),

$$\begin{aligned} E[\hat{c}\,\tilde{c}] &= \sum_{k=1}^{n} a_k E[c(x_k)\,\tilde{c}] \\ &= \sum_{k=1}^{n} a_k \varphi_{c\tilde{c}}(x - x_k) \quad , \end{aligned} \tag{D-13}$$

where $\varphi_{c\tilde{c}}$ is the cross-correlation function given by Eq. (D-10). For the case of uniform sampling, we let

$$a_k = \frac{i}{n} \tag{D-14}$$

and

$$x_k = w\left[\frac{k}{n+1} - \frac{1}{2}\right] \tag{D-15}$$

for k = 1, ..., n. With this choice, the estimate $\hat{c}$ is the average of the instrument responses, and the instruments uniformly cover an interval of width w centered at x = 0. If we use this choice to estimate $\tilde{c}(x)$ at x = 0, we obtain

$$E[\hat{c}\,\tilde{c}] = \frac{1}{n}\sum_{k=1}^{n}\varphi_{c\tilde{c}}\left(w\left[\frac{k}{n+1} - \frac{1}{2}\right]\right). \tag{D-16}$$

Since the argument of $\varphi_{c\tilde{c}}$ ranges from greater than - w/2 to less than w/2, it follows that we only need the first half of Eq. (D-10) for $\varphi_{c\tilde{c}}$, corresponding to the strongly correlated case. Substituting this expression, and using the relation

$$\sum_{j=1}^{n}\theta^j = \theta\,\frac{1-\theta^n}{1-\theta}\quad, \tag{D-17}$$

we obtain

$$E[\hat{c}\,\tilde{c}] = \frac{1}{4} + \frac{1}{4aw}\left[1 - \frac{\theta}{n}\,\frac{1-\theta^n}{1-\theta}\right]\quad, \tag{D-18}$$

where

$$\theta = e^{-\frac{2aw}{n+1}}\quad. \tag{D-19}$$

We note in passing that if n is very large, $\hat{c}$ becomes essentially the same as $\tilde{c}$, and $E[\hat{c}\,\tilde{c}] \to E[\tilde{c}^2]$, given by Eq. (D-7). This can be confirmed by computing the limit of $E[\hat{c}\,\tilde{c}]$ as n approaches infinity. At the other extreme, when n = 1, $\hat{c} = c$ and $E[\hat{c}\,\tilde{c}] = \varphi_{c\tilde{c}}(0)$. This can be confirmed by computing $\varphi_{c\tilde{c}}(0)$ from Eq. (D-10). Our interest, of course, is in values of n between these two extremes.

5.2 $E[\hat{c}^2]$

By Eq. (D-11) and Eq. (D-2),

$$E[\hat{c}^2] = \sum_{j=1}^{n} \sum_{k=1}^{n} a_j a_k E[c(x_j)\, c(x_k)]$$

$$= \sum_{j=1}^{n} \sum_{k=1}^{n} a_j a_k \varphi_{cc}(x_k - x_j) \quad . \qquad \text{(D-20)}$$

Using the uniform sampling assumptions of Eqs. (D-14) and (D-15) and Eq. (D-3) for φ_{cc}, we obtain

$$E[\hat{c}^2] = \sum_{j=1}^{n} \sum_{k=1}^{n} \frac{1}{4n^2} \left(1 + e^{-\frac{2aw}{n+1}|k-j|}\right) \quad , \qquad \text{(D-21)}$$

Again letting $\theta = e^{-\frac{2aw}{n+1}}$ and using Eq. (D-17), after some manipulation we obtain

$$E[\hat{c}^2] = \frac{1}{4} + \frac{1}{4n} \frac{1+\theta}{1-\theta} - \frac{\theta}{2n^2} \frac{1-\theta^n}{(1-\theta)^2} \quad . \qquad \text{(D-22)}$$

6. Mean Squared Error

Eqs. (D-7), (D-18), and (D-22) give the three terms in Eq. (D-12) for the mean squared estimation error. Combining these equations, we obtain our final result:

$$\hat{\sigma}^2 = \frac{1}{4aw} \left\{ \frac{aw}{n} \frac{1+\theta}{1-\theta} + \frac{2\theta(1-\theta^n)}{n(1-\theta)} \left[1 - \frac{aw}{n(1-\theta)}\right] - 1 - e^{-aw} \frac{\sinh aw}{aw} \right\} \quad , \qquad \text{(D-23)}$$

where

$$\theta = e^{-\frac{2aw}{n+1}} \quad . \qquad \text{(D-19)}$$

This equation shows how the expected squared error depends on the mean cloud length $\ell_m = 1/a$, the size of the airport w, and the number of instruments n. Although $\hat{\sigma}^2$ is a relatively simple function of aw and n, its computation requires a certain amount of care, particularly when w/ℓ_m is small. By using a Taylor's series expansion with n fixed, one can obtain the following useful approximations:

$$\hat{\sigma}^2 \simeq \begin{cases} \dfrac{aw}{6\,n(n+1)} & aw \ll n \\ \dfrac{1}{4n} & aw \gg n \end{cases} . \qquad \text{(D-24)}$$

A graph of $\hat{\sigma}^2$ versus w/ℓ_m, which is the same as aw, is shown in Figure D-1. This graph shows that $\hat{\sigma}^2$ increases monotonically with aw and decreases monotonically with n. The worst situation occurs when $aw \gg n$, i.e., when the clouds are very small relative to the distance between instruments. In this case the instrument readings are statistically independent, and it is not possible to improve on the asymptotic result $\hat{\sigma} = 1/2\sqrt{n}$. On the other hand, when the clouds are large relative to the distance between instruments, small values of $\hat{\sigma}$ can be obtained.

Another way to examine these results is to see how many instruments are needed to obtain a specified value for $\hat{\sigma}$. These results are shown in Figure D-2. Of course, only integral value of n are meaningful, and one must select an integer at least as large as the value read from the graph.

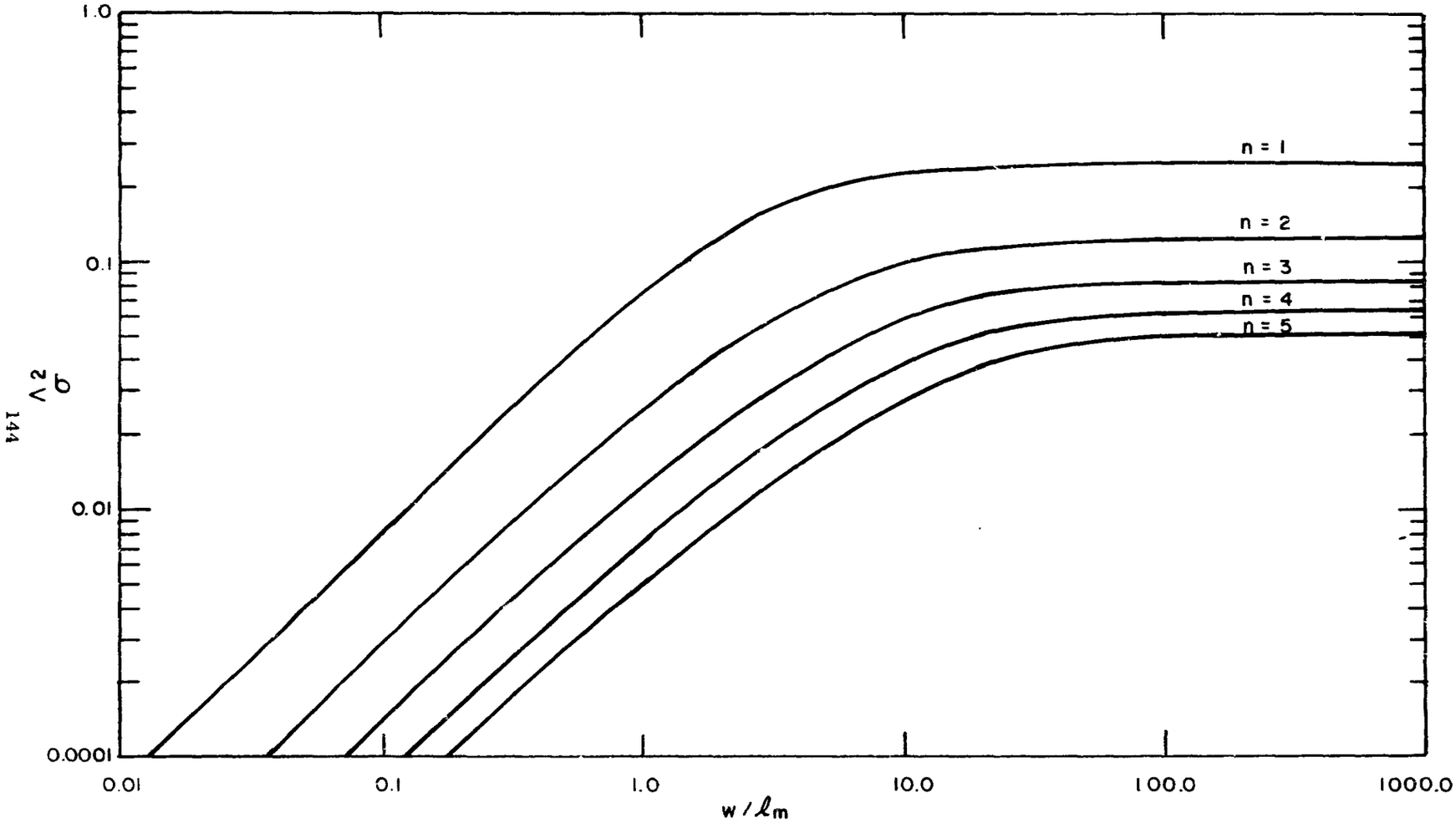

FIGURE D-1 MEAN SQUARED ERROR FOR AN n-INSTRUMENT ESTIMATE OF CLOUD AMOUNT

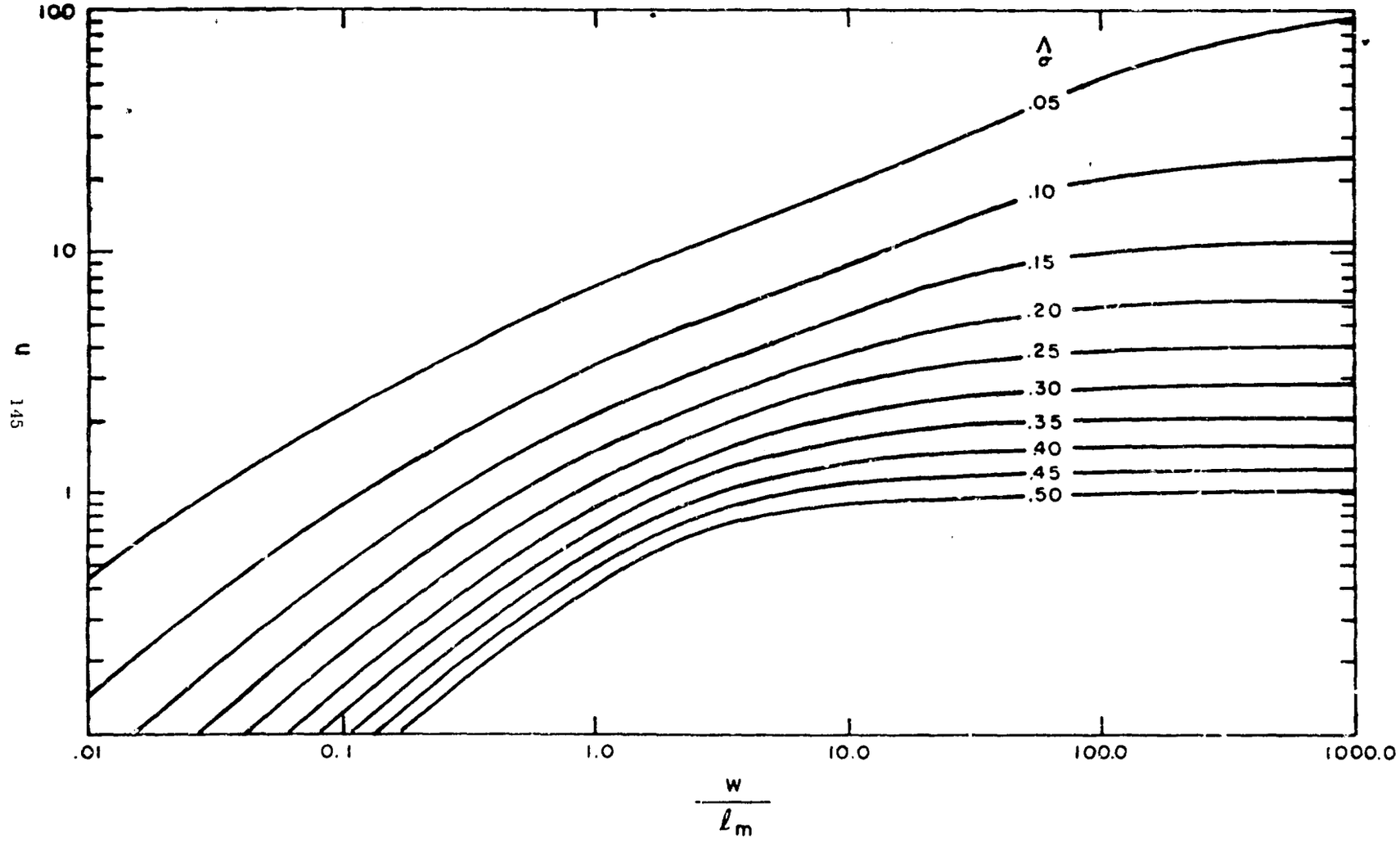

FIGURE D-2 THE NUMBER OF INSTRUMENTS NEEDED TO OBTAIN A ROOT MEAN SQUARED ERROR

Appendix E

EFFECT OF SAMPLING ON BASE-HEIGHT ESTIMATION

This appendix presents an analysis of the effect of sampling on the estimate of the base height of a single unbroken cloud layer. The mathematical steps are essentially the same as those encountered in the cloud amount analysis given in Appendix C. Thus, the following development is done with less detailed explanation.

Let the x-axis be aligned with the direction of cloud motion, and let h(x+vt) give the height of the cloud over point x at time t. Let the autocorrelation function for the cloud base height be given by*

$$E[h(x+\zeta)h(x)] = \bar{h}^2 + \sigma_b^2 e^{-|\zeta|/d}, \qquad \text{(E-1)}$$

where $\bar{h}$ is the mean base height, σ_b is the base height standard deviation, ζ is the correlation shift distance, and d is the base-height correlation distance. Let an instrument located at x_0 sample the cloud layer at times $t_k = t_0 - k\Delta T$ to yield the readings $h_k = h(x_0+vt_0+kv\Delta T)$. Then the correlation between successive readings is given by

$$E[(h_j-\bar{h})(h_k-\bar{h})] = \sigma_b^2 e^{-v\Delta T|j-k|/d}. \qquad \text{(E-2)}$$

This correlation limits the advantage of using a very short sampling interval ΔT to improve the estimate of the mean base height. Let us estimate the mean base height by the mean of m successive readings,

$$\hat{h}_m = \frac{1}{m}\sum_{k=1}^{m} h_k. \qquad \text{(E-3)}$$

Then $\hat{h}_m$ is a random variable with mean $\bar{h}$ and variance $\hat{\sigma}_b^2$, where

*This function is discussed in Appendix A of Duda, Mancuso, and Blackmer (1970).

$$\hat{\sigma}_b^2 = E\left[(\hat{h}_m - \bar{h})^2\right]$$

$$= \frac{1}{m^2} \sum_{j=1}^{m} \sum_{k=1}^{m} E\left[(h_j - \bar{h})(h_k - \bar{h})\right]$$

$$= \frac{\sigma_b^2}{m^2} \sum_{j=1}^{m} \sum_{k=1}^{m} e^{-v\Delta T|j-k|/d}$$

$$= \frac{\sigma_b^2}{m(1-\theta)} \left[1+\theta - \frac{2\theta(1-\theta^m)}{m(1-\theta)}\right] , \qquad \text{(E-4)}$$

where

$$\theta = e^{-v\Delta T/d} . \qquad \text{(E-5)}$$

Clearly, Eq. (E-4) corresponds directly to Eq. (C-9), and Eq. (E-5) corresponds directly to Eq. (C-10). From this, we can conclude immediately that if we fix the averaging time $T = m\Delta T$ and let m increase by letting ΔT go to zero, $\hat{\sigma}_b^2$ will approach the minimum value

$$\hat{\sigma}_{min}^2 = \frac{\sigma_b^2}{vT/2d} \left[1 - \frac{1-e^{-vT/d}}{vT/d}\right] . \qquad \text{(E-6)}$$

Note that $\hat{\sigma}_{min}/\sigma_b$ can be obtained from Figure 2 by replacing vT/ℓ_m by $vT/2d$. If ΔT is not zero, $\hat{\sigma}_b^2$ is greater than $\hat{\sigma}_{min}^2$, but it may not be much greater. The percentage increase in $\hat{\sigma}_b^2$ can be found from Figure C-1 by replacing $v\Delta T/\ell_m$ by $vT/2d$. Thus, in the worst case $\hat{\sigma}_b^2$ is less than 20 percent greater than $\hat{\sigma}_{min}^2$ if $\Delta T = 0.5\ d/v$, and a further reduction in ΔT does not yield much further benefit. For example, if the correlation distance is 100 ft. and the cloud speed is 10 ft./sec., there is little value in sampling faster than once every five seconds.

Appendix F

COMPUTATIONAL REQUIREMENTS FOR HIERARCHICAL CLUSTERING

In this appendix a simple analysis is made of the time required for the modified hierarchical clustering procedure described in Section IV-D-2. The following description is an elaboration of that procedure written in a form that more closely resembles and actual computer program. The input to the program is an array of N=mn base height readings, m readings from each of n ceilometers, taken during an averaging period T. As these readings are processed, the resulting cluster centers are stored in the same array; the array index(i) is used to indicate which entries are cluster centers. Using the notation of Section IV-D-2, the procedure is as follows:

(1) Order the N readings h_i so that $h_1 \leq h_2 \leq \ldots \leq h_N$.

(2) Initialize:

$g \leftarrow N$; $\hat{\sigma}_p^2 \leftarrow 0$;

For i=1 to N:

$n_i \leftarrow 1$; $\hat{h}_i \leftarrow h_i$; index (i) $\leftarrow$ i.

(3) Find nearest clusters:

$d_{min}^2 \leftarrow$ very large number;

For i=1 to g-1:

$j \leftarrow$ index (i);

$k \leftarrow$ index (i+1);

$$d^2 \leftarrow \frac{n_j n_k}{n_j + n_k} (\hat{h}_j - \hat{h}_k)^2;$$

If $d^2 < d_{min}^2$ then $d_{min}^2 \leftarrow d^2$; $i_{min} \leftarrow i$;
else continue.

(4) Update:

$j \leftarrow$ index (i_{min});

$k \leftarrow$ index (i_{min}+1);

$$\hat{\sigma}_p^2 \leftarrow \hat{\sigma}_p^2 + \frac{1}{N-1} d_{min}^2;$$

$$\hat{h}_j \leftarrow \frac{n_j \hat{h}_j + n_k \hat{h}_k}{n_j + n_k} ;$$

$n_j \leftarrow n_j + n_k$; $g \leftarrow g-1$;

For $i = i_{min}+1$ to g

index (i) ← index (i+1).

(5) Test:

If $\sigma_p^2 < (60 \text{ feet})^2$

and $g > 1$

then go to Step 4.

(6) Results:

Number of layers = g

Mean base heights: $\hat{h}_{index(i)}$, i=1 to g

Cloud amount in layers: $\frac{n_{index\ (i)}}{N}$, i=1 to g

Pooled standard deviation: $\hat{\sigma}_p$.

Aside from the program itself, the primary storage requirements are for the three arrays n_i, $\hat{h}_i$, and index(i), requiring 3N words of core memory. The index array could be eliminated by more clever programming, but this might require more execution time.

The most time-consuming part of this procedure is Step 3, since it involves g-1 operations that may have to be repeated N-1 times, with g going from N to 2. That is, the block of steps in the for-loop may have to be executed N(N-1)/2 times. Including the incrementing and testing required for the for-loop itself, this involves 6 fetches, 5 additions or subtractions, 2 multiplications or divisions, 2 tests, and an average of 1 store each time. If t_{add} is the add-time and t_{mul} the multiply-time for the computer, the total time required is bounded by

$$t_{tot} \geq N^2 (7t_{add} + t_{mul}).$$

$$\geq \left(\frac{nT}{\Delta T}\right)^2 (7t_{add} + t_{mul}).$$

Since this computation must be completed in time T if the processing

is not to lag behind the rate at which data is being received, we obtain the requirement

$$7t_{add} + t_{mul} \leq \frac{\Delta T^2}{n^2 T}$$

REFERENCES

I. Andermo, L. Fornaeus, I Svensson, and G. Wilborg, 1965, "Laser-Molnhöjdmätare: Beskrivning och Mätningar Gjorda T.O.M. September 1964, "FOA 2 Rapport, Försvarets Forskningsanstatt, Stockholm, 32 pp.

ASEA (Allmänna Svenska Elektrisk Aktobolaget), 1968, Brochures 8432E and 8352E on Type YLAMB Laser Cloud Ceilometer, Västeras, Sweden.

D. Atlas, 1968, "Clear Air Turbulence Detection Methods: A Review," RAPP Technical Note 1, The University of Chicago, Illinois.

G. H. Ball, 1965, "Data Analysis in the Social Sciences," Proc. Fall Joint Comp. Conf., Vol. 27, pp. 533-560 (Spartan Books, Washington, D.C.).

G. H. Ball and D. J. Hall, 1967, "A Clustering Technique for Summarizing Multivariate Data," Behavioral Science, Vol. 12, No. 2, pp. 153-155.

G. H. Ball and D. J. Hall, 1970, "Application of Cluster Analysis to Bureau of Census Data," Final Report, SRI Project 7600, Stanford Research Institute, Menlo Park, California.

L. G. Bird and N. E. Rider, 1968, "The Laser Cloud-Base Recorder," Met. Mag., London, Vol. 97, pp. 107-115.

R. H. Blackmer, Jr., and S. M. Serebreny, 1962, "Dimensions and Distributions of Cumulus Clouds as Shown by U-2 Photographs," Scientific Report 4, Contract AF 19(604)-7312, Stanford Research Institute, Menlo Park, California.

R. H. Blackmer, Jr., and M. G. H. Lidga, 1963, "Climatological Applications of Vertically Pointing Weather Radar Observations," Scientific Report 5, SRI Project 3245, Stanford Research Institute, Menlo Park, California.

R. Bureau, 1946, "Altimétrie des Nuages par Impulsions Lumineuses," Météorologie, Vol. 3, p. 292.

R. T. H. Collis, 1965, "Lidar Observation of Cloud," Science, Vol. 149, pp. 978-981.

R. T. H. Collis, 1969, "Lidar for Routine Meteorological Observations," B. Amer. Meteor. Soc., Vol. 50, p. 688.

R. T. H. Collis, F. G. Fernald, and J. Alder, 1968, "Lidar Observations of Sierra Wave Conditions," J. Appl. Meteor., Vol. 7, pp. 227-233.

N. E. Davis, 1969, "The Variation of Very Low Cloud Base with Time and Distance and with Height," Meteorological Magazine, Vol. 98, pp. 351-356.

R. O. Duda, R. L. Mancuso, and R. H. Blackmer, Jr., 1970, "Theoretical Considerations for Describing the State of Sky Through Automatic Techniques," Report No. FAA-RD-70-13, Contract FA65WAI-96, SRI Project 7935, Stanford Research Institute, Menlo Park, California.

A. M. Galligan, 1953, "Variability of Subjective Cloud Observations (I)," Air Force Surveys in Geophysics, No. 33.

S. C. Johnson, 1967, "Hierarchical Clustering Schemes," Psychometrika, Vol. 32, No. 3, pp. 241-254.

W. B. Johnson, W. E. Evans, and E. E. Uthe, 1970, "Atmospheric Effects on Laser Eye Safety," Final Report, Contract F41609-69-C-001, U.S. Air Force School of Aerospace Medicine, SRI Project 7472, Stanford Research Institute, Menlo Park, California.

Y. W. Lee, 1960, Statistical Theory of Communication, (John Wiley and Sons, Inc., New York, New York).

M. Lefkowitz, 1970, attachment to a letter of 23 November 1970 from M. Lefkowitz of NOAA to R. O. Duda of SRI.

D. O. Loftsgaarden and C. P. Quesenberry, 1965, "A Nonparametric Estimate of a Multivariate Density Function," Ann. Math. Stat., Vol. 36, pp. 1049-1051.

J. MacQueen, 1967, "Some Methods for Classification and Analysis of Multivariate Observations," 5th Berkeley Symp. on Math., Stat. and Prob., Vol. 1, pp. 281-297.

G. K. Mather and K. R. Hardy, 1970, "Instrumented Aircraft Measurements in the Vicinity of Clear Air Radar Structures," Reprints of Papers Presented at the 14th Radar Meteorology Conference, Boston (Amer. Meteor. Soc., Boston, Massachusetts), pp. 49-52.

P. Medgyessy, 1961, Decomposition of Superpositions of Distribution Functions (Hungarian Academy of Sciences, Budapest, Hungary).

C. A. Northend, R. C. Honey, and W. E. Evans, 1966, "Laser Radar (Lidar) for Meteorological Observations," Rev. Sci. Instr., Vol. 37, pp. 393-400.

E. Parzen, 1962, "On Estimation of a Probability Density Function and Mode," Ann. Math. Stat., Vol. 33, pp. 1065-1076.

A. Perlat and M. Petit, 1961, Mesures en Météorologie (Gauthier-Villars, Paris), 393 pp.

V. G. Plank, 1969, "The Size Distribution of Cumulus Clouds in Representative Florida Populations," J. Appl. Meteor., Vol. 8, No. 1, pp. 46-67.

D. J. Rogers and T. T. Tanimoto, 1960, "A Computer Program for Classifying Plants," Science, Vol. 132, pp. 1115-1118.

G. S. Sebestyen, 1966, "Automatic Off-Line Multivariate Data Analysis," Proc. Fall Joint Comp. Conf., Vol. 28, pp. 685-694.

P. H. A. Sneath, 1969, "Evaluation of Clustering Methods," in Numerical Taxonomy, pp. 257-267, A. J. Cole, ed. (Academic Press, New York, New York).

R. R. Sokal and P. H. A. Sneath, 1963, Principles of Numerical Taxonomy (W. H. Freeman and Co., San Francisco, California).

Sperry Rand Corporation, 1971, "Cloud Base Height Measuring Device," Technical Report AFAL-TR-70-262, AF Avionics Laboratory, AF Systems Command, Wright-Patterson Air Force Base, Ohio.

D. F. Stanat, 1968, "Unsupervised Learning of Mixtures of Probability Functions," In Pattern Recognition, pp. 357-389, L. Kanal, ed. (Thompson Book Co., Washington, D.C.).

M. E. Tarter and R. A. Kronmal, 1968, "Estimation of the Cumulative by Fourier Series Methods and Application to the Insertion Problem," Proc. ACM 23rd Nat. Conf., pp. 491-497.

United States Weather Bureau, 1963, "Climatological Summaries for the Supersonic Aircraft New York-San Francisco Route," Project No. 206-3R (Agreement SRDS-A-178), Department of Commerce, Washington, D.C.

A. Vassiliadis, R. C. Rosan, and H. C. Zweng, 1969, "Research on Ocular Laser Thresholds," Final Report, Contract F41609-68-C-0041, U.S. Air Force School of Aerospace Medicine, SRI Project 7191, Stanford Research Institute, Menlo Park, California.

W. Viezee, 1971, "An Investigation of Mountain Wave Turbulence with Lidar Observations," Final Report, Contract NAS1-9951, NASA Langley Research Center.

W. Viezee, E. E. Uthe, and R. T. H. Collis, 1969, "Lidar Observations of Airfield Approach Conditions--Exploratory Study," J. Appl. Meteor., Vol. 8, pp. 274-283.

Weather Measure Corporation, Undated, "Weather Measure Instruments," a catalog of instruments sold by Weather Measure Corporation, P. O. Box 41257, Sacramento, California.

J. H. Wolfe, 1970, "Pattern Clustering by Multivariate Mixture Analysis," Multivariate Behavioral Research, Vol. 5, pp. 329-350.

P. W. Wyman, 1969, "Laser Radar Eye Hazard Considerations," Appl. Opt., Vol. 8, p. 383.